2020

A THERMODYNAMIC AND FEASIBILITY STUDY OF GREEN SOLVENTS FOR THE FABRICATION OF WATER TREATMENT MEMBRANES

Xiaobo Dong
University of Kentucky, xiaobodong1990@gmail.com
Author ORCID Identifier:
https://orcid.org/0000-0003-2292-9470
Digital Object Identifier: https://doi.org/10.13023/etd.2020.367

STUDENT AGREEMENT:

I represent that my thesis or dissertation and abstract are my original work. Proper attribution has been given to all outside sources. I understand that I am solely responsible for obtaining any needed copyright permissions. I have obtained needed written permission statement(s) from the owner(s) of each third-party copyrighted matter to be included in my work, allowing electronic distribution (if such use is not permitted by the fair use doctrine) which will be submitted to UKnowledge as Additional File.

I hereby grant to The University of Kentucky and its agents the irrevocable, non-exclusive, and royalty-free license to archive and make accessible my work in whole or in part in all forms of media, now or hereafter known. I agree that the document mentioned above may be made available immediately for worldwide access unless an embargo applies.

I retain all other ownership rights to the copyright of my work. I also retain the right to use in future works (such as articles or books) all or part of my work. I understand that I am free to register the copyright to my work.

REVIEW, APPROVAL AND ACCEPTANCE

The document mentioned above has been reviewed and accepted by the student's advisor, on behalf of the advisory committee, and by the Director of Graduate Studies (DGS), on behalf of the program; we verify that this is the final, approved version of the student's thesis including all changes required by the advisory committee. The undersigned agree to abide by the statements above.

Xiaobo Dong, Student

Dr. Isabel C. Escobar, Major Professor

Dr. Stephen Rankin, Director of Graduate Studies

A THERMODYNAMIC AND FEASIBILITY STUDY OF GREEN SOLVENTS FOR THE FABRICATION OF WATER TREATMENT MEMBRANES

DISSERTATION

A dissertation submitted in partial fulfillment of the
requirements for the degree of Doctor of Philosophy in the
College of Engineering
at the University of Kentucky

By
Xiaobo Dong
Lexington, Kentucky
Director: Dr. Isabel C. Escobar, Professor of Chemical and Materials Engineering
Lexington, Kentucky
2020

https://orcid.org/0000-0003-2292-9470

ABSTRACT OF DISSERTATION

A THERMODYNAMIC AND FEASIBILITY STUDY OF GREEN SOLVENTS FOR THE FABRICATION OF WATER TREATMENT MEMBRANES

Nonsolvent induced phase separation (NIPS) has been widely used to fabricate polymeric membranes. In NIPS, a polymer is dissolved in a solvent to form a dope solution, which is then cast on a substrate and immersed in a nonsolvent bath, where phase inversion occurs. Petroleum-derived organic solvents, such as *N*-methyl-2-pyrrolidone (NMP) and dimethylacetamide (DMAc), have been traditionally used to fabricate polymeric membranes via NIPS. However, these solvents may have negative impacts on environmental and human health; therefore, using greener and less toxic solvents, preferably derived from biomass, is of great interest to make membrane fabrication sustainable. In this dissertation, two low-hazard solvents, methyl 5-(dimethylamino)-2-methyl-5-oxopentanoate (Rhodiasolv® PolarClean) and gamma-valerolactone (GVL), were investigated as sole- and as cosolvents to cast polysulfone (PSf) membranes via NIPS.

In the first part of this project, methyl-5-(dimethylamino)-2-methyl-5-oxopentanoate (Rhodiasolv PolarClean) was studied. PolarClean is a bio-derived, biodegradable, nonflammable and nonvolatile solvent. From cloud point curves, PolarClean shows potential to be a solvent for polysulfone. Membranes prepared with PolarClean were investigated in terms of their morphology, porosity, water permeability and protein rejection, and were compared to membranes prepared with traditional solvents. The pores of polysulfone/PolarClean membranes were sponge-like, and the membranes displayed higher water flux values along with slightly higher solute rejection. On the other hand, PSf/DMAc membrane pores were finger-like with lower water flux and slightly lower solute rejection when compared to PSf/PolarClean membranes. Upon reverse-flow filtration to simulate membrane cleaning, it was observed that the pores of PSf/PolarClean membranes collapsed. To address this issue, GVL was investigated as a sole solvent and a cosolvent with PolarClean to fabricate PSf membranes. Membranes prepared using GVL as a sole solvent were observed to be gelatinous, hence not ideal for filtration. On the other hand, when GVL and PolarClean were used as cosolvents, viable membranes were cast with surface charge and hydrophicility not being significantly different from membranes made using PolarClean alone. Furthermore, the average pore size of membranes decreased as the weight percent of GVL in dope solutions increased. Therefore, the use of PolarClean/GVL as cosolvents shows promise for the fabrication of PSf membranes. With respect to operation, membranes cast from dope solutions containing equal amounts of PolarClean and GVL displayed the most similar flux curves and solute rejection to those made using the traditional solvent tested.

Once it was determined that membranes made using PolarClean and GVL as cosolvents were viable and showed similar morphological and operational characteristics to those made using DMAc, the use of PolarClean/GVL cosolvents was then researched at

the production scale. In the last portion of this study, a slot die-roll to roll (R2R) system was used to fabricate polysulfone (PSf) ultrafiltration membranes using low-hazard solvents individually and as cosolvents at a production scale. Production-scale membranes were compared structurally, morphologically and operationally to laboratory-scale membranes made using a doctor's blade. The chemical structure of membranes was not affected by the use of different solvents nor by the differences in scale. On the other hand, cross-sectional images showed that the structures of the membranes were different most likely due to differences in diffusion rates between the different solvents/cosolvents into the nonsolvent, water. Furthermore, it was observed that slot die and doctor's blade casting methods produced membranes with different roughness values likely due to evaporation time differences between the methods. While to protein filtration, all membranes displayed similar operational parameters, i.e., flux decline, permeability and recovery. Overall, this dissertation shows that membranes fabricated using greener/less toxic solvent mixtures are comparable to membranes cast using petroleum-derived solvents, and are scalable using slot die-R2R.

KEYWORDS: Polymeric Membranes, Bio-derived solvent, Non-solvent induced phase separation, Membrane fabrication, Scaleup.

Xiaobo Dong

(Name of Student)

03/27/2020

Date

A THERMODYNAMIC AND FEASIBILITY STUDY OF GREEN SOLVENTS FOR THE FABRICATION OF WATER TREATMENT MEMBRANES

By
Xiaobo Dong

Dr. Isabel C. Escobar
Director of Dissertation

Dr. Stephen Rankin
Director of Graduate Studies

03/27/2020
Date

DEDICATION

To my parents and elder brother.
To Dr. Eric Grulke.

Proverbs 19:2 "Desire without knowledge is not good, and whoever makes haste with his feet misses his way.".

.

ACKNOWLEDGMENTS

First, I would give my sincere gratitude to my advisor, Dr. Isabel C. Escobar. In the past five years, she was a great teacher, a great instructor, and a great mentor for me. She is knowledgeable on any topics related to membranes. She not only gave me advice on research and guided me on the right path, but also taught me how to deal with different situations both in research and life. She has a heart of gold and treats me as her son. Moreover, she was a great running coach for me, and we ran numerous races together. Her presence has been the best thing happened in my life. I cannot thank you more, Dr. Escobar.

I would also thank Dr. Eric Grulke, for his guidance on polymer process engineering for the past four years. His encouragements and sense of humor will always keep in my heart. He will be missed.

I would like to thank Dr. Dibakar Bhattacharyya for many meaningful conversations and help, Dr. Douglass Kalika for his helpful insights on polymer engineering and supports, Dr. Doo Young Kim for his insightful comments on research, Dr. Maria Coleman for all the meetings we had whenever we met during conferences. I cannot imagine I am able to finish this journey without all the help from you.

This dissertation would not be possible without the support provided by the KY NSF EPSCoR program (Grant number: 1355438, 2015-2019). Moreover, through these years, I have collaborated with different research groups. I would like to acknowledge TJ Jeong and Dr. Tequila Harris on the scale up study, Atena Amirsoleimani and Dr. Gail Brion on the bacterial study, Dr. Wenxin Cao and Dr. Fuqian Yang on AFM study, Dr. Nick Linck and Dr. Matt Weisenberger on the viscosity study. This dissertation is truly a teamwork.

During the past five years, the center of membrane sciences at University of Kentucky was the place I stayed longer than any other place. I would like to thank my labmates and friends, Joyner Eke, Dr. Sneha Chede, Dr. Priyesh Wagh, Dr. Andrew Colburn, Dr. Ashish Aher, Dr. Hongyi Wan, Dr. Rupam Sarma, Saiful Islam, Anthony Saad, Michael Detisch, and Francisco Leniz. I had the pleasure to work with some extraordinary undergraduate researchers. You all have helped me through the long journey.

Five years ago, I came to Lexington alone, barely spoke English and knew nobody in this country. Glory to God, he sent me awesome friends and families in the US. I would like to thank three of my closest friends, Conor Sprick, Dr. Matthew Hancock and Dr. Landon Mott. Thank you, my three American brothers. They supported me whenever I need support and they helped me whenever I need help. Kaizer was my emotional dog. I also want to thank my sister Jess Ball for her continuous love and support during this journey. On 2015, I was invited to my language partner Joshua Feinn's family for Thanksgiving lunch. Since then, Feinn's family hosted me five consecutive years for Thanksgiving. Josh, thank you for not only being my English partner, but also a good friend.

I was never left alone in the festivals. The Balls, Feinns, and Motts generously opened their family and hosted me during festivals. The Hancocks, Dena, Skip, Matt, Michael and Mason, always had me when I need a place to go. They treated me as one of their boys and I enjoyed being a Hancock boy. I am very grateful.

I would like to recognize my friends, Sara Vigue Mott, Tammy Sprick, Dr. Yuxin He, Lauren and Dr. Andrew Colburn, Amanda and Logan Warriner, Grace and Cameron Day, Anna and Kevin Thompson, Weibo Shang, Cong Li, Ning Wei, Andrew Meyer, Evan Hyde, Kelley Wiegman, Steven Shofner, Jack Whitewolf, James Riker, Yuyan Xia, Christian Farmer, Joseph Kretz, Chase Thornton, Clay Thornton and Cody Bertram. Thank you for your company.

The communities around me were amazing in the past years. I was honored to serve as different roles in MACE and worked with all the graduate students in our Department. Baptist Campus Ministry, Christian Student Fellowship and Turningpoint Church played important roles in my spiritual life.

最后，我特别想感谢我的家人。过去的三十年，我的父母董振国和李桂珍，含辛茹苦把我抚养成人，无条件地相信我、鼓励我、支持我。因为时代原因和家庭原因，母亲只有小学文化，但是她跟我说过，“我也有过一个博士梦”。您的梦，我替您完成了。感谢我的哥哥嫂嫂董波和吕敏，我常年在外，是他们在家，照顾父母，承担家庭的责任。感谢我的发小张泽天、顾旭舟、王颖和马霄常年来的陪伴、支持和鼓励。

TABLE OF CONTENTS

LIST OF TABLES

LIST OF FIGURES

CHAPTER 1. INTRODUCTION AND LITERATURE REVIEW

1.1 Introduction

Membrane technology has been used in liquid and gas separations for decades because membranes are easy to fabricate, simple to use, have high selectivity and do not need to regenerate sorbents. Membranes have played an increasingly important role in the desalination, water treatment, food and pharmaceutical industries. However, during membrane fabrication, large amounts of organic solvents are used [1], and solvents used in synthesis and post-synthesis steps can have a negative impact on operational safety, cost, the environment and human health [2-4]. Traditional solvents used for membrane preparation include dimethylformamide (DMF), *N*-methyl-2-pyrrolidone (NMP), and dimethylacetamide (DMAc). Due to their toxicity, solvents require specialized control measures. Therefore, the need for greener, low-toxicity and more sustainable solvents has prompted a great amount of research into the processing of renewable feedstocks to obtain platform molecules and downstream end products. The annual global solvent market is in the order of 20 million metric tons and billions of dollars, and bio-based solvent consumption in Europe is predicted to grow to one million metric tons by 2020 [5, 6]. Using renewable solvents derived from biomass, which do not compete with food applications, satisfies both consumer and legislative demands with regards to sustainability.

Therefore, in this dissertation, solvents involved in the manufacturing process of membranes are proposed to be replaced by greener/less toxic alternatives. A green solvent is expected to be non-toxic, non-volatile, and derived from renewable sources [7]. Polysulfone (PSf) was chosen as the membrane polymer material in order to investigate

the ability of two greener/low toxicity solvents to dissolve PSf and then fabricate membranes. The membranes were then characterized and compared with the membranes made of traditional petroleum-derived solvents. This was followed by an investigation of them scaling up of the membranes made with the greener solvents using slot die-roll to roll (R2R).

1.2 Literature review

1.2.1 Membrane Fabrication

Membranes are commonly made of polymeric [8, 9], ceramic [10, 11] and stainless steel materials [12, 13]. Of these, polymeric membranes are the most popular due to the high selectivity, easy operation and easy to perform surface modification, and have been deeply studied [14]. Therefore, the focus of this study is polymeric membranes and their phase separation-based fabrication methods, namely nonsolvent induced phase separation (NIPS), temperature induced phase separation (TIPS), vapor induced phase separation (VIPS), solvent evaporation induced phase separation (EIPS), interfacial polymerization and some other methods. Since phase separation-based methods are the focus of this dissertation, each phase separation method is defined and discussed in terms of a few literature studies, and later compared with respect to advantages and disadvantages.

Nonsolvent induced phase separation (NIPS) is a conventional method to fabricate porous polymeric membranes. Figure 1.1 shows the NIPS method process. First, a polymer or a mixture of polymers with or without additives, such as pore formers, is dissolved by at least one solvent to form a homogeneous dope solution [15, 16]. The dope solution is then cast as a liquid film on a substrate, either a glass plate or a polymeric substrate. The

liquid film on the substrate is then immersed into a coagulation nonsolvent bath, water. Afterwards, phase inversion occurs as the solvent in the film exchanges with the nonsolvent [17]. This process results in an asymmetric polymeric membrane with a dense selective layer and a porous supportive sublayer. These two layers have their different functionality, with the selective layer providing the separation selectivity for the membranes either due to size exclusion or charge, and the porous support layer providing mechanical strength and stability underneath the selective layer [18]. Pagliero et al. [19] used NIPS to prepare polyvinylidene fluoride (PVDF) membranes for membrane distillation They found that the principal factor affecting the membrane structure was the rate of crystallization of PVDF during the liquid-liquid demixing process.

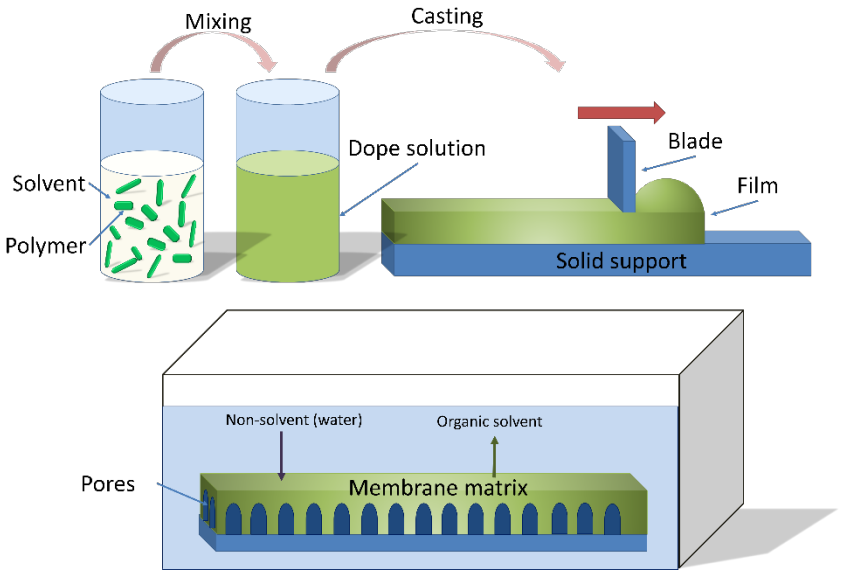

Figure 1.1 Nonsolvent phase inversion casting process [20]

Temperature induced phase separation (TIPS) is a process (Figure 1.2) in which a dope solution of polymers and solvents is prepared at high temperature, and then cooled

down to a low temperature. During the temperature changes, phase separation occurs, and a solid film can form [21].

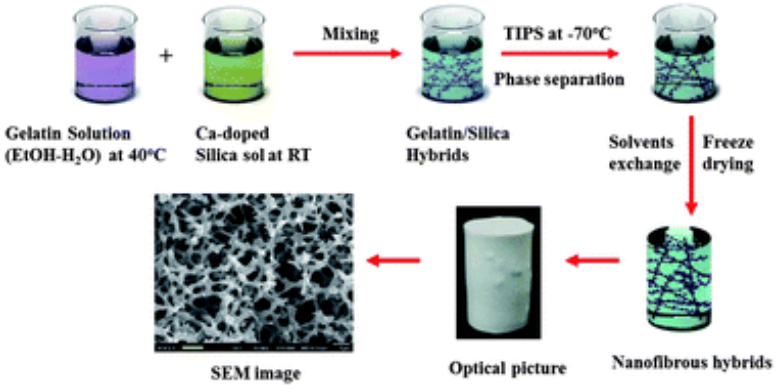

Figure 1.2 Temperature induced phase separation process (Reproduced from Ref [22] with permission from The Royal Society of Chemistry.)

M'barki et al. [23] used TIPS along with crosslinking to prepare porous poly(vinyl alcohol) (PVA) membranes. In this study, water was chosen to dissolve PVA to avoid the use of organic solvents. The membranes showed connected cellular pores throughout the cross-section of the membranes. However, due to water being used as the solvent, with a higher humidity, an open pore structure (larger than 10 μm) was obtained instead of a defect free skin layer.

Vapor induced phase separation (VIPS) is another method to fabricate porous membranes. As shown in Figure 1.3, in VIPS, a dope solution is prepared and cast into a liquid film, and then exposed in the atmosphere of the nonsolvent vapors in a vapor chamber. It is a similar process to NIPS, but phase separation occurs with water vapor transfer into the film while the solvent diffuses into the vapor to form a solid membrane film.

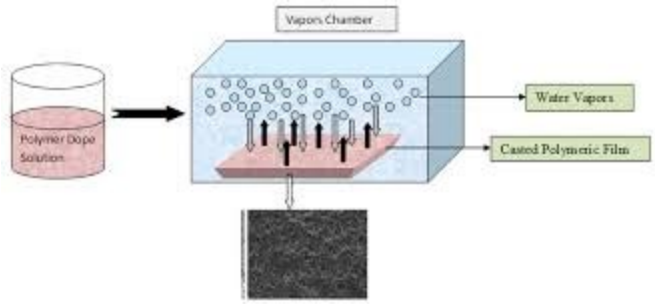

Figure 1.3 Vapor induced phase separation process (Reproduced from Ref [24] published by Longdom Group)

Zhao et al. [25] studied using VIPS to prepare poly(vinylidene fluoride) (PVDF) porous membranes. Membranes showed cellular structure when the vapor temperature was 65 ℃ and relative humidity of 70% for 20 minutes of exposure time. Unlike NIPS, where the dope liquid film immersed into a nonsovent bath, in VIPS, the dope film is exposed to the vapor phase nonsolvent, which delayed the phase separation process and led to cellular membrane structure [25]. They found that with the cellular structures being bicontinuous, mechanical strength was enhanced [25].

In the solvent evaporation induced phase separation (EIPS) method (shown in Figure 1.4), a homogeneous solution is prepared by dissolving a polymer in the mixture of a solvent and a nonsolvent, where the solvent has higher volatility than the nonsolvent. Through evaporation of the solvent, phase separation occurs and the demixing of polymer-solvent-nonsolvent system happens, results in a porous film. The pore structures can be controlled by changing the composition of polymer-solvent-nonsolvent solutions [26].

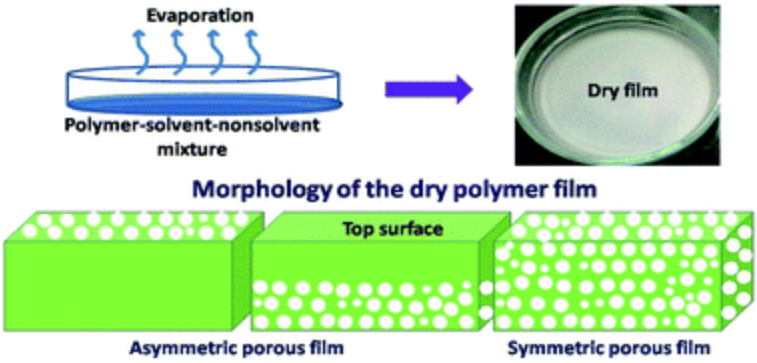

Figure 1.4 Solvent evaporation induced phase separation (Reproduced from Ref [26]- Published by The Royal Society of Chemistry)

Samuel et al. [27] investigated using EIPS to cast polymethylmethacrylate (PMMA) membranes in tetrahydrofuran (THF) solvent with water as the nonsolvent. During the rapid solvent evaporation, condensation of water droplets occurred and formed the porous polymer films. Therefore, water content affected the pore morphology on the membrane surface. The average pore size of the obtained membranes increased along with the water content.

Table 1 summarizes the four phase-separations-based methods including their advantages and disadvantages. It is important to address that while all these phase separations methods convert a dope solution from liquid to solid, most of the phase separation methods are mass transfer processes, while TIPS alone is based on heat transfer. While other processes have significant differences, it is important to differentiate VIPS and EIPS. First, the mechanisms are different, the nonsolvent diffuses into the polymer solution film as vapor in VIPS. In EIPS, originally the solution film is a homogenous polymer/solvent/nonsolvent mixture system, and the solvent evaporation makes the phase separation occurs. Furthermore, the driving force of phase separation in VIPS is the

diffusion of the nonsolvent vapor into the solution film, while for EIPS, the driving force is the solvent diffusing out from the polymer-solvent-nonsolvent liquid film [28].

Table 1.1 Comparison of four phase separation methods [29]

	NIPS [14]	TIPS [21]	VIPS [28, 30]	EIPS [26]
Principle	Mass transfer	Heat transfer	Mass transfer	Mass transfer
Components	Polymer Solvent Nonsolvent	Polymer Solvent	Polymer Solvent Nonsolvent (vapor)	Polymer Solvent Nonsolvent
Advantages	Diverse porous structure, high selectivity, low operation temperature	Easy control, uniform structure, good reproducibility.	Crystallization, Gentle formation process	Good reproducibility
Disadvantages	Many operation parameters, finger-like structures do not have good mechanical strength	High energy consumption; requirements for solvents: low molecular weight, high boiling point, low volatility, high miscibility with polymers, thermal stability.	Many operation parameters, high energy consumption	Difficult to find suitable solvents and nonsolvents used in EIPS

From Table 1 and literature studies, NIPS is able to produce different pore morphology as desired. Also, NIPS is a commonly used method to cast membranes and has been widely employed to fabricate membranes. Therefore, NIPS was chosen in this

dissertation to minimize the variables and focus on investigating greener/less toxic solvents.

1.2.2 Theoretical thermodynamics study

A ternary phase diagram is commonly used to describe the thermodynamic properties of a polymer/solvent/non-solvent system [31-34] , as shown in Figure 1.5 [35]. It can also explain the solvent-nonsolvent exchange phenomena and the kinetics of solvent and nonsolvent exchange during the membrane formation process [34]. The theoretical study of ternary phase diagrams is also used to predict the corresponding binodal curves, spinodal curves and critical points using the calculation methods described in this section [33]. The ternary phase diagram theoretical curves are significant when a new polymer or solvent is to be investigated to fabricate membranes because these curves can quantitatively guide the specific polymeric membrane formation, including the compositions of the polymer/solvent/nonsolvent system, and the prediction of morphology of the membranes.

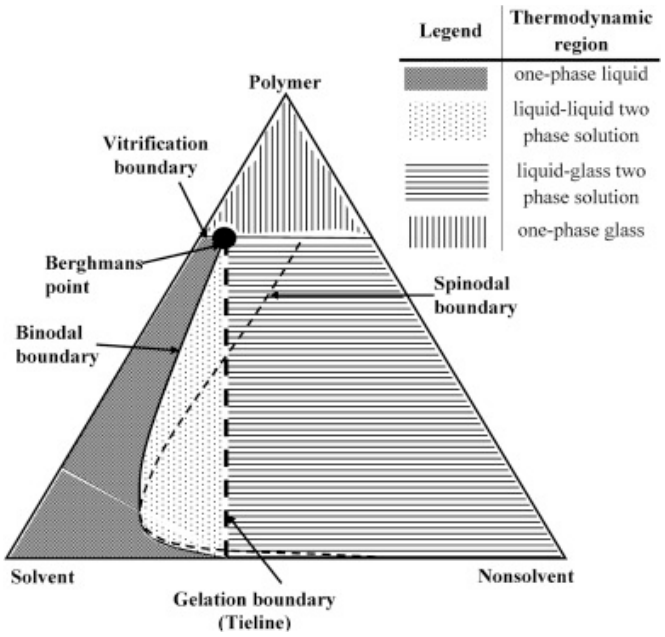

Figure 1.5 A detailed general ternary phase diagram for NIPS process (Reprinted with permission from [35] Copyright © 2015 Elsevier)

To evaluate the thermodynamics of a membrane-forming system, the Flory-Huggins theory of polymer solutions has been extended to the polymer/solvent/nonsolvent ternary system, and is used to predict the binodal curves, spinodal curves and tie lines of the ternary phase diagram in the immersion precipitation process [36]. The Flory-Huggins solution equation represents the Gibbs free energy change (ΔG_m) for mixing a polymer with a solvent[31]. In this theory, the Gibbs free energy (ΔG_m) of the mixing of the membrane casting system is calculated as shown in equation (1):

$$\frac{\Delta G_m}{RT} = n_1 \ln\varphi_1 + n_2 \ln\varphi_2 + n_3 \ln\varphi_3 + g_{12} u_2 n_1 \varphi_2 + g_{13} n_1 \varphi_3 + g_{23} n_2 \varphi_3 \qquad (1)$$

Where subscripts 1, 2 and 3 are respectively nonsolvent, solvent and polymer; while n_i and φ_i are the amount and volume fraction of component i; R is the gas constant and T is temperature; g_{12} is the solvent/nonsolvent parameter, which is assumed to be a function

of u_2 with $u_2 = \varphi_2/(\varphi_1 + \varphi_2)$; g_{13} is the nonsolvent/polymer interaction parameter and g_{23} is the solvent/polymer interaction parameter, which are assumed to be constants. All the interaction parameters are determined through experiments or obtained from literature. The conditions for liquid-liquid equilibrium are as shown in equation (2):

$$\Delta\mu_i^{\alpha} = \Delta\mu_i^{\beta} \qquad (2)$$

Where i represents different components, α and β denote polymer-rich and polymer-lean phases separately. The derivative of the Gibbs free energy of mixing results in the chemical potential of component i, as shown in equation (3):

$$\frac{\Delta\mu_i}{RT} = \frac{\partial}{\partial n_i}\left(\frac{\Delta G_m}{RT}\right)_{P,T,n_j} \qquad (3)$$

For liquid-liquid equilibrium, the conditions can be calculated as equations (4-6):

$$\Delta\frac{\mu_1}{RT} = ln\varphi_1 + 1 - \varphi_1 - \frac{V_1}{V_2}\varphi_2 - \frac{V_1}{V_3}\varphi_3 + [g_{12}u_2\varphi_2 + g_{13}\varphi_3](\varphi_2 + \varphi_3) - \frac{V_1}{V_2}g_{23}\varphi_2\varphi_3 - \varphi_2 u_1 u_2 \frac{dg_{12}u_2}{du_2} \qquad (4)$$

$$\Delta\frac{\mu_2}{RT} = ln\varphi_2 + 1 - \varphi_2 - \frac{V_2}{V_1}\varphi_1 - \frac{V_2}{V_3}\varphi_3 + \left[\frac{V_2}{V_1}g_{12}u_2\varphi_1 + g_{23}\varphi_3\right](\varphi_1 + \varphi_3) - \frac{V_2}{V_1}g_{13}\varphi_1\varphi_3 + \frac{V_2}{V_1}\varphi_1 u_1 u_2 \frac{dg_{12}u_2}{du_2} \qquad (5)$$

$$\Delta\frac{\mu_3}{RT} = ln\varphi_3 + 1 - \varphi_3 - \frac{V_3}{V_1}\varphi_1 - \frac{V_3}{V_2}\varphi_2 + \left[\frac{V_3}{V_1}g_{13}\varphi_1 + \frac{V_3}{V_2}g_{23}\varphi_2\right](\varphi_1 + \varphi_2) - \frac{V_3}{V_1}g_{12}u_2\varphi_1\varphi_2 \qquad (6)$$

Where V_i represents the pure molar volume of species i. Only binary interaction parameters are considered in these equations.

The binodal curve is the boundary between the thermodynamically favorable conditions for the system to be fully mixed and to be phase separated. Every composition inside the binodal curve demixes into a polymer-rich and a polymer-lean phase in thermodynamics equilibrium[32, 34, 37]. The line that connects a pair of equilibrium compositions in the polymer-rich phase ($\varphi_{1,A}$, $\varphi_{2,A}$, $\varphi_{3,A}$) and polymer-lean ($\varphi_{1,B}$, $\varphi_{2,B}$, $\varphi_{3,B}$) phase is a tie line. Thus, there are six unknowns, and the binodal curve should be obtained through determining these six volume fractions. To determine the compositions, a material balance equation is also be needed, as is proposed as equation (7)

$$\sum \varphi_i^I = \sum \varphi_i^{II} = 1 \qquad (7)$$

Where $\varphi_{3,B}$ is considered to be an independent variable in the six unknowns, and then equations (2) and (4)-(7) are solved by the Newton-Raphson method.

The boundary between the unstable and metastable regions is called spinodal, which is defined as equation (8):

$$\frac{\partial^2 \Delta G}{\partial \varphi^2} = 0 \qquad (8)$$

The spinodal curve is evaluated using the Tompa equation, as equations (9) and (10):

$$G_{22} G_{33} = G_{23}^2 \qquad (9)$$

$$G_{ij} = (\partial^2 \overline{\Delta G_m} / \partial \varphi_i \partial \varphi_j)_{v_{ref}} \qquad (10)$$

Where $\overline{\Delta G_m}$ is the Gibbs free energy of mixing on a unit volume basis and v_{ref} is the molar volume of the reference component. For the relationship for $\overline{\Delta G_m}$, the following expressions result as equations (11-13)

$$G_{22} = \frac{1}{\varphi_1} - \frac{V_1}{V_2\varphi_2} - 2g_{12} + 2(u_1 - u_2)\left(\frac{dg_{12}}{du_2}\right) + u_1u_2\left(\frac{d^2g_{12}}{du_2^2}\right) \qquad (11)$$

$$G_{23} = \frac{1}{\varphi_1} - (g_{12} + g_{13}) + g_{23}\frac{v_1}{v_2} + u_2(u_1 - 2u_2)\left(\frac{dg_{12}}{du_2}\right) + u_2^2(1 - u_2)\left(\frac{d^2g_{12}}{du_2^2}\right) \qquad (12)$$

$$G_{22} = \frac{1}{\varphi_1} + \frac{V_1}{V_3\varphi_3} - 2g_{13} - 2u_2^3\left(\frac{dg_{12}}{du_2}\right) + u_2^3(1 - u_2)\left(\frac{d^2g_{12}}{du_2^2}\right) \qquad (13)$$

Choosing φ_3 as the independent variable, equation (9) and the material balance equation (7) are solved numerically using the Newton-Raphson method.

The binodal and spinodal curves intersect at the critical point. It is expressed as equation (14):

$$\frac{\partial^2\Delta G}{\partial\varphi^2} = \frac{\partial^3\Delta G}{\partial\varphi^3} = 0 \qquad (14)$$

The critical point composition is calculated through the following equation (15):

$$G_{222}G_{33}^2 - 3G_{223}G_{23}G_{33} + 3G_{233}G_{23}^2 - G_{22}G_{23}G_{333} = 0 \qquad (15)$$

In this study, the theoretical binodal curves of PolarClean/PSf/water and GVL/PSf/water were calculated using the equations above and then compared with experimental curves. If they corresponded, the calculation method was used to as a standard to employ other green solvents to prepare membranes. If they did not correspond, the reasons causing the differences were analyzed and correction factors were added in the calculation method to improve the accuracy of theoretical curves.

1.2.3 The mechanism of demixing processes

A ternary phase diagram of polymer/solvent/water, as shown in Figure 1.6, is also commonly used to characterize the demixing processes in the phase inversion process. In Figure 1.6, the binodal curve is the liquid-liquid phase boundary, and the line that connects the two points of equilibrium compositions is the tie line, as discussed in section 1.2.2. Any composition point inside the binodal curve demixs into two different composition points, polymer-rich and polymer lean phases, which are in the thermodynamic equilibrium. The composition points outside the binodal curve are in the same liquid phase.

As shown in Figure 1.6 (a), for the instantaneous demixing process, when the liquid film immerses into water, the liquid film demixes immediately into a polymer-rich phase and a polymer-lean phase. For the delayed demixing process, shown in Figure 1.6 (b), after immersion into water, the liquid film remains outside the binodal curve, indicating that no immediate demixing occurred, and the demixing process was relatively slow.

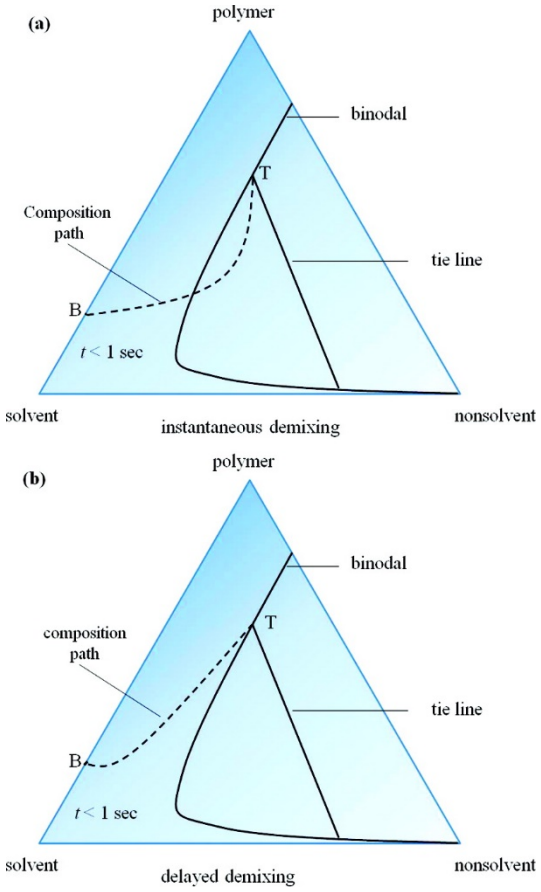

Figure 1.6 Composition paths of liquid film after immediately immersion into nonsolvent bath: (a) instantaneous demixing and (b) delayed demixing: T and B represent the top and the bottom of the film. (Reprinted with permission from [14] Copyright © 2011 American Chemical Society)

Different demixing processes may be due to different factors; for instance, the miscibility of solvent in nonsolvent and the viscosity of the polymer/solvent liquid film [38-41]. Low miscibility of solvent in nonsolvent leads to a delayed demixing process, while high miscibility of solvent in nonsolvent results in an instantaneous demixing process [38, 39]. Similarly, high viscosity of the dope solution may lead to a delayed demixing process, and low viscosity may lead to an instantaneous demixing process [40, 41]. As

shown in Figure 1.7, for an instantaneous demixing process, the solvent/nonsolvent exchange is fast, and finger-like structures form; for a delayed demixing process, the solvent/nonsolvent exchange is slow, which results in spongey-like structures. The mechanism of demixing is used to explain the cross-section morphology in this dissertation. The speed of solvent/nonsolvent exchange was determined using UV-Vis to quantify the diffusion rate of the solvent into nonsolvent, and this method is used in Chapter 6.

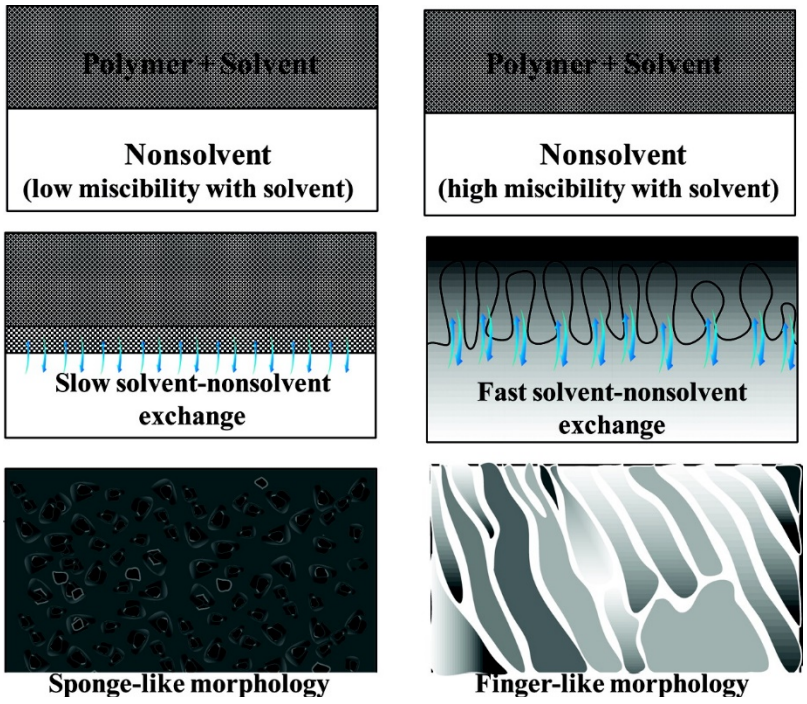

Figure 1.7 Cross sectional morphologies of membranes formed by instantaneous and delayed demixing processes. (Reprinted with permission from [14] Copyright © 2011 American Chemical Society)

1.2.4 Scale up of the membrane fabrication process

Despite extensive research on membrane development and fabrication at the small, laboratory scale [20, 42-46], there is a dearth of studies or reports on scaling up membranes. There is much research activity in laboratories on casting polymeric membranes; however, many of these methods, such as doctor blade casting, spin coating, dip coating, etc., only work in a batch mode and cannot be transferred to large-scale roll-to-roll (R2R) methods [47]. Recently there have been studies on scale-up of plain membranes, using profile roller coating [47] and slot die casting embedded on roll-to-roll (R2R) systems [48, 49]. Slot die

casting is the most prominent method because it is capable of scaling up thin film across a broad array of areas while keeping the functionality of the films [50, 51].

Here, the doctor blade and slot die casting methods are compared as examples of the different fabrication scales. As shown in figure 1.8, in the doctor blade casting process, a dope solution is first placed on a substrate, and the doctor blade is placed at a set height above the substrate. The blade is then moved at a constant velocity to spread the solution onto the substrate to form a film [52].

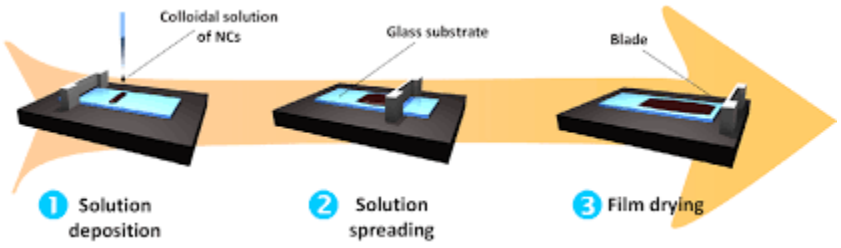

Figure 1.8 The doctor blade coating process (Reproduced from Ref [53]- Published by IOPscience)

In the slot die coating process, a slot die (Figure 1.9 (a) and (b)) is used to deposit a liquid solution onto a substrate that is moving at a constant velocity to form a liquid film on the substrate. The difference between the slot die and doctor blade coating methods is that the slot die is fixed, and the substrate is moving, while for the doctor blade, the substrate is fixed, and the doctor blade is moving.

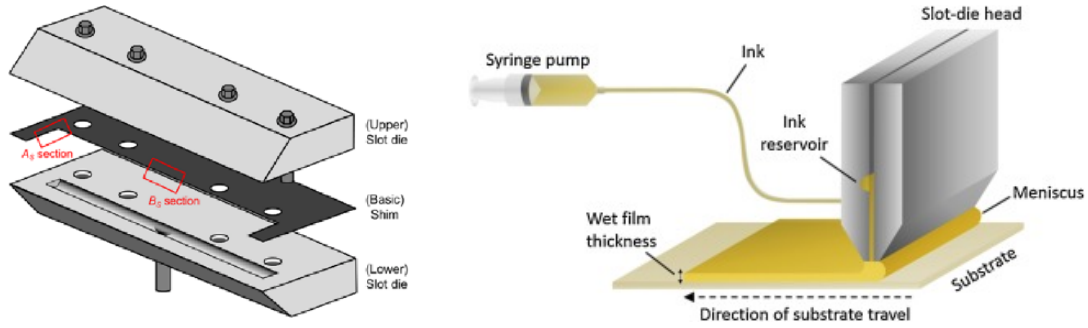

(a) *(b)*

Figure 1.9 The slot die coating process: (a) the slot die head structure (Reprinted with permission from [54] copyright ©2016 Springer Nature); (b) the schematic of slot die coating process (Reprinted with permission from [55] copyright ©2020 Elsevier)

1.2.4.1 Comparison of doctor blade casting and slot die casting of membranes

Doctor blade casting has been a popular primary film casting method in the laboratory [56, 57], but it is not always the best method to fabricate membranes on an industrial scale because the membrane morphology is largely reliant on the viscosity of the dope solutions, and therefore, not suitable for continuous casting [48]. On the other hand, slot die casting is a well-developed and commonly used method to manufacture polymer films. It is suitable for continuous casting of liquid films and, therefore, has been investigated to scale up polymeric membranes [49]. There is a constant demand to increase the processing speed of the thin film since the processing speed can increase the production output. At the same time, there is also a constant demand for maintaining low thicknesses of the film considering its applications in coating and polymer industry [48]. However, if these two key factors are not balanced, the polymer film quality cannot be maintained

properly. Film quality is dependent upon several factors, such as the solution properties, fabrication process and processing parameters, and defects arise when these factors are altered [48, 49].

Scaling up from a small production scale, such as doctor blade, to a larger one, such as slot die, is not intuitively obvious, and several parameters must be identified in order to determine dope flow rate and substrate velocity. One such parameter is the surface tension of the polymer since coating speed depends on surface tension values, and solutions with lower surface tension can restrict the coating speeds to lower values [48]. Another key parameter is viscosity, which plays a significant role in determining the processing conditions because fabrication defects, such as air bubble entrapment, highly depends on the solution viscosity [49]. Air entrainment rate is lower at lower solution viscosities [48].

1.2.4.2 Advantage of Slot Die Casting for Scale Up

Often laboratory methods, such as doctor blade casting, spin coating and solution casting, are not scalable and/or do not introduce the same stress on the membrane as those formed using scalable approaches e.g., slot die casting. Furthermore, different manufacturing techniques may lead to significantly different membrane properties (e.g. mechanical, chemical, etc.), particle distribution, overall membrane functionality, and its ability to treat water.

Integration of slot die casting into a R2R system allows for continuous casting of polymeric membranes. An illustration of a simple R2R system is shown in Figure 1.10, which has been used to study scale up of AgNP membranes previously [58].

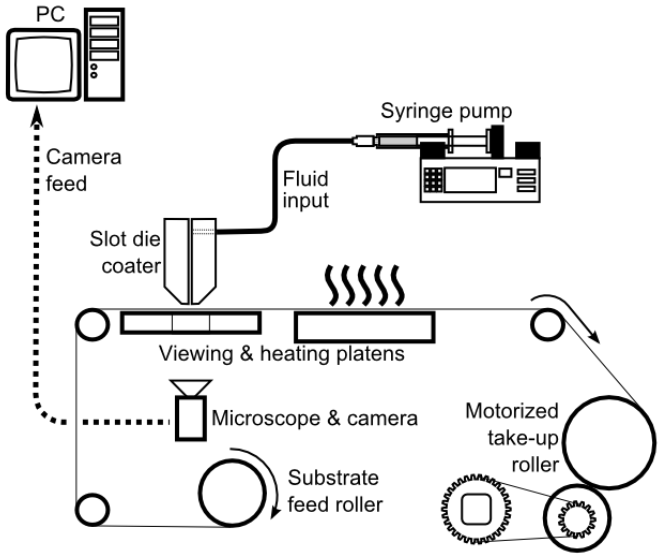

Figure 1.10 Schematic of a simple R2R experimental setup with a slot die coater (Reprinted with permission from [57] copyright ©2020 John Wiley and Sons)

The slot die coating process consists of pumping a dope solution at a preset flow rate between two die halves set apart by a small gap onto a substrate moving with a relative velocity to the dies, as depicted in Figure 1.11.

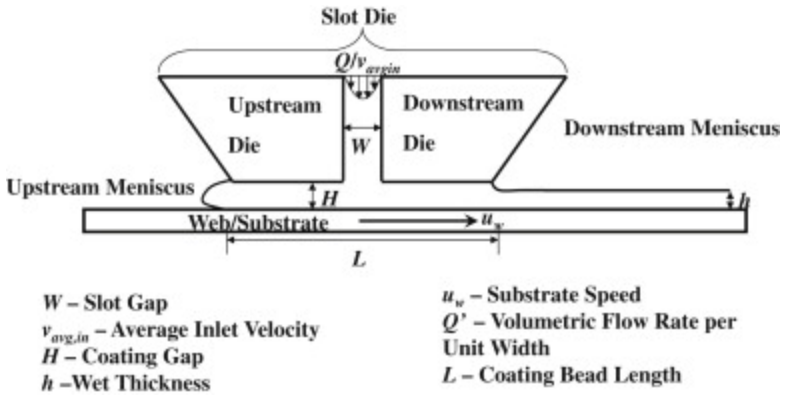

Figure 1.11 Schematic of the lower section of a slot die coater with key parameters identified (Reprinted with permission from [49] copyright ©2013 Elsevier)

The slot die process offers the advantage of controlled coating thickness (h) as it is only a function of specific process parameters, the pre-metered flow rate of solution per unit die (Q') and substrate speed (u_w) [48]. That is, $h = Q'/u_w$. Other process parameters such as the slot gap width (W) and the coating gap height (H) can affect the quality of the film as cast, with defects being introduced into the film if the process is not properly controlled. The space of process parameters in which defect-free casting can occur for a given coating fluid is called the casting/coating window [59]. A graphical representation of this space as a function of the volumetric flow rate and the substrate speed during the coating process and the associated defects seen at the boundaries is shown in Figure 1.12.

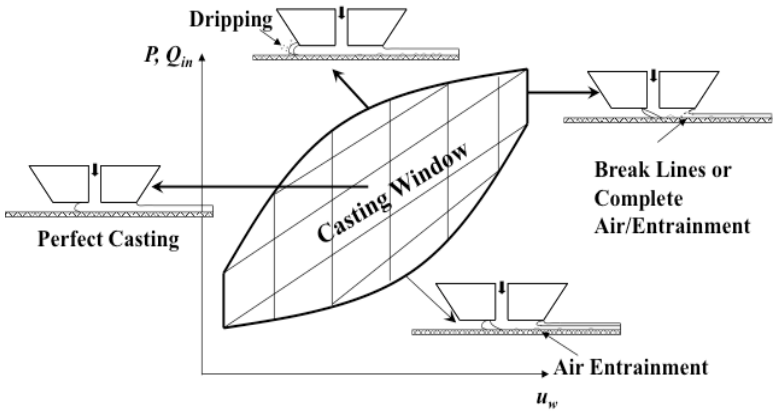

Figure 1.12 Schematic of a generic casting window to illustrate the upper and lower boundaries of a slot die casting process before the onset of defects. (Reprinted with permission from [49] copyright ©2013 Elsevier)

1.2.5 Materials used in NIPS method

This dissertation focuses on the NIPS method using doctor blade casting for membrane development and later on slot die-R2R systems for scale up. Materials involved in these fabrication methods include polymers, solvents, nonsolvents and additives. Additives, such as polyvinylpyrrolidone (PVP) [60, 61], polyethylene glycol (PEG) [62, 63], propionic acid (PA) [64], and LiCl [65, 66], have been used to enhance the selectivity and/or mechanical strength of polymeric membranes [67-69]. However, this makes the analysis of polymer-solvent-nonsolvent systems significantly more complicated; therefore, only polymers and solvents are discussed here.

1.2.5.1 Polymers

Polymers play an important role as the backbone in the membrane matrix. Specifically, multiple polymers have been investigated in membrane fabrication including

conventional polymers such cellulose acetate (CA), polysulfone (PSf), polyethersulfone (PES), polyvinylidene fluoride (PVDF), and some sustainable polymers.

CA is one of the most common polymers employed to fabricate membranes and has been widely researched. CA can be used to prepare microfiltration (MF) [70], ultrafiltration (UF) [71, 72], nanofiltration (NF) [73], and reverse osmosis (RO) [74] membranes, and it is usually used as a material for the application of dialysis [75]. However, CA has several disadvantages, such as low chemical and thermal resistance and mechanical strength [14]. Addition of additives or surface modification are often needed to improve the properties of CA membranes [71, 76, 77].

PSf is another common polymer used in membrane fabrication. The popularity of PSf is not only because it is commercially available, but also easy to process. Compared to CA, PSf provides a portfolio of better thermal and chemical resistance, and better mechanical strength [14]. PES is similar to PSf structurally, with good chemical and thermal stability [78]. The ether groups make it easier to perform chemical modifications on PES than PSf [78-80].

Lastly, PVDF exhibits high chemical and thermal resistance and mechanical strength, but it is also hydrophobic [81]. The hydrophobicity of PVDF makes it possible to be used in membrane distillation [82, 83]. Moreover, in order for the membranes to be used in water treatment, surface modification is necessary to increase the hydrophilicity of membranes [84].

Besides these conventional petroleum-derived polymers, much research has been performed on sustainable polymers; for example, celluloses [85], poly(lactic acid) (PLA)

[86], bamboo fiber, chitosan, and others. Sustainable polymers have been investigated to minimize the use of petroleum-derived polymers to meet the requirements of membranes [87-89]. These polymers are derived from natural products, which significantly decrease the carbon footprint of the manufacturing process [90].

Chitosan is a polysaccharide, a polymer derived from the deacetylation of chitin [91, 92]. It has numerous advantages such as being commercially available, environmentally friendly, and having good chemical and thermal stability, biodegradability, and mechanical strength. However, looking for a solvent that can dissolve chitosan might be challenging [93-96]. Acetic acid is usually used to decrease the pH of a chitosan solution and then enable the solubility of chitosan in solution [97, 98]; however, it is a hazardous solvent [98, 99]. Cui et al. [100] used an ionic liquid (IL), 1-ethyl-3-methylimidazolium acetate ([EMIM]AC), to dissolve chitosan and then prepare membranes. The obtained membranes had a smooth surface without curling, and a strong tensile strength of up to 24 Mpa, proving that ILs have the potential to be used as alternatives to acetic acid to cast chitosan membranes.

Phuong et al. [101] investigated the use of PLA and bamboo fibers as membrane support materials. PLA is a polyester derived from biomass, and it is biodegradable. However, the low thermal stability and low mechanical strength restricted the use of PLA. Bamboo fiber was then introduced to increase the mechanical stability of the PLA matrix. PLA/bamboo matrix was then investigated as a membrane support. With an optimized recipe, the membrane support matrix was found to provide comparable tensile strengthen to that of a commercial membrane support as well as higher water permeance.

1.2.5.2 Solvents

In NIPS, solvents play an essential role in shaping the morphology of obtained membranes and even affecting properties and performance of the membranes [14]. During membrane fabrication, large amounts of traditional organic solvents are used [1]. Solvents used in synthesis steps can have a negative impact on operational safety, cost, the environment and human health [2-4]. Traditional solvents used for membrane preparation include dimethylformamide (DMF), N-methyl-2-pyrrolidone (NMP), dimethylacetamide (DMAc), dimethyl sulfoxide (DMSO), and tetrahydrofuran (THF). Some of these solvents are volatile and hazardous to the environment or living cells. [102] Solvents, such as cyclohexanes, DMAc, and DMSO are mutagenic and tumorigenic; acetone is highly flammable; and NMP is an irritant [102, 103]. Acute effects of DMF include skin irritation and dizziness, while its long-term effects are known to cause birth defects [104]. Due to their hazard, solvents require specialized control measures. In addition to the high toxicity of the solvents used during polymeric membrane fabrication processes [1], energy consumption to remove or recycle solvents from the water is significant [105].

While petroleum-derived solvents have been traditionally used in membrane fabrication, greener/low toxicity solvents are starting to attract attention due to decreased impacts on human health and the environment from their use [1]. The annual global solvent market is in the order of 20 million metric tons and billions of dollars, and bio-based solvents consumption in Europe has been predicted to grow to one million metric tons by 2020 [5, 6]. Using renewable solvents derived from biomass, which do not compete with food applications, satisfies both consumer and legislative demands with regards to sustainability. As Europe moves towards a more bio-derived manufacturing base, the

opportunities for new and bio-derived low hazardous solvents are only expected to increase worldwide. Recently, low hazardous solvents have been investigated for membrane fabrication, and these include but are not limited to methyl lactate, triethylphosphate, ionic liquids, PolarClean, γ-valerolactone, and others.

1.2.5.2.1 METHYL LACTATE

Methyl lactate is biodegradable, versatile, and has the potential to dissolve CA powders leading to a homogeneous dope solution [7]. Gonzalez et al. [7] produced a membrane polymer dope solution using CA and methyl lactate by phase inversion. Resulting membranes were defect-free, ultrafiltration range, and pressure resistant. The membranes prepared with methyl lactate followed a green process. Alqaheem et al. [106] investigated methyl lactate to fabricate polyetherimide (PEI) membranes based on the fact that the Hansen solubility parameter showed that methyl lactate had the potential to dissolve PEI but methyl lactate did not dissolve PEI in their experiments. Membranes prepared with methyl lactate have been found not to be homogeneous, to have micro-voids appearing on the surface, and their water permeability has been observed to vary significantly [7]. Another disadvantage of methyl lactate is that it cannot dissolve a broad spectrum of polymers.

1.2.5.2.2 TRIETHYLPHOSPHATE (TEP)

TEP is an industrial catalyst and an intermediate product in the manufacturing of pesticides and other chemicals. TEP may serve as the substitute for traditional toxic solvents, considering its low toxicity, high acid resistance, and good thermal stability [107]. Wang et al. [108] prepared polyvinylidenedifluoride (PVDF) flat-sheet membrane

and a hollow-fiber membrane using TEP as a solvent. Their studies suggested that when TEP was used as a solvent for copolymer blends, it led to delayed phase separation and as a result, sponge-like void membranes were formed. Sponge-like membranes result in low flux compared to finger-like membranes. Tao et al. [109] fabricated PVDF membranes using four different solvents, dimethylformamide (DMF), trimethylphosphate (TMP), hexamethylphosphoramide (HMPA), and TEP by phase inversion and evaluated the resulting membrane performance. They observed that the membranes prepared using TEP showed the lowest flux decline, highest pure water, and lowest rejection of proteins as compared to other membranes. This was mainly due to the larger pore size and less compaction of PVDF/TEP membranes as compared to other membranes. They suggest that PVDF membranes prepared using TEP have potential to become successful microfiltration membranes; however, the mechanical strength of the PVDF/TEP membrane was poor, which limited the use of TEP. Chang et al. [42] also employed TEP to fabricate PVDF hollow fiber membranes for membrane distillation. Without additives, the membranes processed a flux of 20 kg/m^{2}h at 60 °C with the rejection of NaCl as 99.99%; however, the mechanical strength of the membrane was compromised and to improve it, TEP had to be introduced in the coagulation bath, which increased the amount of TEP used. Karkhanechi et al. [110] investigated TEP to prepare polyvinylidenedifluoride-co-chlorotrifluoroethylene (PVDF-co-CTFE) hollow-fiber membranes and compared them to NMP. The trinary phase diagram and rheological properties were studied. The results showed that it was easier for phase separation to occur with the TEP system than with the NMP system and that the viscosity of the TEP system increased dramatically when water was added into the system.

However, the disposal of TEP/water mixtures may increase the concentration of phosphorus in receiving bodies of water, which can lead to the eutrophication in rivers and lakes [1]. Eutrophication can stimulate algae growth, which may lead to toxic algal blooms, such as red tides and brown tides, and can devastate the habitat for aquatic animals and plants [111-113].

1.2.5.2.3 IONIC LIQUIDS (ILS)

Ionic liquids are types of organic salts, which consist of an organic cation and a polyatomic inorganic anion. The cation can be imidazolium or pyridinium, whereas the anion can be a halogen, triflate, or trifluoroborate. Ionic liquids are widely used to replace environmentally toxic organic solvents [7, 114-116]. Their vapor pressure is often negligible [117]. It should be noted that some ILs (for example, [EMIM][BF_4] and [BMIM][PF_6]) have been synthesized with a measurable vapor pressure [118, 119]. Moreover, the adequate selection of the organic cation and inorganic anion can change the physical and chemical properties of ILs, such as melting point, density, and viscosity, to meet different requirements. Another advantage is that ILs are nonflammable and have high thermal stability. Ionic liquids have been used in preparation of supported IL membranes, which use a porous solid polymer or ceramic membrane to support the liquid membrane phase [94].

Chichowska-Kopczynska et al. [120] used imidazolium ILs with alkyl fluoride anions in CO_2 separation. They found that the supported IL membranes were stable, and the increase of alkyl chain length would lead to the decrease in permeation values of CO_2. If a trifluoromethanesulfonate anion was used in CO_2 separation, the solubility of CO_2

could be lower. Supported IL membranes can also be used in hollow fibers. Xing et al. [121] used 1-butyl-3-methylimidazolium thiocyanate ([BMIM][SCN]) to prepare flat-sheet and hollow-fiber CA membranes and compared them to membranes prepared using traditional NMP and acetone solvents. The membranes prepared by IL showed a denser structure. The group also showed that the IL could be recycled and reused to make membranes. Xing et al. [122] used 1-ethyl-3-methylimidazolium thiocyanate ([EMIM]SCN) and 1-ethyl-3-methylimidazolium acetate ([EMIM]OAc) to fabricate CA hollow-fiber membranes. [EMIM]OAc interacted with CA more than [EMIM]SCN, and the CA/[EMIM]OAc dope solution presented a more highly entangled network than the CA/[EMIM]SCN dope solution. Therefore, the CA/[EMIM]OAc system was more practical to fabricate CA membranes. Colburn et al. [123] also investigated [EMIM]OAc to fabricate cellulose/graphene quantum dots (GQD) membranes. Cellulose is difficult to dissolve in common solvents but has the potential to be dissolved in this IL. Within the IL, GQDs were incorporated homogeneously into the cellulose membranes and improved the membranes performance on the perspectives of photoactivity and sensing. However, the viscosity of dope solutions significantly increased, which has the potential to lead to deficits on the surface of the membranes during the phase inversion process.

However, the synthesis of ILs is neither clean nor energy-efficient; hence, the cost of using ILs could be high [114]. The toxicities of ILs may vary significantly across organisms and tropic levels [114, 124-127]. Furthermore, the biodegradability of ILs is slow [124]. Considering these perspectives, ILs are adequate but they are not “green” substitutes for conventional solvents.

1.2.5.2.4 Rhodiasolv® PolarClean

PolarClean is a water-soluble, eco-friendly, and biodegradable polar solvent with no reported health hazards when used for the casting PVDF membranes [128, 129]. It is a green solvent commercialized by Solvay Novecare, and it is derived from the valorization of 2-methylglutaronitrile (MGN), which is a byproduct from the synthesis of Nylon 6,6 [130, 131]. The production of PolarClean can reduce the carbon footprint and minimize the environmental impact [130]. Hassankiadeh et al. [128] used PolarClean to fabricate PVDF hollow-fiber membranes via TIPS. However, in the PVDF/PolarClean system, the rate of PolarClean outflow was observed to be higher than the rate of water inflow, and this difference resulted in dense hollow-fiber membranes with low-water permeability. Due to PolarClean's high miscibility with water, Jung et al. [129] further investigated its NIPS effect on the membrane surface during the TIPS process, along with the kinetics of the membrane formation process. In this study, over-dense top layers were also reported, and required a pore-former, such as Pluronic F-127, to improve water permeability at the expense of mechanical properties.

1.2.5.2.5 Gamma-valerolactone

Gamma-valerolactone (GVL) is a 5-carbon cyclic ester with 5 atoms in the ring. It is water-soluble and can be bio-derived from lignocellulosic biomass, specifically from hemicellulose and cellulose, according to the process shown in Figure 1.13 [132]. Briefly, hemicellulose is converted to furfural and furfural alcohol as intermediates by acid hydrolysis, and then furfural alcohol is esterified with ethanol to produce ethyl levulinate [132-134]. Cellulose is converted to hydroxymethylfurfural (HMF) as an intermediate

and then converted to levulinic acid also through acid hydrolysis [133, 135]. Both of ethyl levulinate and levulinic acid are hydrogenated to GVL [132]. Rasool et al [136] prepared membranes using GVL using a variety of different polymers, most notably CA and cellulose triacetate (CTA). Specifically, 15% CA/GVL and 10% CTA/GVL dopes were used to cast nanofiltration (NF) that rejected 90% Rhodamine B, at permeances of 1.8 $Lm^{-2}h^{-1}bar^{-1}$ (LMH/bar) and 11.7 LMH/bar, respectively.

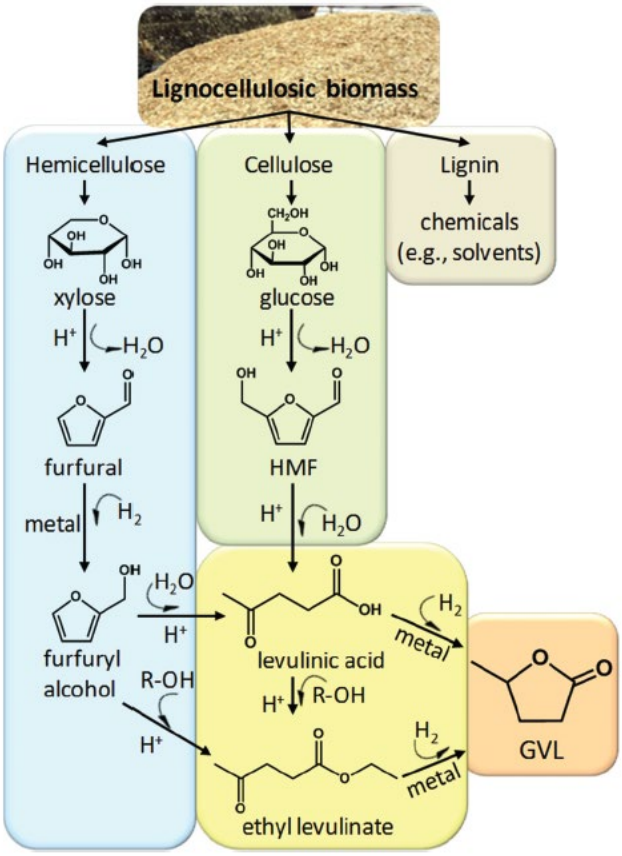

Figure 1.13 Lignocellulosic biomass and reaction pathways to produce GVL (Reprinted with permission from [132] copyright ©2013 The Royal Society of Chemistry)

1.3 Hypotheses and Objectives

The overarching goal of this dissertation was to investigate PolarClean and GVL as sole solvents and as solvent mixtures to replace a traditional petroleum-derived solvent, DMAc, in the fabrication of PSf membranes, along with the ability of scaling up these membranes. Based on the goal of replacing traditional petroleum-derived solvents with greener alternatives, the four hypotheses of this study were developed as follows

- The first hypothesis was that because of the similar chemical structures between PolarClean and DMAc, PolarClean would be able to be used as a replacement of DMAc to fabricate polymeric membranes using NIPS.
- The second hypothesis was that based on the similarity of chemical structures between γ-Valerolactone (GVL) and NMP, a cellulosic biomass derived solvent, GVL would be able to replace NMP to fabricate polymeric membranes using NIPS.
- The third hypothesis built on the fact that based on the Hansen solubility parameter model, the dispersive force, the polar force and the hydrogen bonding of the cosolvent mixture fell in between those of the individual solvents, and were closer to the solubility parameters of PSf; thus, making the cosolvent mixture more suitable to fabricate polymeric membranes using NIPS.
- The fourth hypothesis was that due to the Newtonian fluid behavior of dope solutions prepared using the greener solvents, the membranes developed using a laboratory-scale doctor blade could be scaled up using slot die-R2R.

To test these hypotheses, the following objectives were identified

- Objective 1: The thermodynamics of mixing and demixing using PolarClean to fabricate polysulfone membranes in a NIPS process as compared to DMAc were investigated experimentally and theoretically. (Chapter 3)
- Objective 2: PSf membranes were fabricated using PolarClean and characterized in terms of their morphology, porosity, water permeability and protein rejection, and compared to membranes prepared with DMAc. (Chapter 3)

- Objective 3: The thermodynamics of mixing and demixing using PolarClean and GVL as sole solvents and as a solvent mixture (or co-solvents) to fabricate polysulfone membranes in a NIPS process as compared to DMAc were investigated experimentally and theoretically. (Chapter 4 and Chapter 5)
- Objective 4: PSf membranes were fabricated using PolarClean and GVL as sole solvents and solvent mixtures and characterized in terms of their morphology, porosity, water permeability and protein rejection, and compared to membranes prepared with DMAc. (Chapter 4 and Chapter 5)
- Objective 5: Using dope solution viscosity, the kinetic of dope solution mixing process was quantified and used to characterize the homogeneity of dope solutions. (Chapter 5)
- Objective 6: The scaling up of PSf membranes prepared using PolarClean and GVL as sole solvents and cosolvents along with DMAc via slot die-R2R systems was investigated, and then the structural, morphological and operational properties of the membranes were determined. (Chapter 6)

CHAPTER 2. OVERVIEW OF GENERAL METHODS

2.1 Membrane preparation

2.1.1 Choice of solvents

The choice of solvent–nonsolvent system in NIPS membrane formation is crucial because it influences the morphology, mechanical properties, interfacial characteristics, and separation performance [14]. Several properties, including molecular weight, flash point, boiling point, and solubility in water, should be considered when choosing a NIPS solvent [1, 3, 7, 14, 137-139]. Toxicity is also a factor considered herein. The main properties of NMP, DMAc, GVL, and PolarClean are listed in Table 2 [131, 132, 140].

Table 2.1 Main properties of selected solvents

Property	NMP	DMAc	PolarClean	GVL
CAS no.	872-50-4	127-19-5	1174627-68-9	108-29-2
Formula	C5H9NO	C4H9NO	C9H17NO3	C5H8O2
MW (g/mol)	99.133	87.122	187.239	100.112
Density (g/mL)	1.03	0.94	1.043	1.05
Flash point (°C)	95	69	144–146	96
Boiling point (°C)	202	165	278–282	207–208
Solubility in water (%)	Miscible	Miscible	Miscible	Miscible
Signal	Danger	Danger	Warning	Warning
Toxicity	Reproductive toxicity	Reproductive toxicity		

2.1.2 Hansen solubility parameter

Based on the Hansen solubility parameter theory, the affinity of a polymer and a solvent is described as R_a, which is calculated by equation 1:

$$R_a = \sqrt{4(\delta_{d2}-\delta_{d1})^2 + \left(\delta_{p2}-\delta_{p1}\right)^2 + (\delta_{h2}-\delta_{h1})^2} \quad (1)$$

Where δ_d is the dispersive force, δ_p is the polar force, and δ_h is hydrogen bonding [141]. A solvent is deemed to have good compatibility with a polymer when the value of R_a is small [136, 141]. In this study, PSf was dissolved using two co-solvents simultaneously (i.e., a binary solvent mixture) instead of a single solvent. Therefore, the corresponding parameters of the binary solvent mixture needed to be calculated by the two following procedures: first, the volume fraction of each solvent was calculated by equations 2 and 3; second, the values of solubility parameters were then calculated using equation 4, 5, and 6 [141]:

$$V_1 = \frac{W_1/\rho_1}{W_1/\rho_1+W_2/\rho_2} \quad (2)$$

$$V_2 = \frac{W_2/\rho_2}{W_1/\rho_1+W_2/\rho_2} \quad (3)$$

$$\delta_d = V_1\delta_{d1} + V_2\delta_{d2} \quad (4)$$

$$\delta_p = V_1\delta_{p1} + V_2\delta_{p2} \quad (5)$$

$$\delta_h = V_1\delta_{h1} + V_2\delta_{h2} \quad (6)$$

Where 1, 2 represents solvent 1 and solvent 2; V_i represents the volume fraction, and W_i represents the weight fraction.

2.1.3 Relative energy difference

In Hansen solubility parameter theory, three parameters of a polymer or solvent form a sphere [141]. The relative energy difference (RED) is used to describe the interaction between a polymer and a solvent [45]. A good solvent for a polymer is defined as having a RED value less than or equal to 1, which can be calculated by equation 7 [20, 141]:

$$\mathrm{RED} = \frac{R_a}{R_0} \qquad (7)$$

Where R_o represents the radius of the Hansen solubility parameter sphere for the polymer.

2.1.4 Preparation of dope solutions

Dope solutions were prepared using a sonicator (Elmasonic P70H, from Elma Electronic Inc., Munich, Germany) and a planetary centrifugal mixer (Mazerustar KK-250S, from Kurabo Industries Ltd., Osaka, Japan). The dope solutions were sonicated at 65 °C at a frequency of 80 kHz and power of 900 W under pulse mode for 24 h to accelerate the mixing process, allowed to return to room temperature, and then mixed in the planetary mixer for 10 min. The process was repeated until the solutions became homogenous. After storing in room temperature for three months, the dope solutions did not turn cloudy, which indicated that no separations occurred during this period and the solutions remained homogenous.

2.1.5 Membrane fabrication

2.1.5.1 Doctor blade

To study the scale up of the membranes prepared using low-hazardous solvents, an aluminum doctor blade (AP-G10/10, Paul N. Gardner company, Florida, United States) is used to cast membranes in laboratory scale and an aluminum slot die is used to fabricate the membranes in a production scale, to understand the viability of scaling up the fabrication process. When the doctor blade method is used, the gap between the blade and the glass plate is set at 200 μm.

2.1.5.2 Slot die method

In the slot die casting method, the slot gap is set at 90 μm, and the coating gap is set at 200 μm above the glass plate substrate, which is placed on top of the poly(ethylene terephthalate) (PET) film. The PET film is the moving conveyor that is pulled at a speed of 1.3 mm/s from a feed roller to the take-up roller. A syringe pump is used to set the flow rate of the dope solution dispensed from the slot die to fabricate defect free membranes. All casting is performed at 25 ˚C and 48% humidity.

The glass substrates are cleaned with DI water and are then rinsed using isopropyl alcohol to guarantee no residual water on the surface before casting. After casting, the liquid films are inversed into a solid film via the NIPS method. Membranes pieces are then cast in the shape of 305×100 mm×mm (length×width).

2.2 Membrane characterization methods

2.2.1 Morphology

Flat sheet membranes, prepared using the phase inversion method, were immersed and fractured in liquid nitrogen and then sputtered with palladium. The top layers and the

cross sections of the PSf membranes were sampled by focused ion beam (FIB) and then observed by SEM (FIB-SEM, FEI Helios Nanolab 660 from Thermo Fisher Scientific, Waltham, MA, USA). FIB is an advanced method to sample preparation prior to SEM imaging to characterize the morphology of membranes [142]. FIB-SEM provides a more effective method to observe the cross sections of membranes as compared to the common SEM [143]. Moreover, the higher quality of FIB-SEM images shows the internal structure of polymeric membranes and shows the distribution of pores. FIB-SEM images showed the detailed images at scales of 5 nm. In order to observe the entire morphology of cross sections, the PSf membranes were observed by SEM (SEM, Hitachi S-4300 from Hitachi Group, Troy, MI, USA).

2.2.2 Contact Angle

The contact angle was characterized to represent hydrophilicity of the membranes. It was measured by the sessile drop method using a drop shape analyzer connected to a high definition camera (DSA 100S, Kruss Company, Hamburg, Germany.) One drop water of 12 μL was deposited on the membrane surface. The interface between the water drop and the membrane surface was captured by the camera and the contact angle was calculated according to the image. The measurement was repeated six times and then the average values and deviations were calculated.

2.2.3 Roughness

The topography of membranes is measured at the atomic scale to characterize the roughness on the membranes surface. The surface roughness values of the six membranes were measured using an atomic force microscope (AFM, Quesant Instrument Co., United

States). The surface roughness was measured under the tapping mode and then evaluated by root-mean-squared (RMS) roughness. Six areas of 20 × 20 μm on each membrane surface were randomly chose and measured.

2.2.4 Surface pore analysis

The pore size on the selective layer of a membrane is used to estimate the selectivity of a membrane based on size exclusion. The surface pores of membranes were measured using a Liquid-Liquid porometer (LLP-11000A, Porous Materials Incorporated, Ithaca, New York, United States). Two immiscible wetting liquids, silwick (purchased from PMI, Ithaca, New York, United States) and isopropyl alcohol (IPA, purchased from VWR international), were used for the measurement. The membranes were wetted with silwick for ten minutes, and IPA was pressurized to displace the silwick in the membrane pores. The pressure was increased gradually from 0 kPa to 5400 kPa. The silwick was forced to flow through the pores and the amount was measured using a balance equipped in the porometer. The mean flow pore diameter and bubble point pore diameter were used to represent the mean value of pore size and the largest pore on the membrane surface.

2.2.5 Porosity and MWCO

The porosity (Pr, %) of PSf membranes were tested using differences in membrane weight [144-146]. Due to the hydrophobicity of PSf, water was not used in this measurement. Membranes were first wet by silwick (from Porous Materials Inc., Ithaca, NY, USA), then isopropyl alcohol (IPA, ≥99.7%, FCC, FG, from Sigma-Aldrich, St. Louis, MI, USA) was filtered through the membranes under 2 bars for 10 min [146]. The membranes with IPA were exposed to clean and dry air for three days. The wet and dried

state weights of membranes at the equilibrium were collected separately [144-147]. Then the porosity was calculated using the Equation (8):

$$Pr = V_{sil}/V_{total} = (W_{sil}/\rho_{sil})/(W_{sil}/\rho_{sil} + W_{PSf}/\rho_{PSf}) \quad (8)$$

where W_{sil} and W_{PSf} are the weights of the silwick and PSf membranes; ρ_{sil} is the density of the silwick, 0.93 g/mL and ρ_{PSf} is the density of PSf, 1.24 g/mL [146, 148, 149].

Molecular weight cut off (MWCO) represents the lowest molecular weight of solute which could be 90% rejected by the membrane [150, 151]. Polyethylene glycol (PEG) with molecular weight from 200, 400, 1 k, 4 k, 10 k, 20 k, 40 kDa were used as feed to determine MWCO values for the different membranes. Since PEGs are linear polymers, the regression model of hydrodynamic radius (nm) and molecular weight (kDa) is given by Equation (9) [152]:

$$r_H = 0.06127(MW)^{0.3931} \quad (9)$$

Table 2 shows the corresponding hydrodynamic radius (nm) to tested molecular weights of PEGs calculated using Equation (9).

Table 2.2 Molecular weights and hydrodynamic radius of PEG used in MWCO study.

Molecular Weight (kDa)	Hydrodynamic Radius (nm)
PEG 200	0.49
PEG 400	0.65
PEG 1000	0.93
PEG 4000	1.60
PEG 10,000	2.29
PEG 20,000	3.01
PEG 40,000	3.95

2.2.6 FTIR

Attenuated total reflectance-Fourier transform infrared spectroscopy (ATR-FTIR, Thermo Nicolet iS50 FTIR Spectrometer, Thermo Scientific, Waltham, Massachusetts, USA) was performed to characterize the surface structure of membranes prepared using different solvents. A piece of each PSf membrane was freeze dried overnight and then placed on ATR-FTIR crystal (diamond) for analysis. The absorbance spectra of different membranes were normalized[153-156] and then adjusted in the same figure for comparison.

2.2.7 Filtration Studies

2.2.7.1 Dead-end filtration

Water permeation experiments were carried out at a constant pressure of 4 bars in an Amicon dead-end filtration cell (Amicon Stirred Cell 8010-10 mL from Millipore Sigma Company, Burlington, MA, USA). The pure water flux was measured using deionized water until the water flux became constant, which is called precompaction. In this study, all the precompaction were performed by filtering 20 mL DI water at a constant pressure of 4 bars for consistency. After precompaction, 20 mL of solutions containing 1000 mg/L BSA; that is, 20 mg of BSA, were filtered through the membranes at a constant pressure of 4 bars and room temperature. BSA has a molecular weight of 66.5 kDa, is hydrophobic, and its isoelectric point is 4.7, which means it is negatively charged at neutral pH values. The permeability was recorded for every 2-mL filtration period, and permeate samples were collected to analyze the concentrations of BSA in the feed and permeate using a Fusion UV/Persulfate TOC analyzer (14-9600-100 from Teledyne Tekmar Company, Mason, OH, USA). All experiments were performed in triplicate.

After BSA filtration, reverse flow filtration using deionized water was performed at a constant pressure of 2 bars for 30 min to remove foulants that were not adsorbed to the membrane (i.e., reversibly attached), and then flux recovery ratio (Re, %) was measured. The recovery ratio is related to the resistance of the fouled membrane.

2.2.7.2 Crossflow filtration

Filtration performance of membranes is characterized by using a crossflow apparatus Sterlitech HP4750 stirred cell (Kent, Washington, USA) to perform convective studies.

The crossflow filtration cell is run at a flowrate of 1.2 L/min through the precompaction stage, fouling stage and tangential washing stage. DI water permeability is determined for each membrane by precompacting at 6.9 bar overnight and then measuring the volumetric flux of deionized ultrafiltered (DIUF) water at 1.4, 2.8, 4.1, 5.5, 6.9 bar, respectively. The linear correlations of membranes are analyzed accordingly. 50 mg/L BSA solution is then filtered through the membranes to investigate long-term filtration. At the fouling stage, the initial flux is measured. When the flux reached 70% of the initial value, the membrane surface is tangentially rinsed with DI water for 10 min. This process is repeated until the flux reaches 35% of the initial flux, and the overall filtration time is recorded. Then BSA solution is used to filter through the membrane again. This process is repeated three times. The permeate is collected and the BSA samples for the feed and permeate are analyzed using a VWR UV-6300PC Spectrophotometer (Radnor, Pennsylvania, USA). The flux linearity study and the BSA filtration are duplicated for reproducibility.

CHAPTER 3. INVESTIGATION OF THE USE OF A BIO-DERIVED SOLVENT FOR NON-SOLVENT-INDUCED PHASE SEPARATION (NIPS) FABRICATION OF POLYSULFONE MEMBRANES

This chapter has been published in the following report on an open access journal:

Dong, X.; Al-Jumaily, A.; Escobar, I.C. Investigation of the Use of a Bio-Derived Solvent for Non-Solvent-Induced Phase Separation (NIPS) Fabrication of Polysulfone Membranes. *Membranes* **2018**, *8*, 23. [20]

3.1 Introduction

Membrane technology has proven to be effective in recent years due to its promising benefits such as reduced footprint, easy control and easy scale-up, simple operational parameters, high throughput and automation [157]. Asymmetric membranes typically consist of a porous support layer that provides mechanical strength and stability, and which is covered by a thin selective layer or film responsible for providing the membrane with separation capabilities [137, 157, 158]. Phase inversion usually includes non-solvent-induced phase separation (NIPS), thermally induced phase separation (TIPS), or a combination of both [158-160]. In the NIPS method, shown in Figure 3.1, a dope solution is prepared by dissolving a polymer in a solvent [15, 16]. A membrane is then formed by the precipitation of the polymer in an anti-solvent bath, such as water. Briefly, through the immersion of a substrate in a coagulation bath, a solvent in the casting solution film is exchanged with a non-solvent in the precipitation media, and phase separation occurs. This process results in an asymmetric membrane with a dense top layer and a porous sublayer.

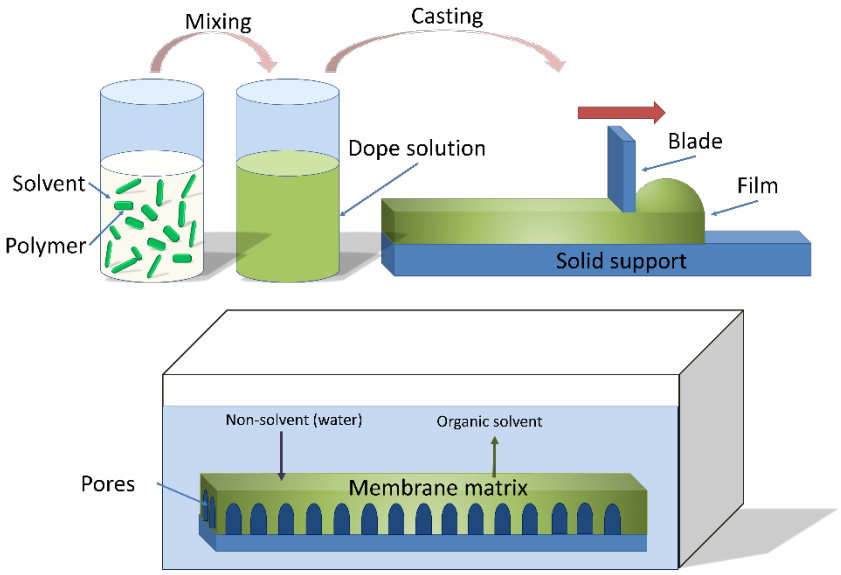

Figure 3.1 Non-solvent phase inversion casting process.

During membrane fabrication, large amounts of traditional organic solvents are used [1]. Solvents used in synthesis and post-synthesis steps can have a negative impact on operational safety, cost, the environment and human health [2-4]. Traditional solvents used for membrane preparation include dimethylformamide (DMF), *N*-methyl-2-pyrrolidone (NMP), dimethylacetamide (DMAc), dimethyl sulfoxide (DMSO), and tetrahydrofuran (THF). Some of these solvents are volatile and hazardous to the environment or living cells [102]. Solvents, such as cyclohexanes, DMAc, and DMSO are mutagenic and tumorigenic; acetone is highly flammable; and NMP is an irritant [102, 103]. Acute effects of DMF include skin irritation and dizziness, while its long-term effects are known to cause birth defects [104]. Due to their hazardousness, solvents require specialized control measures. Therefore, the need for greener, sustainable chemicals has prompted a great amount of research into the processing of renewable feedstocks to obtain platform molecules and downstream end products. The annual global solvent market is in the order of 20 million

metric tons and billions of dollars, and bio-based solvents consumption in Europe has been predicted to grow to one million metric tons by 2020 [5, 6]. Using renewable solvents derived from biomass, which do not compete with food applications, satisfies both consumer and legislative demands with regards to sustainability.

Therefore, solvents involved in the membrane manufacturing process are proposed to be replaced by greener alternatives. A green solvent is expected to be non-toxic, non-volatile, and derived from renewable sources [7]. In this research, a solvent produced from renewable sources, Methyl-5-(dimethylamino)-2-methyl-5-oxopentanoate (Rhodiasolv® PolarClean, Solvay Novecare (Princeton, NJ, USA)), was used to replace the traditional solvents [128]. PolarClean is derived from the valorization of 2-methylglutaronitrile (MGN), a byproduct from the synthesis of Nylon 6,6 [130, 161]. PolarClean has been previously shown to be a water-soluble, eco-friendly and biodegradable polar solvent with an excellent toxicological and eco-toxicological profile [130, 131], and the major physicochemical properties of PolarClean are shown in Table 3.1 [102, 131, 140].

PolarClean has been previously investigated to cast polyvinylidene fluoride (PVDF) and polyethersulfone (PES) membranes [128-130, 162]. Hassankiadeh et al. [128] used PolarClean as a green solvent to fabricate PVDF hollow fiber membranes via temperature induced phase separation (TIPS) process. Due to PolarClean's high miscibility with water, Jung et al. [129] further investigated its NIPS effect on the membranes surface during TIPS process, along with the kinetics of the membrane formation process. Marino et al. [130] prepared PES ultrafiltration and microfiltration membranes using PolarClean using NIPS and vapor induced phase separation (VIPS) processes. However, the thermodynamics of polymer/solvent/non-solvent mixing and demixing processes when

PolarClean is used as a NIPS solvent for the fabrication of polysulfone (PSf) membranes is unknown. Therefore, the research project described here first investigated the thermodynamics of mixing and demixing processes of PolarClean/PSf and compared them to NMP/PSf and DMAc/PSf. After mixing/demixing analysis (i.e., cloud point determination), DMAc was determined to be a more appropriate comparison for its greater similarity to PolarClean; subsequently, PolarClean was used to fabricate PSf membranes in a NIPS process and compared only to DMAc.

Table 3.1 Physicochemical properties of NMP, DMAc and PolarClean.

Property	NMP	DMAc	PolarClean
CAS-No	872-50-4	127-19-5	1174627-68-9
Formula	C5H9NO	C4H9NO	C9H17NO3
MW ($g \cdot mol^{-1}$)	99.133	87.122	187.239
Density ($g \cdot mL^{-1}$)	1.03	0.94	1.043
Flash point (°C)	95	69	144–146
Boiling point (°C)	202	165	278–282
Solubility in water (%)	miscible	miscible	miscible
Signal	Danger	Danger	Warning
Toxicity	Reproductive toxicity	Reproductive toxicity	

Polysulfone was chosen as the polymer to fabricate membranes due to its thermal stability, strong mechanical strength, good chemical resistance, and antifouling properties [163]. To dissolve PSf, NMP and DMAc were used as the traditional petroleum-based solvents since they are two of the most commonly used solvents in membrane fabrication and their performance has been studied for decades [14, 18, 139, 150, 163-167].

3.2 Experimental

3.2.1 Materials

Polysulfone (PSf, average MW 35,000 by LS, average Mn 16,000 by MO, pellets) was purchased from Sigma-Aldrich (Saint Louis, MO, USA). Methyl-5-(dimethylamino)-2-methyl-d-oxopentanoate (Rhodiasolv® PolarClean) was provided by Solvay Novecare (Princeton, NJ, USA). *N*,*N*-Dimethylacetamide (DMAc) was purchased from Tokyo Chemical Industry Co., Ltd. (Tokyo, Japan), and 1-Methyl-2-pyrrolidone (NMP, for peptide synthesis) was purchased from EMD Millipore Corporation (Burlington, MA, USA). Bovine Serum Albumin (BSA) was purchased from VWR Life Science (Radnor, PA, USA), and different sizes of polyethylene glycols (PEGs) were purchased from Alfa Aesar (Haverhill, MA, USA).

3.2.2 Thermodynamics

3.2.2.1 Hansen Solubility Parameter Calculation

To choose the appropriate solvent for a polymer, the polymer must be soluble or easily dispersible in the specific solvent [14]. To select potentially compatible solvents, the relative energy difference (RED) is calculated using Equation (1):

$$\mathrm{RED} = R_a/R_o \tag{1}$$

where R_o is the radius of interaction of a Hansen solubility parameter sphere and R_a is the solubility parameter distance between polymer (1) and solvent (2). R_a can be calculated based on their individual Hansen solubility parameters (δ_d represents the dispersive force,

δ_p represents the polar force and δ_h represents hydrogen bonding) using Equation (2) [168]:

$$Ra = \sqrt{4(\delta_{d2}-\delta_{d1})^2 + (\delta_{p2}-\delta_{p1})^2 + (\delta_{h2}-\delta_{h1})^2} \quad (2)$$

The solubility increases as the value of R_a decreases towards 0 [168].

3.2.2.2 Cloud Point Curve Measurement

In order to determine the compatibility of a solvent to fabricate membranes by the non-solvent phase inversion method, a cloud point curve must be obtained for the solvent/non-solvent/polymer ternary system [169]. For the PolarClean/PSf/water system, a cloud point curve was experimentally determined by titration [37]. In experiments, dope solutions were prepared using 1, 3, 5, 10, 15, 20, 25 and 30 wt % concentrations of PSf in NMP, PolarClean and DMAc. Each of these dope solutions was mixed using a sonicator (Elmasonic P70H, from Elma Electronic Inc., Munich, Germany) at 65 °C (with frequency of 80 kHz, power of 900 W under pulse mode) for 24 h. All dope solutions were then cooled to room temperature, and deionized water was gradually added to the dope solutions using a micropipette until the solutions were observed to become cloudy. Afterwards, the cloudy solution was sonicated for one additional hour to determine if it changed to a clear solution. If the solution was still cloudy, the composition of water/solvent/polymer was determined as the cloud point.

3.2.3 Preparation of PSf Flat Sheet Membranes

The homogeneity of the dope solution is important for the fabrication of membranes [170-172]. Two methods were used to achieve full mixing of the dope solution, sonication and planetary mixing. Sonication is a traditional mixing method, while planetary mixing is a 3-D mixing process to mix dry and wet materials using a planetary mixer [173]. The planetary mixing process combines high speed revolution and rotation to accelerate the mixing of polymer/solvent [174], therefore, it has the potential to be used in dope solution preparation [175].

Dope solutions of 17% PSf in NMP, DMAc and PolarClean were prepared using a sonicator (Elmasonic P70H, from Elma Electronic Inc., Munich, Germany) and a planetary centrifugal mixer (Mazerustar KK-250S, from Kurabo Industries Ltd., Osaka, Japan). The planetary mixer is set up to mimic planetary motion to accelerate the mixing process, where the sample rotates and revolves simultaneously, as shown in Figure 3.2. The dope solutions were sonicated at 65 °C at a frequency of 80 kHz and power of 900 W under pulse mode for 24 h to accelerate the mixing process, allowed to return to room temperature, and then mixed in the planetary mixer for 10 min. The process was repeated until the solutions became homogenous. After storing in room temperature for three months, the dope solutions did not turn cloudy, which indicated that no separations occurred during this period and the solutions remained homogenous. Room temperature was used for cooling the dope solutions, casting and phase inversion.

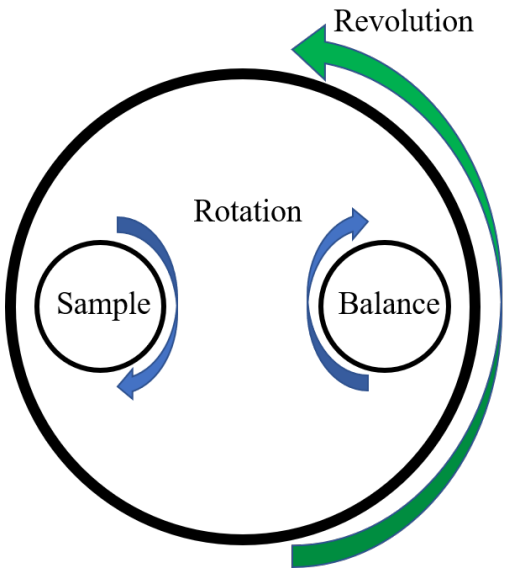

Figure 3.2 The illustration of the working principle of the planetary centrifugal mixer.

Distilled water was used as the non-solvent. Once the dope solutions were fully dissolved, as determined by the solution becoming clear, the solution was degassed in an ultrasonic bath at room temperature for approximately three hours to remove any air bubbles. After the dope solution was prepared, membranes were cast using the NIPS casting process [176-179], in which a thin film of the casting solution is deposited onto a glass plate using an aluminum casting knife under room temperature and evaporated for a period between 30 and 120 s in air before being immersed in the non-solvent. Membrane films were cast with thicknesses ranging from 80 to 100 microns. After fabrication, the membranes were stored in deionized (DI) water at room temperature for seven days.

Numerous membrane treatment methods have been applied to polymeric membranes after casting to achieve desired properties, such as permeability and selectivity [180-182]. Some of these include using room temperature ovens, solvent exchange and

freeze drying processes to improve membrane performance as measured by flux values [180]. However, to minimize the number of design variables here, only the effect of evaporation time on PSf/PolarClean dope solution prior to casting was investigated using 30, 45, 60, 90 and 120 s. It was determined that evaporation time had a strong effect on water permeability. With increasing evaporation time, the polymer concentration of the polymer-rich phase increases, and a denser and thicker selective layer forms on the surface of the membranes [183]; as a consequence of the increase in selective layer thickness, the permeability of membranes decreases [184, 185]. All filtration experiments were performed by first precompacting the membranes using DI water, and then filtering BSA solutions through an Amicon dead-end filtration cell (Amicon Stirred Cell 8010-10 mL from Millipore Sigma company, Burlington, MA, USA) under a constant pressure at 4 bars at room temperature.

As shown in Figure 3.3, after precompaction, water flux values for evaporation times of 30 s (1633 ± 449 LMH), 45 s (1769 ± 509 LMH) and 60 s (2423 ± 125 LMH) were not significantly different. As evaporation time increased from 60 s to 120 s, in agreement with literature studies [183-186], membrane pure water permeability decreased by over one order of magnitude (Figure 3.3). Specifically, the water flux value decreased from 2423 ± 124.9 LMH for 60 s to 1055 ± 346.7 LMH for 90 s, and continued decreasing to 67 ± 26.7 LMH for 120 s. Furthermore, at the start of filtration of 1000 ppm BSA feed solution, all membranes displayed declined flux values likely due to instantaneous fouling. For PSf/PolarClean membranes, the initial BSA flux values were 131 ± 41.5 LMH for an evaporation time of 30 s, 151 ± 41.0 LMH for 45 s, 176 ± 8.8 LMH for 60 s, 108 ± 18.7 LMH for 90 s, and 17 ± 9.2 LMH for 120 s.

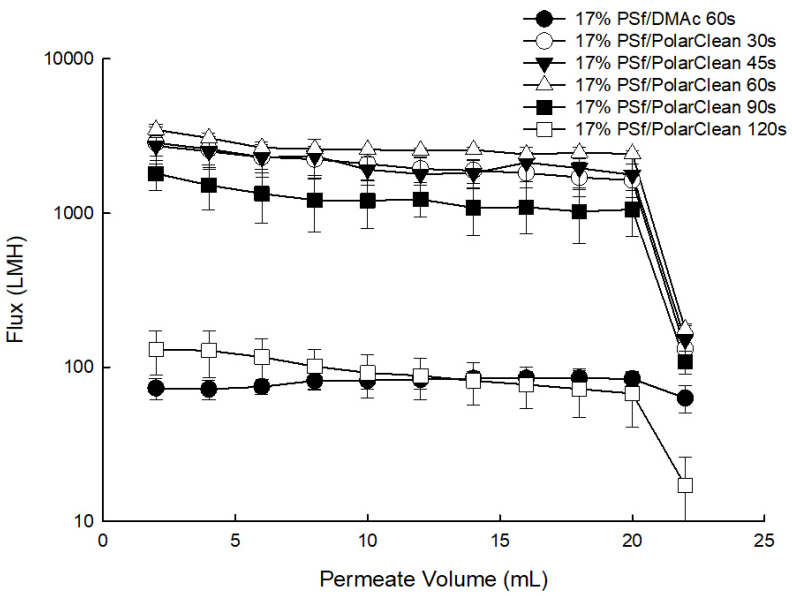

Figure 3.3 Pure water and BSA solution permeability (at 4 bar).

For PSf/DMAc membrane, an evaporation time of 60 s was studied, and the associated BSA flux value was 63 ± 12.4 LMH. The probable reason for the significant difference as compared to PSf/PolarClean might be that the selective layers of PSf/PolarClean membranes made with short evaporation times were relatively thinner as compared to PSf/DMAc, as later discussed in Section 3.5. Without a thick selective layer, BSA molecules might have blocked the pores faster, which would lead to instantaneous cake formation, and therefore, a larger decrease the water flux [187-191]. Since 60 s was originally used for DMAc membranes, it was decided to use 60 s evaporation time for PolarClean membranes for a direct comparison.

3.2.4 Characterization of PSf Membranes

3.2.4.1 Morphology

Flat sheet membranes, prepared using phase the inversion method, were immersed and fractured in liquid nitrogen and then sputtered with palladium. The top layers and the cross sections of the PSf membranes were sampled by focused ion beam (FIB) and then observed by SEM (FIB-SEM, FEI Helios Nanolab 660 from Thermo Fisher Scientific, Waltham, MA, USA). FIB is an advanced method to sample preparation prior to SEM imaging to characterize the morphology of membranes [142]. FIB-SEM provides a more effective method to observe the cross sections of membranes as compared to the common SEM [143]. Moreover, the higher quality of FIB-SEM images shows the internal structure of polymeric membranes and shows the distribution of pores. FIB-SEM images showed the detailed images at scales of 5 nm. In order to observe the entire morphology of cross sections, the PSf membranes were observed by SEM (SEM, Hitachi S-4300 from Hitachi Group, Troy, MI, USA).

3.2.4.2 Contact Angle

The contact angle data of PSf membranes prepared with different solvents were determined by the sessile drop method using a drop shape analyzer equipped with a high definition camera (DSA100S from Krüss company, Hamburg, Germany).

3.2.4.3 Porosity and MWCO

The porosity (Pr, %) of PSf membranes were tested using differences in membrane weight [144-146]. Due to the hydrophobicity of PSf, water was not used in this measurement. Membranes were first wet by silwick (from Porous Materials Inc., Ithaca, NY, USA), then isopropyl alcohol (IPA, ⩾99.7%, FCC, FG, from Sigma-Aldrich, St. Louis, MI, USA) was filtered through the membranes under 2 bars for 10 min [146]. The

membranes with IPA were exposed to clean and dry air for three days. The wet and dried state weights of membranes at the equilibrium were collected separately [144-147]. Then the porosity was calculated using the Equation (3):

$$Pr = V_{sil}/V_{total} = (W_{sil}/\rho_{sil})/(W_{sil}/\rho_{sil} + W_{PSf}/\rho_{PSf}) \quad (3)$$

where W_{sil} and W_{PSf} are the weights of the silwick and PSf membranes; ρ_{sil} is the density of the silwick, 0.93 g/mL and ρ_{PSf} is the density of PSf, 1.24 g/mL [146, 148, 149].

Molecular weight cut off (MWCO) represents the lowest molecular weight of solute which could be 90% rejected by the membrane [150, 151]. Polyethylene glycol (PEG) with molecular weight from 200, 400, 1 k, 4 k, 10 k, 20 k, 40 kDa were used as feed to determine MWCO values for the different membranes. Since PEGs are linear polymers, the regression model of hydrodynamic radius (nm) and molecular weight (kDa) is given by Equation (4) [152]:

$$r_H = 0.06127(MW)^{0.3931} \quad (4)$$

Table 2 shows the corresponding hydrodynamic radius (nm) to tested molecular weights of PEGs calculated using Equation (4).

Table 3.2 Molecular weights and hydrodynamic radius of PEG used in MWCO study.

Molecular Weight (kDa)	Hydrodynamic Radius (nm)
PEG 200	0.49
PEG 400	0.65
PEG 1000	0.93
PEG 4000	1.60
PEG 10,000	2.29
PEG 20,000	3.01
PEG 40,000	3.95

3.2.5 Filtration Studies

Water permeation experiments were carried out at a constant pressure of 4 bars in an Amicon dead-end filtration cell (Amicon Stirred Cell 8010-10 mL from Millipore Sigma Company, Burlington, MA, USA). The pure water flux was measured using deionized water until the water flux became constant, which is called precompaction. In this study, all the precompaction were performed by filtering 20 mL DI water at a constant pressure of 4 bars for consistency. After precompaction, 20mL of solutions containing 1000 mg/L BSA; that is, 20 mg of BSA, were filtered through the membranes at a constant pressure

of 4 bars and room temperature. BSA has a molecular weight of 66.5 kDa, is a hydrophobic, and its isoelectric point is 4.7, which means it is negatively charged at neutral pH values. The permeability was recorded for every 2-mL filtration period, and permeate samples were collected to analyze the concentrations of BSA in the feed and permeate using a Fusion UV/Persulfate TOC analyzer (14-9600-100 from Teledyne Tekmar Company, Mason, OH, USA). All experiments were performed in triplicate.

3.2.6 Recovery and Fouling Performance

After BSA filtration, reverse flow filtration using deionized water was performed at a constant pressure of 2 bars for 30 min to remove foulants that were not adsorbed to the membrane (i.e., reversibly attached), and then flux recovery ratio (Re, %) was measured. The recovery ratio is related to the resistance of the fouled membrane.

3.3 Results and Discussion

3.3.1 Hansen Solubility Parameter Calculation

RED values of selected solvents (including water as comparison) and PSf are shown in Table 3. The RED value of PolarClean is slightly larger than that of NMP and DMAc; however, a solvent is determined to be a good solvent when the RED value is equal to or smaller than 1 [14]; thus, PolarClean has the potential to fabricate PSf membranes.

Table 3.3 Relative energy density calculation for picked solvents and PSf.

Polymer	δ_d (MPa1/2)	δ_p (MPa1/2)	δ_h (MPa1/2)	Ro (MPa1/2)	
PSf	19.7	8.3	8.3	8.00	
Solvents	$\boldsymbol{\delta_d}$ (MPa1/2)	$\boldsymbol{\delta_p}$ (MPa1/2)	$\boldsymbol{\delta_h}$ (MPa1/2)	Ra (MPa1/2)	RED
NMP	18	12.3	7.2	5.36	0.67
DMAc	16.8	11.5	10.2	6.89	0.86
PolarClean	15.8	10.7	9.2	8.21	1.03
Water	15.5	16	42.4	35.95	4.49

3.3.2 Cloud Point Curve

The ternary phase diagram is the general method to illustrate the thermodynamics of a polymer/solvent/non-solvent system [37, 163, 169, 192]. The cloud point curve, which is considered as the experimentally binodal curve, represents the composition where the solution is not thermodynamically stable and phase transition occurs. Experimental cloud point curves were developed here for PSf/NMP/H_2O and PSf/DMAc/H_2O, and these agreed with literature reported curves [163, 192, 193]. Thus, the experimental cloud point curve of PSf/PolarClean/H_2O using the same method was considered valid. The experimental cloud point curves for polymer/solvent/non-solvent are shown in Figure 3.4. The cloud point curves illustrate that the NMP/PSf solution system had the highest non-

solvent (i.e., water) tolerance, while the water tolerance of PolarClean/PSf and DMAc/PSf solutions were not significantly different. Therefore, the miscibility area of the PolarClean/PSf/water and DMAc/PSf/water systems was found to be less than NMP/PSf/water system, while the precipitation rate of PolarClean/PSf and DMAc/PSf solutions was higher than then NMP/PSf solution.

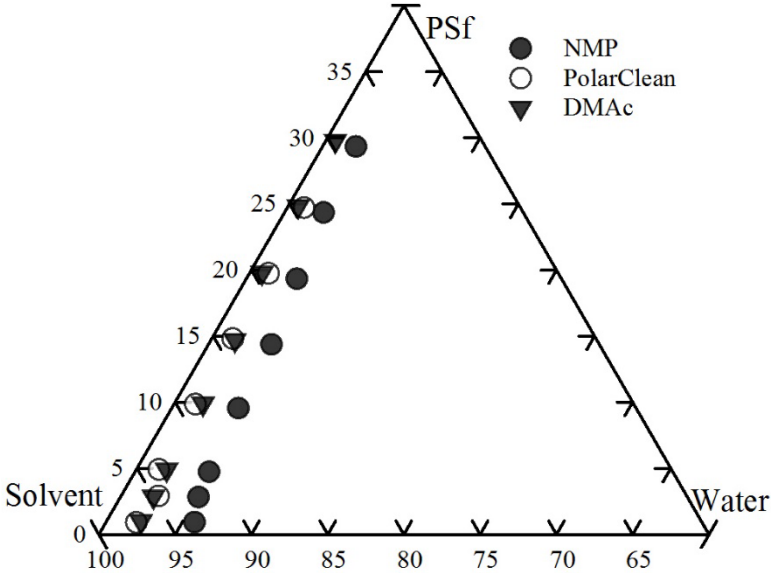

Figure 3.4 Experimental cloud point curves of PSf/solvent/water system.

Moreover, as shown in Figure 3.5, NMP has a 5-membered ring, which is a distinctly different structure as compared to DMAc and PolarClean since the latter two have similar chain structures, specifically, the structure of PolarClean is a combination of DMAc and isopropyl acetate. Therefore, based on the similar cloud point curves and chemical structures, it was concluded that PSf membranes prepared with PolarClean were best compared to membranes prepared with DMAc for this research.

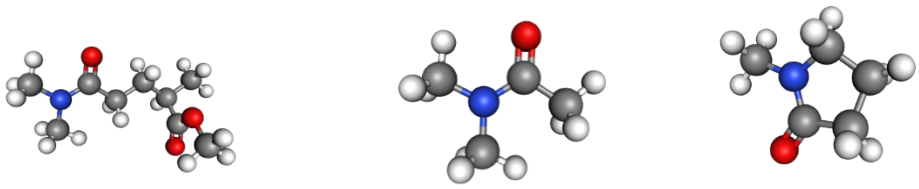

(a) (b) (c)

Figure 3.5 Chemical structure of three solvents: (a) PolarClean (b) DMAc (c) NMP. (Blue: Nitrogen, Red: Oxygen, Grey: Carbon, White: Hydrogen).

3.3.3 Porosity and MWCO

To determine the types of membranes made here and predict their filtration performance, molecular weight cut-off (MWCO) and porosity studies were performed. Figure 3.6 showed that there was no significant difference in the MWCO of 17% PSf membranes cast using DMAc and PolarClean, with all the membranes showing rejection to large molecules in the range of 400–1000 Daltons (0.65–0.93 nm of hydrodynamic radius) through the size-exclusion process. The PSf/DMAc membranes showed 68 ± 5% overall porosity, while the PSf/PolarClean membranes showed 71 ± 1%. As with MWCO, the porosity of these two different membranes showed no significant difference.

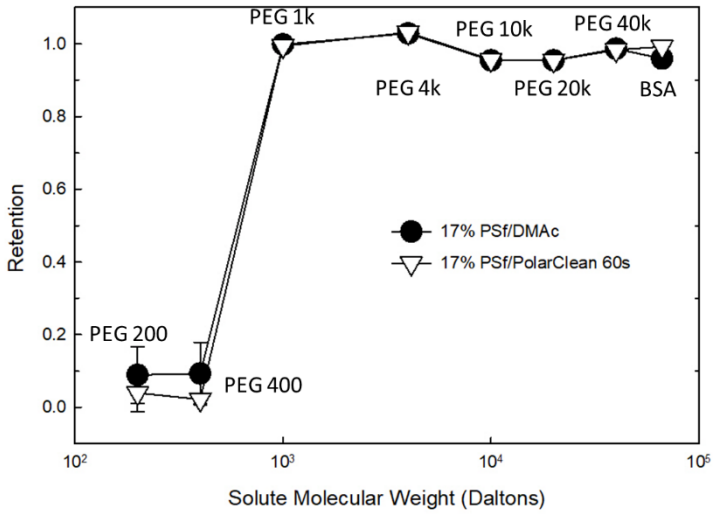

Figure 3.6 Molecular weight cut-off of PSf membranes.

3.3.4 Hydrophobicity of Membranes

Membrane hydrophobicity affects permeability, rejection and fouling behavior of membranes [137, 194-197]. The contact angle of 17% PSf membranes prepared using DMAc was found to be 64 ± 4°, while that using PolarClean was 68 ± 2°. Therefore, the hydrophobicity of membranes would not account for any differences in water permeability, selectivity or fouling observed here, and differences were more likely due to structural differences, as discussed in Section 3.5.

3.3.5 Morphology

The cross sections of the selective layers of 17% PSf membranes prepared with the two solvents are shown in Figure 3.7 a,b, and the entire cross sections of the PSf membranes are shown in Figure 3.7 c,d. Figure 3.7 a,b show, at a magnification of 5 μm, the details of the selective layers of the membranes and also the thicknesses of the selective layers, while Figure 3.7 c,d show the entire cross section morphology of the membranes at

a magnification of 50 μm. Figure 3.7 a–d show that the PSf membranes prepared with DMAc had finger-like pore structures, whereas membranes prepared with PolarClean had sponge-like pore structures. This difference in morphology is influenced by several factors, including the polymer type, additives, solvent and non-solvent combinations, as well as fabrication techniques [160, 198, 199]. In NIPS, an instantaneous liquid-liquid demixing process leads to finger-like pore structures, while a delayed liquid-liquid demixing process results in sponge-like pore structures [14, 183]. The demixing process happens when the composition profile intersects with the binodal line and the delayed demixing process leads to the slow precipitation, and therefore forms the spongy-like structures [14]. The speed of the liquid-liquid demixing process is determined by the diffusion rate between the solvent and non-solvent. Therefore, from Figure 3.7c, d, it was hypothesized that the diffusion rate of DMAc and water was faster than that of PolarClean and water. Furthermore, it has been shown that finger-like pores result in higher water fluxes along with lower solute rejection rates as compared to sponge-like pores [81, 200, 201]. Therefore, it was expected that the membranes prepared using the two different solvents would display differences in permeability.

Another observation was that the thicknesses of the selective layers of the membranes were different. From Figure 3.7a, PSf/DMAc membranes displayed an approximate selective layer thickness of 400 to 800 nm, while PSf/PolarClean membranes (Figure 3.7b) did not show an obvious selective layer. The thickness of the selective layer is influenced by several factors, including polymer concentration, evaporation time and coagulation bath conditions [183-186]. In this case, it is proposed that evaporation time might have been the most probable cause of the difference in thicknesses. Since different

solvents have different volatilities, the evaporation time to form the selective layers with same thicknesses may differ significantly. If the boiling point is used to represent the volatility [202], for a given solvent, the higher the vapor pressure and the lower boiling point, the higher volatility [202]. The vapor pressure at 20 ℃ is 300 Pa for DMAc [203] and less than 0.01 Pa for PolarClean [204]. The boiling points at 101.3 kPa of DMAc and PolarClean are reported to be 165 ℃ and 282 ℃ [131, 205], respectively, which indicated that DMAc had higher volatility than PolarClean. Therefore, a longer evaporation time would be needed to form the same thickness of selective layer for PSf/PolarClean membranes as PSf/DMAc membranes, which agrees with experimental effects of evaporation time (Figure 3.3). From Figure 3.3, an evaporation time of 120 s for PSf/PolarClean led to membranes of similar permeability as an evaporation time of 60 s for PSf/DMAc.

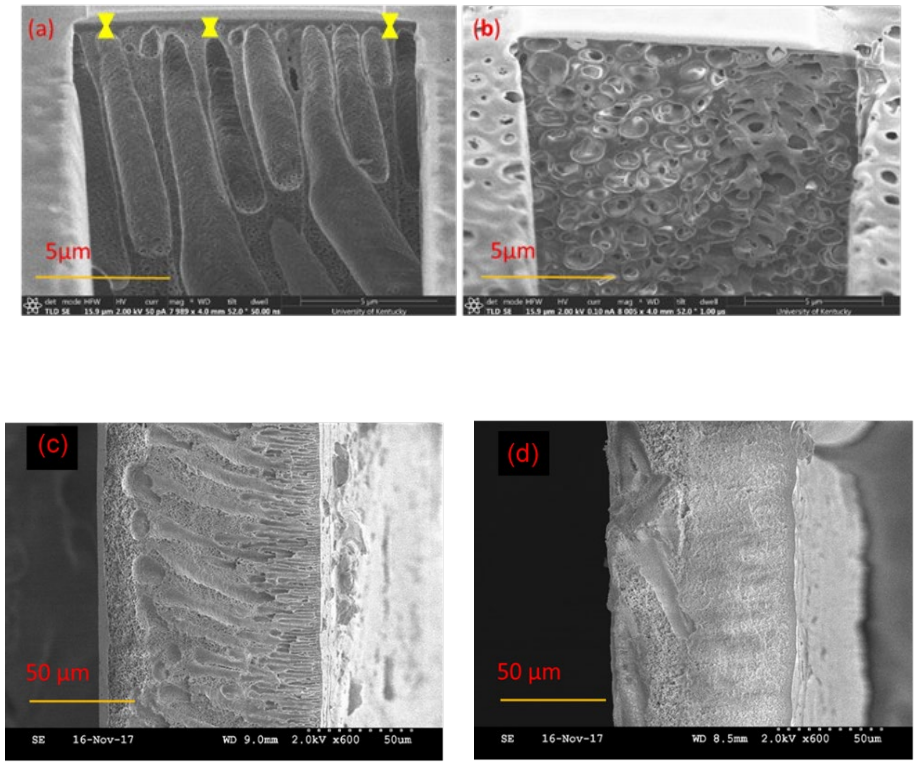

Figure 3.7 Cross-sectional FIB-SEM images of the top layers of PSf ultrafiltration membranes prepared with: (a) DMAc; (b) PolarClean. Cross-sectional SEM images of PSf ultrafiltration membranes prepared with: (c) DMAc; (d) PolarClean.

3.3.6 Filtration performance

From Figure 3.8, during BSA filtration, the flux of PSf/DMAc membranes declined from 63.1 ± 12.4 to 40.0 ± 13.6 L/m^2·h (LMH), while the flux of PSf/PolarClean membranes declined from 176.0 ± 8.8 to 125.0 ± 4.5 LMH. This decline was likely due some compression under the 4-bar pressure [206, 207] along with accumulation of BSA on the surface of the membrane, which increased resistance to flow. It was also observed that the water flux values of PSf/PolarClean membranes were higher than PSf/DMAc membranes, which did not agree the expectation from the morphology (Figure 3.7).

However, as previously mentioned, for different solvents, the evaporation time impacted the thickness of the selective layer of the membranes, which consequently impacted the water permeability [185, 186, 208], which may explain the higher flux values observed with PSf/PolarClean membranes. In this case, the thickness of the selective layers of membranes were the dominant parameter influencing water permeability.

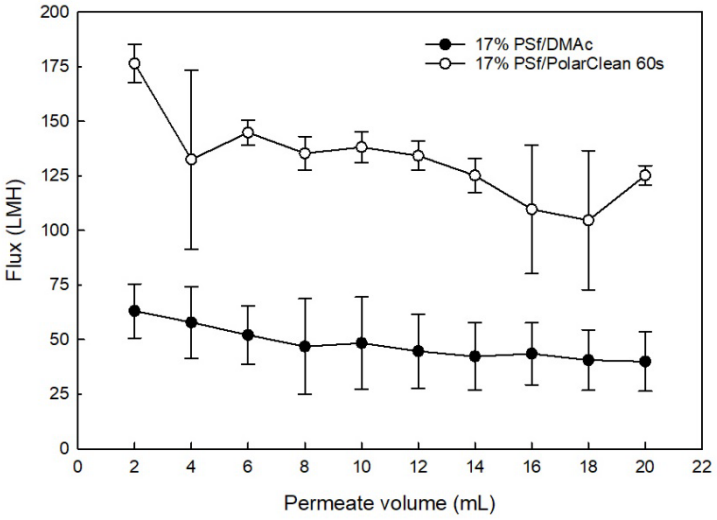

Figure 3.8 BSA solution permeability (at 4 bar).

BSA rejection analysis was also performed, and it was determined that 99 ± 1% of BSA was removed by the PSf/PolarClean membranes, which was slightly higher than 96 ± 2% BSA rejection by the PSf/DMAc membranes. The higher rejection rate of PSf/PolarClean membranes agreed with their sponge-like pore structures as shown in Figure 3.7b. In addition to comparing the performance of PSf/PolarClean membranes fabricated here to the performance of PSf/DMAc membranes fabricated using similar controlled conditions, a comparison was made to literature PSf/DMAc membranes [158, 209-212]. It is important to note that evaporation times were not available for membranes from the literature. It is clearly observed that PSf/PolarClean membranes are within the

acceptable range of pure water flux, permeability and BSA rejection. This validates the potential of PolarClean to be used as a bio-derived greener alternative equivalent to DMAc.

To determine the extent of the irreversible adsorption of BSA to the membranes after filtration, or the amount of irreversible fouling, reverse-flow filtration using DI water was performed after BSA filtration to represent a backwash cycle. The flux was then measured after reverse-flow filtration to determine the recovered flux, or the percentage of the flux decline due to reversible fouling. The average recovered flux for PSf/PolarClean membranes was 30 ± 1%, which was lower than that for PSf/DMAc membranes (77 ± 13%). The lower flux recovery using PolarClean was hypothesized to have been due to the sponge-like pores collapsing after filtration, which would make it more difficult for water to pass through the pores. In order to verify this hypothesis, PSf/PolarClean membranes were analyzed using FIB after BSA filtration and reverse-flow filtration. Figure 3.9 shows the surface morphology, while Figure 3.10 displays the cross-sectional structures. As observed from Figure 3.9b, BSA molecules accumulated on the surface of the membranes to foul them, and reverse-flow filtration was able to remove most of the foulants (Figure 3.9c). However, comparing Figure 3.7b (cross-section using PolarClean) and Figure 3.10a (cross-section using PolarClean after BSA filtration) shows that the pores of the PSf/PolarClean membranes slightly collapsed after BSA filtration, which might have been due to the pressure applied on the membranes [213-215]. Likewise, by comparing Figure 3.10a (cross-section using PolarClean after BSA filtration) and Figure 3.10b (cross-section using PolarClean after backwash), it was observed that the pores collapsed further and the thickness of the selective layer increased after backwash. This was likely the cause of the lower recovery rate observed for PSf/PolarClean membranes. One reason for the collapse

of the pores might have been that the mechanical strength of the sponge-like pores was lower than finger-like pores; hence, the sponge-like pores might have been easier to compress under the same backwash pressure.

Another reason might be the selective layer of the PSf/PolarClean membranes were thin, in agreement with Figure 3.7b, and possibly fragile. Considering that the MWCO of PSf/PolarClean membranes was less than 1 nm (Figure 3.6) while the apparent the pore size of PSf/PolarClean membranes was at micrometer level (from SEM images, Figure 3.7b, a thin selective layer might have been present. This selective layer might have collapsed or been damaged during filtration and/or recovery. Then, the selectivity of the membrane became a function of the porous structure and tortuosity, indicating it started to behave as a depth filter instead of a membrane. This also correlates with the low recovery following backwashing, indicating that the pores collapsed.

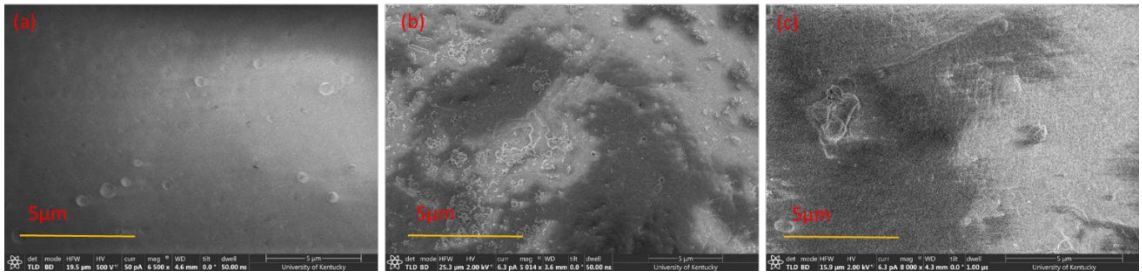

Figure 3.9 FIB-SEM images of PSf/PolarClean membranes surface: (a) Original; (b) After BSA filtration; (c) After DI water backwash.

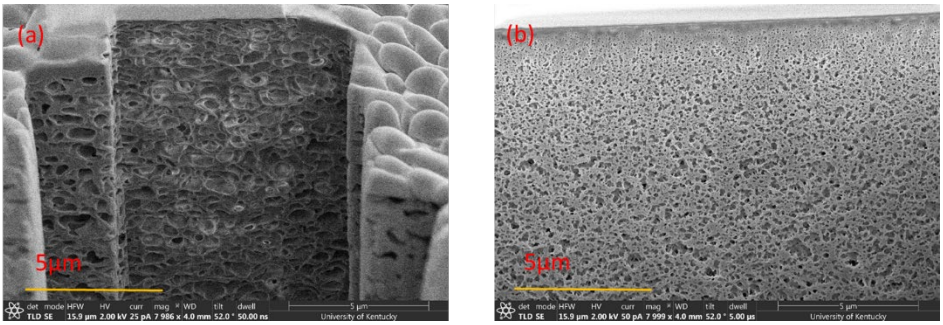

Figure 3.10 Cross-sectional FIB-SEM images of PSf/PolarClean ultrafiltration membranes: (a) After BSA filtration; (b) After DI water backwash.

3.4 Conclusions

In this study, PolarClean was used as a NIPS solvent to cast PSf membranes and then compared with DMAc. Based on the ternary phase diagram, the cloud point curve of PSf/PolarClean/water was similar to that of PSf/DMAc/water. Dope solutions for PSf/PolarClean and PSf/DMAc were prepared at 65 °C and membranes were cast and characterized afterwards. The overall porosity, MWCO and hydrophobicity of membranes made using PolarClean and DMAc were not significantly different. However, the cross-sections images of the membranes were different, with PSf/DMAc membranes showing finger-like structures and PSf/PolarClean membranes showing sponge-like structures.

Regarding membrane performance, PSf/PolarClean membranes showed slightly higher BSA rejection rates (99 ± 1%) as compared to PSf/DMAc membranes (96 ± 2%), which agreed with their sponge-like pores structures. Furthermore, PSf/PolarClean membranes also showed higher flux values (176.0 ± 8.8 LMH) than PSf/DMAc membranes (63.1 ± 12.4 LMH), which disagreed with the sponge-like structure theory and might have been due to evaporation time. However, pore collapsing was observed in the study, which means the stability of PolarClean membranes is uncertain. In conclusion, bio-derived solvents should be investigated further and may become promising replacements to traditional solvents.

CHAPTER 4. INVESTIGATION OF POLARCLEAN AND GAMMA-VALEROLACTONE AS SOLVENTS FOR POLYSULFONE MEMBRANE FABRICATION

This chapter has been published in the following report and adapted with permission from:

Dong, X.; Shannon, H.D.; Escobar, I.C. Investigation of PolarClean and Gamma-Valerolactone as Solvents for Polysulfone Membrane Fabrication *Green Polymer Chemistry: New Products, Processes, and Applications.* **January 1, 2018** , 385-403 [46]

4.1 Introduction

Immersion precipitation, or nonsolvent induced phase separation (NIPS), is a conventional method used to fabricate porous polymeric membranes. In this method, a polymer is first dissolved in a solvent. The polymer and the solvent are mixed often through mechanical mixing with or without heating until a homogenous dope solution is obtained. In the laboratory, flat-sheet membranes are often obtained using a doctor blade or the spin coating method. A doctor blade is used to cast the dope solution on a substrate, usually a glass plate or a polymeric support film, to form a liquid film with a desired thickness [1, 170]. The doctor blade is easy to operate, controls the conditions of the membranes formed, and it wastes minimum dope solution [216, 217]. However, it is difficult to keep consistency because different operators have different habits and the speed of casting is hard to control. In spin coating, a small amount of coating material is applied on a solid substrate by spinning at low speed [218, 219]. Spin coating is more suitable to fabricate small sizes of films and easier to keep the consistency; however, the homogeneity of the

membranes is often a concern [216, 218, 219]. With both the doctor's blade and spin coating method, after casting, the substrate with the film is immersed into a coagulation nonsolvent bath, typically water [16]. Through immersion, solvent in the film is exchanged with the nonsolvent in the coagulation bath, where the phase separation occurs [17]. The phase separation is due to the presence of nonsolvent and so it is named NIPS.

The NIPS process leads to a membrane with two layers, a dense surface layer and a porous support layer, where the porous support layer, which provides mechanical strength and stability and which is covered by a thin selective layer or film, is responsible for providing the membrane with separation capabilities. After phase inversion, the solvent from the dope solution remains in the nonsolvent bath, which is a hazardous liquid waste that must be treated to minimize environmental impacts because large amounts of traditional petroleum-derived solvents are used to prepare the dope solutions. As Europe and China move toward a more bio-derived manufacturing base, the opportunities for new and bio-derived solvents are only expected to increase worldwide. To address this issue, traditional solvents involved in the membrane manufacturing process are proposed to be replaced by environmentally friendly solvents. Two recently developed and bio-derived solvents show structures similar to traditional solvents along with similar properties. These solvents are methyl-5-(dimethylamino)-2-methyl-5-oxopentanoate (Rhodiasolv PolarClean) and gamma-valerolactone (GVL). The structure of PolarClean is similar to Dimethylacetamide (DMAc), whereas GVL has a similar structure to N-Methyl-2-pyrrolidone (NMP). Therefore, PolarClean and GVL were investigated individually and as a mixture of solvents for their ability to cast membranes.

4.2 Experimental Section

4.2.1 Materials

Polysulfone (PSf, average Mw 35000 by LS, average Mn 16000 by MO, pellets) was purchased from Sigma-Aldrich (St. Louis, Missouri, United States); GVL was purchased from Acros Organics (Fair Lawn, New Jersey, United States); Methyl-5-(dimethylamino)-2-methyl-d-oxopentanoate (Rhodiasolv® PolarClean) was kindly provided by Solvay Novecare (Princeton, New Jersey, United States).

4.2.2 Preparation of Dope Solution

Dope solutions were prepared as described in Table 1. Each dope solution was mixed using a magnetic stirring bar at 65 ℃ for 24 h, and then a planetary centrifugal mixer (Mazerustar KK-250S, Kurabo Industries Ltd., Osaka, Japan) was used to ensure the homogeneity of the dope solutions [20]. The dope solutions with different solvent compositions are numbered in Table 1 for convenience. The main purpose of choosing 17 wt. % of polysulfone was to target the casting ultrafiltration membranes, which has been previously determined to be at 17% [20]. The same polymeric dope solutions were used in this research to maintain consistency.

Table 4.1 Composition of PSf dope solutions in this study

Polymer	Weight percent	Solvent 1	Weight percent	Solvent 2	Weight percent	Number
PSf	17	PolarClean	0	GVL	83	1
PSf	17	PolarClean	1/4 × 83	GVL	3/4 × 83	2
PSf	17	PolarClean	1/2 × 83	GVL	1/2 × 83	3
PSf	17	PolarClean	3/4 × 83	GVL	1/4 × 83	4
PSf	17	PolarClean	83	GVL	0	5

4.2.3 Membrane Casting

Once the dope solutions were homogenous, they were degassed in an ultrasonic bath at room temperature for 1 h to remove air bubbles. The membranes were cast afterward using the NIPS process [14, 20]. A thin film of dope solution was deposited on a glass plate at room temperature, and then cast using a doctor casting blade which was set at the thickness of 200 μm. According to previous studies [20], the evaporation rate of different solvents in air vary. In this study, to minimize the influence of evaporation rates of different

solvents, the evaporation time was chosen to be 0 s before the dope solutions were immersed into water. The thickness of membranes was measured using a digimatic deep throat digital thickness gage (547-520S, Mitutoyo Co., Kawasaki, Japan) with the range of 80–100 μm. Afterward, the membranes were store in deionized water at room temperature for 1 week.

4.2.4 Characterization Methods

The viscosity of dope solutions was measured using a rheometer (AG-G2, TA Instruments, Delaware, United States). The average pore size of membranes was measured through a Liquid-Liquid porometer (LLP-11000A, Porous Materials Incorporated, Ithaca, New York, United States). The zeta potential values (i.e., membrane surface charge) were determined by an electrokinetic analyzer (Anton Paar SurPASS, Ashland, Virginia, United States), and the adjustable gap cell was adjusted to a gap with 90–110 μm with 0.01 M KCl used as the electrolyte solution. The contact angles of membranes in this study were measured by sessile drop method, using a drop shape analyzer (DSA 100S, Kruss Company, Hamburg, Germany). The tests were repeated 6 times and contact angles were calculated with deviation. The surface roughness of membranes was investigated in atmosphere under tapping mode using an atomic force microscope (AFM, Quesant. Instrument Co., United States). It was evaluated by root-mean-squared (RMS) roughness over six membrane surface areas of 20 × 20 μm (2), which were randomly picked on the top layer of membranes.

4.2.5 Membrane Performance

For membranes #1 to #5, pure water filtration (PWF) tests were performed at a constant pressure of 4.1 bars in an Amicon dead-end filtration cell (Amicon Stirred Cell 8010-10 mL, Millipore Sigma Co., Burlington, Massachusetts, United States). When the water flux became constant, the flux was recorded. Afterward, 100 mg/L BSA solution was filtered through the membranes at 4.1 bars. The permeability was recorded. The permeate samples were collected and then the concentration was analyzed using a UV/Vis spectrophotometer (UV-6300PC, VWR International bvba/sprl, Leuven, Belgium).

4.3 Results and Discussion

4.3.1 Viscosity of Dope Solutions

The viscosity values of different dope solutions are presented in Table 2. For all the dope solutions, the viscosity decreased slightly while the shear rate increased from 0.1/s to 1/s and then 10/s. This indicated that the viscosity of PSf dope solutions did not change significantly with shear rate.

At the shear rate of 0.1/s, from #1 to #5, the viscosity increased gradually from 1.44 Pa.s to 5.448 Pa.s, showing that the viscosity increased as the percent of GVL decreased in the dope solutions. Hence, dope solutions prepared using PolarClean alone (membrane #5) showed the highest viscosity, while the dope solutions using GVL alone (membrane #1) showed the lowest. At the same shear rate of 0.1/s, the viscosity of PSf membranes made using traditional petroleum-derived solvents, NMP and DMAc, was 0.3517 and 0.1657 Pa.s, respectively. Based on the viscosity of dope solutions made using traditional solvents,

low viscosity values were targeted here. Therefore, adding GVL as a co-solvent mixture with PolarClean can effectively decrease the viscosity of dope solutions. It is important to note that membranes made using GVL as the sole solvent would stick to themselves like glue, while membranes made with PolarClean alone were found to not produce membranes with stable pore structures after cleaning using backwash [20].

Table 4.2 Viscosity of dope solutions under certain shear rates

Shear rate (1/s)	Viscosity (Pa.s)				
	#1	#2	#3	#4	#5
0.1	1.44	1.967	2.864	4.086	5.448
1	1.431	1.899	2.689	4.081	5.417
10	1.424	1.875	2.668	4.046	5.326

4.3.2 Membrane Hydrophobicity

Membrane hydrophobicity is measure by contact angles, with smaller contact angles reflecting more hydrophilic materials. Contact angles for membranes tested are presented in Figure 4.1. The contact angles of the membranes decreased gradually from 78.46 ± 1.73° (pure GVL) to 60.01 ± 3.71° as the weight percent of PolarClean increased from 0% to 75%. The contact angle of membrane #5, pure PolarClean, was approximately 64.13 ± 2.08°, which is higher than the membrane #4. However, the contact angles of membranes #2 to #5 displayed overlapping standard deviations; therefore, the membranes

prepared using PolarClean, and PolarClean/GVL solvents mixture presented similar hydrophilicity. Moreover, the membranes prepared using GVL were significantly more hydropobic than the membranes prepared using PolarClean and PolarClean/GVL solvent mixtures.

Hydrophilicity represents the surface property of membranes. Since the polymer used and the weight percent of polymer in dope solution were same, the reason that PSf/GVL membranes had higher hydrophobicity may be that water is harder to penetrate a rougher surface with smaller pores. This agreed the results in the roughness and the average pore size sections.

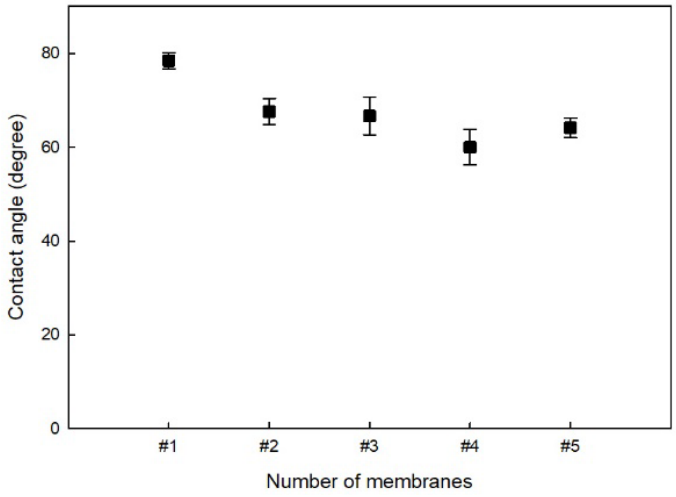

Figure 4.1 Contact angles of different membranes.

4.3.3 Membrane Surface Charge

The surface charge of membranes, measured by the zeta potential of the membrane, is an important factor in the designing of membranes because it can be manipulated to reject charged solutes via charge repulsion and aid in fouling control [220]. As shown in

Figure 4.2, the zeta potential value of membranes #1 to #5 were measured to be –10.58 ± 0.05 mV, –20.85 ± 1.34 mV, –21.32 ± 0.56 mV, –18.99 ± 0.26 mV, and –23.76 ± 0.41 mV, respectively. All the PSf membranes were negatively charged, which is desirable since most dissolved organic matter in water is negatively charged. It was noticed that the membranes prepared using PolarClean (#5) and PolarClean/GVL (#2 to #4) showed no significant difference with respect to surface charge, and showed higher negative charge density as compared to the membranes prepared using GVL alone (#1). This again shows that the addition of GVL to PolarClean produced membranes with properties closer to PolarClean alone membranes.

The reason that the surface charges are different with the same amount of polymer may be due to the use of GVL. The use of GVL may lead to less functional groups on the membrane surface than the circumstance of using PolarClean, which would account for the lower charge; however, this should be further verified.

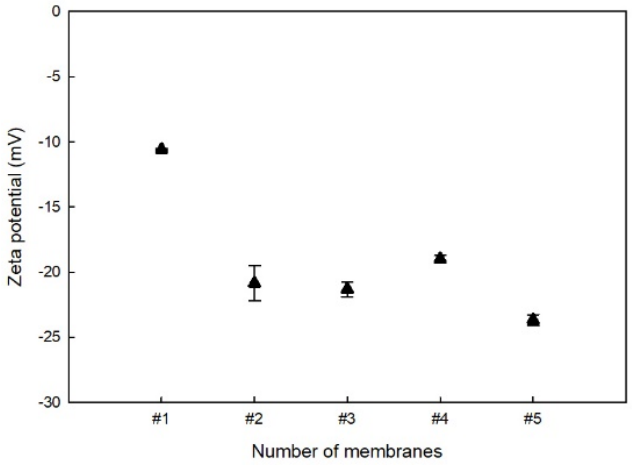

Figure 4.2 Zeta potential of different membranes.

4.3.4 Membrane Surface Roughness

The surface roughness was determined by the root-mean-squared (RMS) roughness of the surface of membranes, and is shown in Figure 4.3. The RMS roughness values of membranes #2 to #4 were measured as 72.46 ± 28.49 nm, 10.36 ± 4.78 nm, and 8.97 ± 6.15 nm, respectively. The RMS roughness value of membrane #1 was 39.78 ± 18.71 nm, whereas the value of membrane #5 was 30.55 ± 17.71 nm. The results indicate that the membranes prepared using pure PolarClean or GVL showed overlapping surface roughness values. When 25% GVL was added into the dope solutions, the membrane surface was smoothest. After adding GVL to 50%, the membrane surface became slightly rougher. The membrane surface was the roughest when 75% GVL was added to the dope solutions. The same conclusion could be observed from the 3D images of membrane surfaces shown in Figure 4.4.

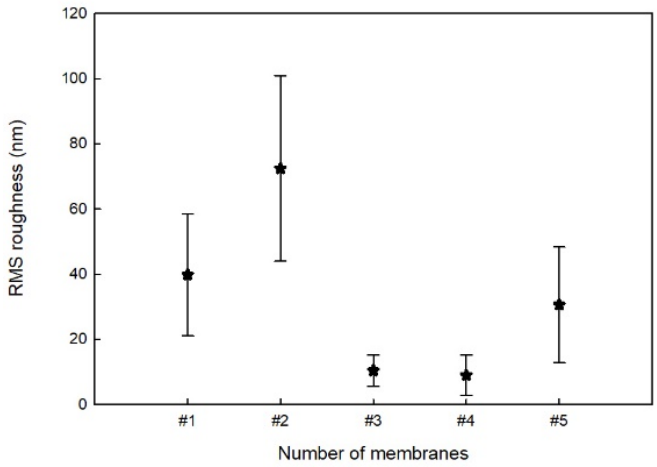

Figure 4.3 RMS roughness of membranes.

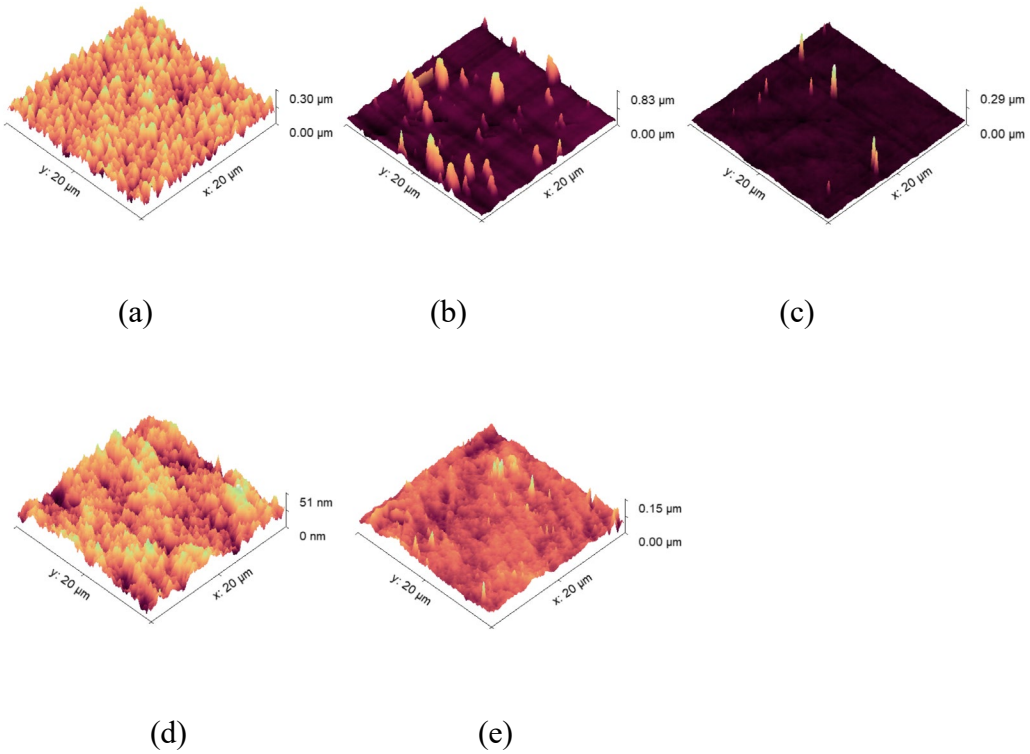

Figure 4.4 AFM 3D images of PSf membranes using different solvent: (a) GVL, (b) 25%PolarClean/75%GVL, (c) 50%PolarClean/50%GVL, (d) 75%PolarClean/25%GVL, and (e) PolarClean.

4.3.5 Membrane Average Pore Size

Figure 4.5 shows that the average pore size of membranes #1 to #5 was <1 nm, 1.7 nm, 9.3 nm, 21.8 nm, and 48.1 nm, respectively. For membrane #1 (GVL alone), the result was less than 1 nm since it was below the detection limit of the porometry. For membranes #2 to #5, the average pore size increased as a function of decreasing the GVL percentage in the dope solution.

The influence of weight percent of GVL in dope solutions on the average pore size of membranes may be due to the difference in the water solubility of the two solvents. At

room temperature, the water solubilities of PolarClean and GVL are larger than 490 g/L and larger than 100 g/L, respectively [131]. Therefore, a larger amount of PolarClean may diffuse into the water bath, resulting in larger pores on the membrane surface.

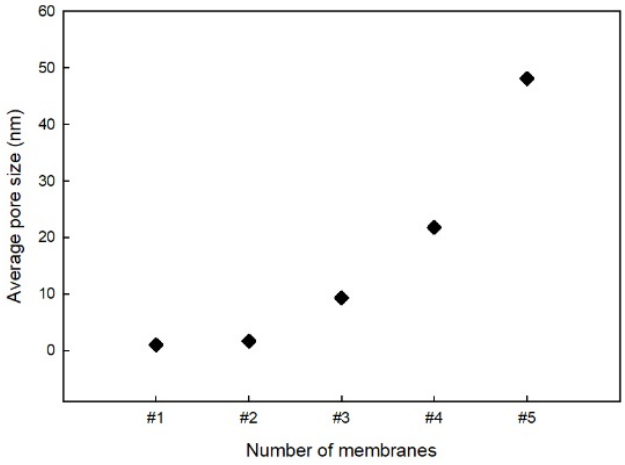

Figure 4.5 Average pore size of different membranes.

4.3.6 Filtration Performance

During the precompaction process, the pure water flux and the flux during BSA filtration were measured. In Figure 4.6, the DI water flux of membranes #1 to #5 was 0.53 ± 0.02 LMH, 33 ± 2 LMH, 320 ± 90 LMH, 500 ± 98 LMH, and 660 ± 84 LMH. The pure water flux increased with the increase in the amount of PolarClean in the dope solution. The tendency of increasing pure water flux from membranes #1 to #5 also agreed with the increasing average pore size of the membranes as shown in Figure 4.5.

The flux of membrane #1 was too low to continue the BSA filtration study. Therefore, membranes #2 to #5 were used to filter BSA solutions. The flux values of #2 to #5 were 29 ± 2 LMH, 198 ± 23 LMH, 258 ± 37 LMH, and 314±20 LMH, respectively. The

trend was similar to that observed with pure water. Moreover, the BSA rejection of all membranes were measured to all be above 99.9%. It should be mentioned that although the average pore size of PSf/PolarClean (#5) membranes was larger (as shown in Figure 4.5), the rejection rate was not significantly different because of the sponge-like structures of the membranes, as previously observed [20]. Other substances can be used to distinguish the size selectivity of different membranes in future work.

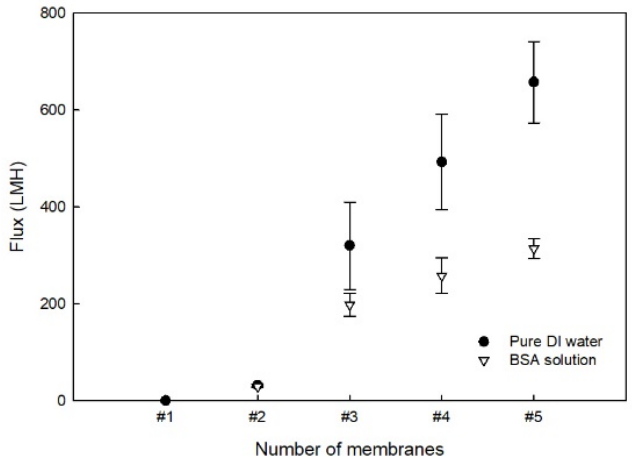

Figure 4.6 Average flux of different membranes.

4.3.7 Implications

Membranes fabricated using PolarClean alone were found to be similar to those made using traditional petroleum-derived solvents with respect to flux and solute rejection. However, the pores of these membranes may collapse during filtration [20]. Thus, GVL was investigated as an individual and as a co-solvent to PSf membranes. Membranes made using GVL as a sole solvent were observed to be gelatinous, so they were not likely to be mechanically strong for filtration. On the other hand, the mixture of these two solvents seemed to be promising, as the hydrophilicity and charge of fabricated membranes were

determined to be similar with the membranes using PolarClean. Moreover, membranes fabricated using mixtures (50%PolarClean/50%GVL and 75%PolarClean/25%GVL) showed a smoother surface than membranes made using PolarClean alone. The average pore size of the membranes using mixtures was within the range of membranes using GVL or PolarClean.

The results of the membranes prepared using the mixture of green solvents showed their potential to replace petroleum-derived traditional solvents, which can make the process of membrane fabrication eco-friendlier. Therefore, using these two solvents can reduce dependency on petroleum products; hence, the price of petroleum would not influence the cost of manufacturing membranes. The use of environmentally friendly solvents also has the potential to lessen environmental impacts and reduce the carbon footprint of membranes. Moreover, the utilization of PolarClean and GVL is a method to use by-products [130] and biowastes [132, 221] from the chemical and agricultural processes; thus, finding uses for what would otherwise be waste to be disposed. Due to these reasons, fabricating membranes using PolarClean and/or GVL supports the principles of green chemistry [222, 223].

On the other hand, there are drawbacks and concerns toward the use of green solvents. From the most updated (July 20, 2018) prices listed online (www.alibaba.com): PolarClean is approximately $6/kg; GVL fluctuates around $2/kg; NMP is about $2.7/kg; and the price of DMAc is around $1/kg. The cost of distillation of these different solvents should be investigated and compared to determine the economic feasibility of solvent recovery. Lastly, these solvents are biodegradable, so they may cause eutrophication of receiving waters.

4.4 Conclusions

As an individual solvent, PSf/GVL membranes showed an average zeta potential value of –10.58 ± 0.05 mV, while PSf/PolarClean membranes showed –23.67 mV ± 0.41 mV. The average contact angle of PSf/GVL membranes was 78.46 ± 1.73°, while PSf/PolarClean showed 64.13 ± 2.08°. The average pore size of PSf/GVL membranes was less than 1 nm, while it was 48.1 nm for PSf/PolarClean membranes. The surface roughness of PSf/PolarClean and PSf/GVL membranes were overlapping. The addition of GVL in dope solutions was able to significantly decrease the viscosity of dope solutions, which is desirable because the viscosity of dope solutions prepared using traditional petroleum-derived solvents, NMP and DMAc, were lower than the viscosity of PSf/PolarClean dope. The zeta potential values and the contact angles did not vary significantly by adding GVL to dope solutions. On the other hand, the surface roughness of membranes prepared using GVL/PolarClean solvent mixtures varied significantly, with the smoothest membranes arising from the 75% PolarClean/25% GVL solvent mixture in the dope solution. Lastly, the average pore size of the membranes decreased as the weight percent of GVL in dope solutions increased. Therefore, the use of PolarClean and GVL as co-solvents for PSf membrane fabrication has the potential to be a promising replacement to traditional solvents, and to be a better option than using PolarClean or GVL alone.

CHAPTER 5. COMPARISON OF TWO LOW-HAZARD ORGANIC SOLVENTS AS INDIVIDUAL AND CO-SOLVENTS FOR THE FABRICATION OF POLYSULFONE MEMBRANES

This chapter has been published in the following report and adapted with permission from:

Dong, X.; Shannon, H.D.; Parker, C.; De Jesus, S.; Escobar, I.C. Comparison of two low-hazard organic solvents as individual and cosolvents for the fabrication of polysulfone membranes. *AIChE J*. 2020; 66:e16790. [224]

5.1 Introduction

Membranes possess the ability to treat a wide variety of source waters such as brackish and seawater for desalination[83, 225-227], as well as low quality surface water[228] and even wastewater[229-231]. They can produce water that is of higher quality than traditional water treatment processes, such as coagulation, flocculation, sedimentation, sand filtration, etc. For this reason, membranes and membrane processes have gained much popularity in recent years. In liquid separations, polymeric membranes tend to be widely used. For example, ultrafiltration (UF) commercial membranes are made of selective layers ranging from highly hydrophilic polymers such as cellulose acetate (CA), to hydrophobic polymers such as polypropylene (PP) and polyethylene (PE). Various polymers with intermediate hydrophilicity such as the polysulfone (PS) / polyether sulfone (PES) family, polyacrylonitrile (PAN) and polyvinylidene fluoride (PVDF) are also used as selective layers for the membranes.

To cast the polymeric membranes in a laboratory scale, different methods have been investigated, for instance, non-solvent induced phase separation (NIPS)[232], temperature

induced phase separation (TIPS)[21], vapor induced phase separation (VIPS)[233], etc. In this study, NIPS was chosen to fabricate polymeric membranes, as shown in Figure 5.1. First, a solvent is used to dissolve a certain concentration of polymers to form a homogenous dope solution. Then, the dope solution is deposited on a substrate and then cast using a doctor's casting blade to form a thin liquid film on a substrate, which is immersed into a non-solvent bath. The solubilities of the polymer and solvent are different; therefore, the solvent diffuses into the non-solvent while the polymer remains on the substrate to form the polymer film, which is the membrane. However, in this process, the solvent remains in the non-solvent. If the solvent is toxic or environmentally hazardous, the mixture of solvent/non-solvent threatens not only the environment, but also the health of operators[1]. Currently, traditional solvents are derived from petroleum, such as N-methyl-2-pyrrolidone (NMP), dimethylacetamide (DMAc), dimethylformamide (DMF) etc., are used for the NIPS process. The toxicity profiles of these solvents are well-known and have been discussed in the previous studies[234-237]. However, due to their highly toxic nature, the European Registration, Evaluation, Authorisation and Restriction of Chemicals (REACH) has banned the use of NMP and DMAc by 2020 and listed the use of DMF on the watching list[46]. Therefore, the search for low-hazard/low toxicity solvents to substitute traditional solvents in membrane fabrication is necessary and urgent.

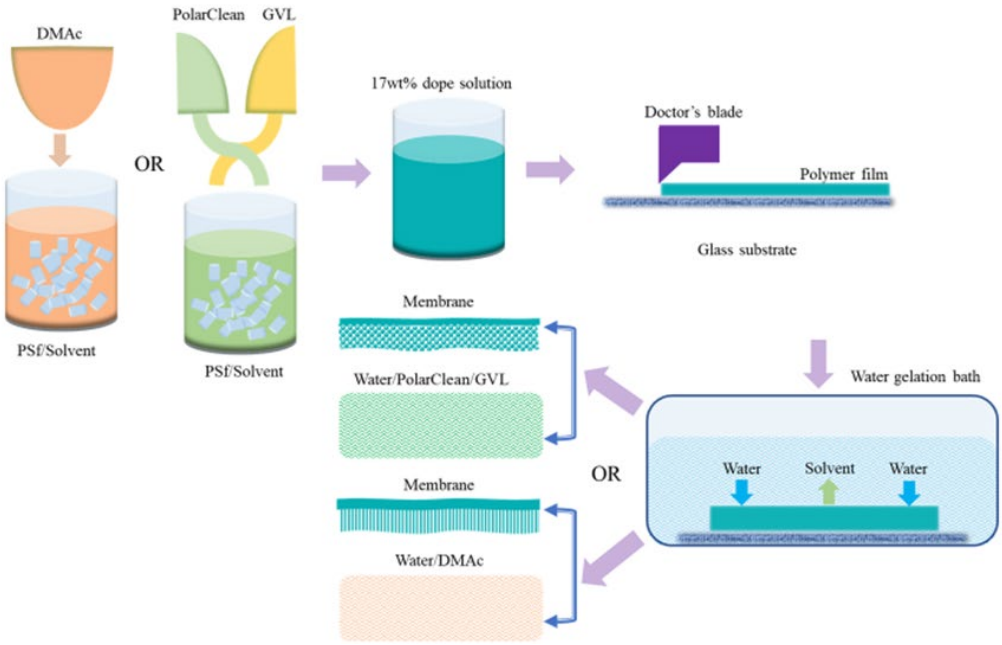

Figure 5.1 NIPS process using green solvents or a traditional solvent

Multiple solvents have been explored in the fabrication of polymeric membranes in the recent years. In previous studies, several low-hazard solvents have been studied, including methyl lactate, ehtyl lactate, triethylphosphate (TEP), ionic liquids (ILs), etc[46]. Recently, additional ones have been reported. Marino et al.[238] presented dihydrolevoglucosenone (Cyrene^{TM}) to cast polyethersulfone (PES) and poly(vinylidene fluoride) (PVDF) membranes via the VIPS/NIPS method. Cyrene^{TM} was synthesized from cellulose and had a nontoxicity, environment-friendly profile. PES and PVDF membranes cast using Cyrene^{TM} were characterized and showed that Cyrene^{TM} was a promising option for casting PES and PVDF membranes; however, these membranes were not used in filtration experiments. Recently, dimethylsulfoxide (DMSO) has become the focus of several studies. Xie et al.[45] used DMSO to partially replace traditional solvents to cast poly(vinyl chloride)-graft-poly(ethylene glycol) methyl ether methacrylate (PVC/PVC-g-

PEGMA) UF membranes via the NIPS method. The reason to partially instead of fully replacing traditional solvents was that DMSO cannot dissolve PVC, so traditional solvents were still needed. Evenepoel et al.[239] proposed DMSO as a benign solvent to replace NMP in the fabrication of PES ultrafiltration membranes and, potentially, nanofiltration membranes. Marino et al.[240] reported an improved version of DMSO, DMSO EVOL™ in casting PES microfiltration membranes via the NIPS/VIPS method. Dong et al.[46] investigated Methyl 5-(dimethylamino)-2-methyl-5-oxopentanoate (Rhodiasolv® PolarClean) and gamma-valerolactone (GVL) for PSf membrane fabrication, but found that PolarClean made membranes that did not stand well to reverse-flow filtration while GVL was not effective for the casting of PSf membranes. Lastly, Rasssl et al.[136] theoretically explored GVL and glycerol derivatives as environment-friendly solvents for membrane preparation using different polymers; however, fabricted membranes were not fullly characterized or analyzed.

In this study, PSf was chosen because PSf membranes can be applied over a wide pH range from 2 to 12 and can be used at temperatures up to 105 ℃[20, 46, 158, 241, 242]. PSf is also resistant to chlorine oxidation[241, 243-245]. Moreover, PSf is commercially available and has been widely used. However, casting PSf membranes using low-hazard solvents has not been significantly explored as compared to PVDF and PES membranes. Therefore, an in-depth investigation of low-hazard solvents, namely PolarClean and GVL, as compared to a traditional petroleum-derived solvent, DMAc, for the fabrication of PSf membranes was the main objective of this study. The chemical structures of DMAc, PolarClean and GVL are shown in Figure 5.2, and their chemical/physical properties are shown in Table 1. PolarClean is the byproduct of the manufacturing process of Nylon 6-6,

and it is an environment-friendly product commercialized by Solvay Novecare. GVL is a bio-derived solvent from lignocellulosic biomass, specifically, from hemicellulose and cellulose. Hemicellulose is converted to furfural and furfural alcohol as intermediates by acid hydrolysis, and then furfural alcohol is esterified with ethanol to produce ethyl levulinate[132-134]. Cellulose is converted to hydroxymethylfurfural (HMF) as an intermediate and then converted to levulinic acid also through acid hydrolysis[133, 135]. Both ethyl levulinate and levulinic acid are hydrogenated to GVL[132]. While this current method of producing GVL can minimize the use of petroleum-derived products, it is not sustainable because of high energy consumption and water usage[246], as well as the requirement of strong acidic catalysts[247]. However, more sustainable approaches to produce GVL are currently being investigated[221].

In this work, the term "low hazardous" refers to low toxicity to human contact. The Globally Harmonized System (GHS) classification, toxicity of PolarClean, GVL and DMAc, shown in Table 1, verify that PolarClean and GVL have lower toxicities as compared to DMAc. PolarClean was classified as H319 because its use might lead to eye irritation[130, 248], while GVL did not meet the GHS hazard criteria[249, 250]. On the other hand, DMAc was classified as H312, H332 and H360D[251]; that is, harmful in contact with skin, harmful if inhaled and may damage unborn children, respectively. Furthermore, all of these three solvents are reported as biodegradable in the environment and will not cause bioaccumulation[248, 250, 251]; however, biodegradable compounds might lead to eutrophication. Regarding toxicity to fish, the lethal concentration required to kill 50% of population is defined as LC50. For DMAc, the LC50 is >500 mg/L after an

exposure time of 96 h[251]. There are no reported GVL and PolarClean studies on their toxicity to fish.

Since in the previous studies, membranes produced using PolarClean suffered from pores collapsing during filtration and backwash, while those fabricated using GVL hydrolyzed, PolarClean and GVL were investigated as co-solvent, here, to cast PSf membranes and then compared to the membranes cast using DMAc.

Figure 5.2 Chemical structure of (a) DMAc, (b) PolarClean, and (c) GVL

Table 5.1 Properties of solvents studied here

Properties	DMAc	PolarClean	GVL	Water
CAS no.	127-19-5	1174627-68-9	108-29-2	7732-18-5
Formula	C_4H_9NO	$C_9H_{17}NO_3$	$C_5H_8O_2$	H_2O
MW (g/mol)	87.122	187.239	100.112	18.02
Density (g/mL) at 25°C	0.94	1.043	1.05	0.997
Viscosity (mPa·s)	0.945	9.78	2.18	0.890
Boiling point (°C)	165	278–282	207–208	100
Flash point (°C)	69	144–146	96	
Solubility in water (%)	Miscible	Miscible	Miscible	
Signal	Danger	Warning	Warning	
Toxicity	Reproductive toxicity			

5.2 Experimental

5.2.1 Materials

The polymer used was PSf (average MW 35000 by LS, average Mn 16000 by MO, pellets) purchased from Sigma-Aldrich (St. Louis, Missouri, United States). Three solvents were investigated in this study, (1) GVL, purchased from Acros Organics (Fair Lawn, New Jersey, United States); (2) Rhodiasolv® PolarClean, provided by Solvay Novecare (Princeton, New Jersey, United States); and (3) DMAc, purchased from Tokyo Chemical Industry Co., Ltd. (Tokyo, Japan). Lastly, to study the filtration performance of membranes, bovine serum albumin (BSA), purchased from VWR Life Science (Radnor, PA, USA), was used. Grade I deionized water (DI) of resistivity of 18.2 mΩ • cm at 25℃ was provided by the Chemical Engineering Undergraduate Laboratory at University of Kentucky.

5.2.2 Mixing Studies

Based on the Hansen solubility parameter theory, the affinity of a polymer and a solvent is described as R_a, which is calculated by equation 1:

$$R_a = \sqrt{4(\delta_{d2}-\delta_{d1})^2 + \left(\delta_{p2}-\delta_{p1}\right)^2 + (\delta_{h2}-\delta_{h1})^2} \quad (1)$$

Where δ_d is the dispersive force, $\delta_p$is the polar force, and δ_h is hydrogen bonding[141]. A solvent is deemed to have good compatibility with a polymer when the value of R_a is small[136, 141]. In this study, PSf was dissolved using two co-solvents simultaneously (i.e., a binary solvent mixture) instead of a single solvent. Therefore, the corresponding parameters of the binary solvent mixture needed to be calculated by the two following

procedures: first, the volume fraction of each solvent was calculated by equations 2 and 3; second, the values of solubility parameters were then calculated using equation 4, 5, and 6[141]:

$$V_1 = \frac{W_1/\rho_1}{W_1/\rho_1+W_2/\rho_2} \quad (2)$$

$$V_2 = \frac{W_2/\rho_2}{W_1/\rho_1+W_2/\rho_2} \quad (3)$$

$$\delta_d = V_1\delta_{d1} + V_2\delta_{d2} \quad (4)$$

$$\delta_p = V_1\delta_{p1} + V_2\delta_{p2} \quad (5)$$

$$\delta_h = V_1\delta_{h1} + V_2\delta_{h2} \quad (6)$$

Where 1, 2 represents solvent 1 and solvent 2; V_i represents the volume fraction, and W_i represents the weight fraction.

In Hansen solubility parameter theory, three parameters of a polymer or solvent form a sphere[141]. The relative energy difference (RED) is used to describe the interaction between a polymer and a solvent[45]. A good solvent for a polymer is defined as having a RED value less than or equal to 1, which can be calculated by equation 7[20, 141]:

$$\text{RED} = \frac{R_a}{R_0} \quad (7)$$

Where R_o represents the radius of the Hansen solubility parameter sphere for the polymer.

5.2.3 Preparation of dope solutions

The following combinations of solvents and co-solvents were used to dissolve PSf: (1) PolarClean, (2) 75 wt% PolarClean/25 wt% GVL, (3) 50 wt% PolarClean /50 wt%

GVL, (4) 25 wt% PolarClean/75 wt% GVL, (5) GVL, and (6) DMAc. The weight percentages of polymer and solvent were maintained constant at 17% and 83%, respectively, for proper comparison of membranes. These weight percents of polymer and solvent were chosen to cast ultrafiltration membranes based on literature recipes[20, 46], and the different compositions were labeled M1-M6 as shown in Table 2. Each dope solution was mixed using a magnetic stirring bar at 65℃ for 72 h.

In order to study PSf dissolution kinetics in different solvents/co-solvents, 2 mL samples were taken at 1 h, 2 h, 3 h, 4 h, 6 h, 8 h, 16 h, 24 h and 72 h, and the viscosity of each sample was measured using a rheometer (AG-G2, TA instrument, Delaware, United States) at the shear rate of 1/s. This experiment was triplicated for reproducibility. M4 was not included in the dissolution study due to the previous study showed the recipe was not ideal to fabricate PSf membranes[46]. The concept of Normalized viscosity (NV) is introduced here to represent the homogeneity and estimate the required mixing time of different dope solutions. To calculate NV, the ultimate viscosity (as defined by the viscosity at the 72^{th} hour) of each dope solution was used as the baseline for homogeneity and, hence, complete dissolution. Viscosities were then measured as a fraction/percentage of the ultimate viscosity, which was called NV.

Table 5.2 Recipes of PSf/solvent membranes (all dope solutions were made using 17% PSf and 83% solvent)

Weight percent (%)	M1	M2	M3	M4	M5	M6
PSf	17	17	17	17	17	17
PolarClean	83	75%×83	50%×83	25%×83		
GVL		25%×83	50%×83	75%×83	83	
DMAc						83

5.2.4 Fabrication of membranes

After dope solution homogeneity was achieved, based on 90% NV (i.e. dope viscosity equal to 90% of the ultimate viscosity of the dope after 72 hours of mixing), the membranes were cast using the NIPS method, as shown in Figure 5.1. In this study, distilled water was used as the non-solvent. Briefly, dope solutions were first degassed in an ultrasonic bath at room temperature for 1 h to remove air bubbles. Then, a small amount (approximate 3 mL) of dope solution was poured on a glass plate and cast using an aluminum casting knife. The gap of the casting knife was set at 200 μm. Thin films produced were evaporated for 30 seconds for consistency before immersion into the distilled water/non-solvent bath in order to allow phase inversion to occur. The thickness of produced membranes was measured using a thickness gage with the thickness range of 100-130 μm. The thickness of membrane was less than the gap of the casting knife because

the casting knife was applied on the liquid dope with 83 wt% solvent in it, while after phase inversion occurs, only the solid polymer was left on the glass substrate. Fabricated membranes were stored in DI water for a week before use.

In this case, the gap of the casting knife was set at 200 μm but the membranes obtained were about 100-130 μm, which is an acceptable range for membranes prepared using the NIPS method[232]. A mass balance was used to analyze the thickness under the following two lower and upper boundaries: (1) if there were no pores in the structure (a film formed with polymer without any void/microvoid space), the thickness should be the doctor's blade thickness setting multiplied by the polymer weight percentage, or 200 × 17% = 34 μm; (2) if the solvent diffused into the non-solvent while the membrane structure was maintained as liquid film, the thickness should be the setting of the doctor's blade, or 200 μm[232, 252]. The thickness of 100-130 μm is in between the boundaries, meaning that after depositing on the substrate and before immersion into the nonsolvent bath, the dope solutions spread on the substrate[253], which might have decrease the thickness. Furthermore during phase inversion, the solvent diffused into the nonsolvent, and resulted in some of decrease of the thickness of the film[20, 232, 252].

5.2.5 Membrane Characterization

Membranes were characterized using several different techniques to determine how similar or different membranes fabricated using different solvents/co-solvents were. The membrane fabricated using DMAc was set as the standard since this solvent is commercially used[20]. Therefore, optimal membrane recipes were defined as being most

similar to DMAc membranes with respect to roughness, pore size distribution, morphology, hydrophobicity and surface charge.

5.2.5.1 Roughness

The topography of membranes is measured at the atomic scale to characterize the roughness on the membranes surface. The surface roughness values of the six membranes (M1- M6) were measured using an atomic force microscope (AFM, Quesant Instrument Co., United States). The surface roughness was measured under the tapping mode and then evaluated by root-mean-squared (RMS) roughness. Six areas of 20 × 20 μm on each membrane surface were randomly chose and measured.

5.2.5.2 Surface pore analysis

The pore size on the selective layer of a membrane is used to estimate the selectivity of a membrane based on size exclusion. The surface pores of membranes were measured using a Liquid-Liquid porometer (LLP-11000A, Porous Materials Incorporated, Ithaca, New York, United States). Two immiscible wetting liquids, silwick (purchased from PMI, Ithaca, New York, United States) and isopropyl alcohol (IPA, purchased from VWR international), were used for the measurement. The membranes were wetted with silwick for ten minutes, and IPA was pressurized to displace the silwick in the membrane pores. The pressure was increased gradually from 0 kPa to 5400 kPa. The silwick was forced to flow through the pores and the amount was measured using a balance equipped in the porometer. The mean flow pore diameter and bubble point pore diameter were used to represent the mean value of pore size and the largest pore on the membrane surface.

5.2.5.3 Morphology

To prepare membrane samples for SEM image, the PSf membranes were immersed and fractured in liquid nitrogen, freeze dried overnight and then sputtered with palladium for 4 minutes. The surfaces and the cross sections of the PSf membranes were observed by a scanning electron microscope (SEM, Hitachi S-4300 from Hitachi Group, Troy, MI, USA). All the images were presented as a scale bar of 50 μm.

5.2.5.4 Hydrophilicity

The contact angle was characterized to represent hydrophilicity of the membranes. It was measured by the sessile drop method using a drop shape analyzer connected to a high definition camera (DSA 100S, Kruss Company, Hamburg, Germany.) One drop water of 12 μL was deposited on the membrane surface. The interface between the water drop and the membrane surface was captured by the camera and the contact angle was calculated according to the image. The measurement was repeated six times and then the average values and deviations were calculated.

5.2.5.5 FTIR

Attenuated total reflectance-Fourier transform infrared spectroscopy (ATR-FTIR, Thermo Nicolet iS50 FTIR Spectrometer, Thermo Scientific, Waltham, Massachusetts, USA) was performed to characterize the surface structure of membranes prepared using different solvents. A piece of each PSf membrane was freeze dried overnight and then placed on ATR-FTIR crystal (diamond) for analysis. The absorbance spectra of different membranes were normalized [153-156] and then adjusted in the same figure for comparison.

5.2.5.6 Permeability and separation performance

While characterization comparisons determine which membranes are chemically and morphologically similar, filtration experiments were used to investigate operational similarities between membranes cast using the solvents/co-solvents. Filtration experiments were performed using a dead-end filtration cell (Amicon Stirred Cell 50 mL, UFSC05001, provided by Millipore Sigma, Burlington, MA, United States). First, a circular membrane piece with diameter of 44.5 mm and effective area of 13.4 cm^2 was cut. Then, 20 mL of deionized water were filtered through the membrane for precompaction[20, 254, 255], followed by 20 mL of 1 g/L BSA. All experiments were performed at a pressure of 400 kPa under room temperature. The permeability was recorded for every 2 mL of permeate samples. The concentrations of BSA in the feed and permeate were analyzed using a UV/Vis spectrophotometer (UV-6300PC, VWR International bvba/sprl, Leuven, Belgium) at a wavelength of 277 nm in order to calculate the rejection of BSA. The experiments were triplicated.

After the BSA filtration, reverse flow filtration using deionized water was performed at 200 kPa for 30 minutes to remove any reversibly attached BSA (i.e. reversible fouling) from the membranes. Then, flux recovery ratio (Re, %) was calculated to characterize the resistance of the fouled membrane.

5.3 Results and Discussion

This chapter focused on the fabrication of ultrafiltration membranes, using viscosity to characterize the kinetics of the dope solution mixing process, using normalized viscosity as a parameter to determine the homogeneity of dope solution, and the influence of viscosity of dope solutions. Therefore, to isolate the impact of viscosity on the above-

mentioned parameters, we kept all the other parameters unchanged. The thickness of membranes was maintained at 100-130 μm. Furthermore, 17 wt% PSf dope solution, which is approximately 14.6 volume percent, was chosen based on literature studies that show this is suitable for the fabrication of ultrafiltration membranes[20, 46].

5.3.1 Mixing Studies

R_a and RED values for dope solutions made by mixing polysulfone and different solvents, including individual solvents and co-solvents, were calculated using the Hansen Solubility Parameter theory and are shown in Table 3. Ra represents the affinity of a polymer and a solvent, with high affinity being calculated as a small R_a value because it requires that the solubility parameters of the polymer and solvent need to be similar, based on the equation (1). Likewise, a good solvent for a polymer has a RED value smaller than or approximately 1 because it represents that the interaction between solvent and polymer is within the sphere of the polymer. The similarity of polymer and solvent results in a good affinity[136, 141].

For baseline, R_a and RED values were calculated for the traditional solvent DMAc, and were 6.9 $MPa^{1/2}$ and less than 1, respectively. RED values of PolarClean and GVL were slightly larger than 1, which indicated that PolarClean and GVL might not be ideal as sole solvents for PSf. However, when PolarClean and GVL were used as co-solvents, the RED values dropped to below 1, which indicated that the co-solvents may be a promising option. The reason is that the Ra value is calculated by three parameters, δ_d, δ_p, and δ_h. The difference of the dispersive force between PSf and PolarClean is 3.9 $MPa^{1/2}$, which is larger than the difference between PSf and GVL (0.7 $MPa^{1/2}$). Likewise, the

difference of the polar force between PSf and PolarClean is 2.4 $MPa^{1/2}$, less than the difference between PSf and GVL (8.3 $MPa^{1/2}$). The difference between PSf and PolarClean is the same with PSf and GVL at 0.9 $MPa^{1/2}$. By using them as co-solvents, the differences of dispersive forces and polar forces decreased, leading to a decrease in the RED values of the PSf/co-solvent systems. It implicated that, theoretically, the use of PolarClean and GVL as co-solvents might be a promising option. The lowest RED value was obtained at 50% PolarClean and 50% GVL, as shown in Table 3.

Table 5.3 R_a and RED values of polymer, solvents and co-solvents used in this study

Polymer	δ_d ($MPa^{1/2}$)	δ_p ($MPa^{1/2}$)	δ_h ($MPa^{1/2}$)	R_o ($MPa^{1/2}$)		
PSf	19.7	8.3	8.3	8.0		
Solvent	δ_d ($MPa^{1/2}$)	δ_p ($MPa^{1/2}$)	δ_h ($MPa^{1/2}$)	R_a ($MPa^{1/2}$)	RED	Membrane label
PolarClean	15.8	10.7	9.2	8.2	1.03	M1
75% PolarClean 25% GVL	16.6	12.2	8.8	7.3	0.92	M2
50% PolarClean 50% GVL	17.4	13.6	8.3	7.1	0.88	M3
25% PolarClean 75% GVL	18.2	15.1	7.9	7.5	0.93	M4
GVL	19.0	16.6	7.4	8.5	1.06	M5
DMAc	16.8	11.5	10.2	6.9	0.86	M6
Water	15.5	16.0	42.4	36.0	4.49	

5.3.2 Dissolution kinetics

The achievement of a homogeneous dope solution is the key to the fabrication of polymeric membranes since it prevents the formation of defects during casting. In this study, viscosity was used as the parameter to demonstrate the dissolution process of the PSf/solvent system since viscosity is related to water transport during phase inversion. The viscosity of polymeric dope solution reflects hydrogen bonds in between the solvent and polymer[123, 256]. High viscosities are undesirable since they retard the transport of water during phase inversion and ultimately form dense outer layers. At the beginning of dissolution, the solvent and the polymer are not fully in contact with each other. Therefore, in this stage, the viscosity of the dope solution mainly reflects the viscosity of solvents. As time moves along the dissolution process, the polymer swells, so the polymer and solvent diffuse into each other[257]. The viscosity increases exponentially during the swelling phase because hydrogen bonds increase exponentially with the diffusion of polymer/solvent. Once the polymer fully swells and the polymer/solvent is fully diffused, an equilibrium state is reached, and the viscosity of dope solution reaches its highest sustained value.

Dope viscosities as a function of time are shown in Figure 5.3. It needs to be mentioned that 25wt% PolarClean/ 75wt% GVL (M4) was not included in Figure 5.3- 5.5 because this recipe was proved not ideal for PSf fabrication based on the reported study[46]. As previously stated, the dope solution made using DMAc was used as baseline for comparison. During mixing, the viscosity of PSf/DMAc dope solution mainly increased during the 2nd hour, from 0.069 to 0.174 Pa·s, and then remained approximately constant at 0.18 - 0.19 Pa·s; therefore, homogeneity was achieved after two hours of mixing. On the

other hand, the viscosity of PSf/PolarClean dope solution increased gradually during the first 8 hours, then increased exponentially from 8^{th} h (0.45 Pa·s) to 24^{th} h (5.50 Pa·s), indicating that PolarClean required additional dissolution time to reach dope homogeneity. Another observation was that PolarClean led to the most viscous dope solutions, which poses issues during casting[50, 253]. The PSf/GVL dope solution increased majorly during 2^{nd} h to 6^{th} h, from 0.12 to 1.18 Pa·s and then remained approximately constant, which was faster than the PSf/PolarClean dope solution. However, it is important to note that GVL is not desirable when water is the non-solvent to cast membranes[46], which is needed to keep the NIPS process greener; therefore, co-solvents were investigated.

When PolarClean and GVL were used as co-solvents, the viscosity of the produced dope solutions stayed in between the individual curves for PolarClean and GVL, as shown in Figure 5.3. At the beginning of the mixing, the standard deviations were large (average viscosity and their corresponding standards). Therefore, there was no significant decrease in the viscosity when comparing M2, M3 and M5. The most likely reason for this initial large standard deviation might be because dope solutions might not have yet reached equilibrium mixing, so individual samples used to measure viscosity might not have been representative of the mixture. The large standard deviation supported the notion that the mixing process required a minimum period of time for the polymer to swell and diffuse with the solvent.

Both co-solvent dopes showed similar trends of viscosity increasing during the first 24 h, before reaching homogeneity and constant viscosity values. Therefore, while the use of PolarClean/GVL as co-solvents did not change the time required for the dissolution process/homogeneity, as measured by reaching a constant viscosity values, of PSf dope

solutions, it did decrease the ultimate viscosity of the dope solution. While the ultimate viscosities of the co-solvent dope solutions still were over one order of magnitude higher than PSf/DMAc, they were lower than that of PolarClean alone.

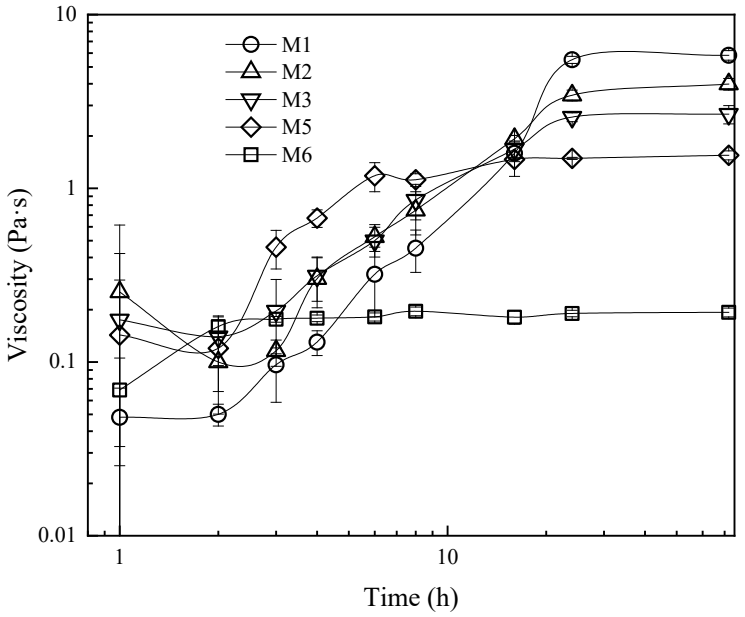

Figure 5.3 Viscosity changes of dope solutions as a function of time

The effect of the use of co-solvents on reaching complete dissolution/homogeneity was deconvoluted for adequate comparison using the concept of normalized viscosity (NV), as shown in Figure 5.4. For each dope solution, the ultimate viscosity (as defined by the viscosity at the 72th hour) was used as the baseline for homogeneity and, hence, complete dissolution. Viscosities were then measured as a fraction/percentage of the ultimate viscosity, called NV. For M6, 3 hours were required to achieve 90% of the ultimate viscosity, and 8 hours later, the NV was 100%, indicating a completely dissolved polymer. For M1, NV values were at 7.7% at the 8th h, 27.3% at the 16th h, and 98.4% at the 24th h.

For M5, NV values were 7.5%, 72.2% and 94.6% at the 2nd, 16th and 24th h, respectively. For the co-solvents, NV values of 75 M2 were 18.8% after 8 h and 48.4% after 16 h, while the NV values of M3 were 32.0% after 8 h and 62.7% after 16 h. It was observed that after 8 h and 16h, NV values were M5>M3>M2>M1. The reason might be that the dispersive forces and polarity of solvents increased as the weight percent of GVL increased, as shown on Table 3. At 24 h, all the dope solution displayed NV values at or over 90%, indicating that the dope solutions were mostly homogenous.

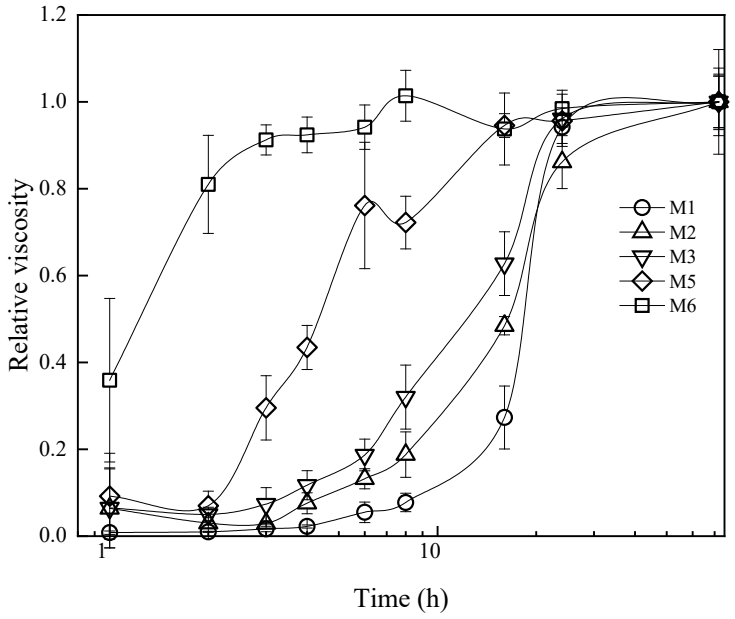

Figure 5.4 Related viscosity (RV) changes of dope solutions as a function of time

In a laboratory setting, a casting knife is usually manually controlled. In this case, a Newtonian fluid is preferred because the viscosity does not change as a function of shear rate; moreover, it is difficult to control the shear rate manually. However, the effect of shear rate on viscosity is important since it defines large-scale casting conditions. Therefore, the

behavior of viscosity changes as a function of the shear rate was investigated in Figure 5.5. The viscosity of PSf/DMAc and PSf/PolarClean dope solutions did not change significantly as a function of shear rate over the 0.1 /s to 10 /s range, which supported that the dope solutions were Newtonian fluids. On the other hand, the viscosity of PSf/GVL decreased from 1.69 to 1.27 Pa·s, a 24.8% decline, which meant that the PSf/GVL dope solution showed shear thinning behavior, an undesirable trait for laboratory casting[253]. However, when PolarClean/GVL were used as co-solvents, the dope solutions were Newtonian fluids because the viscosity of these solutions did not change as a function of shear rate, as shown in Figure 5.5.

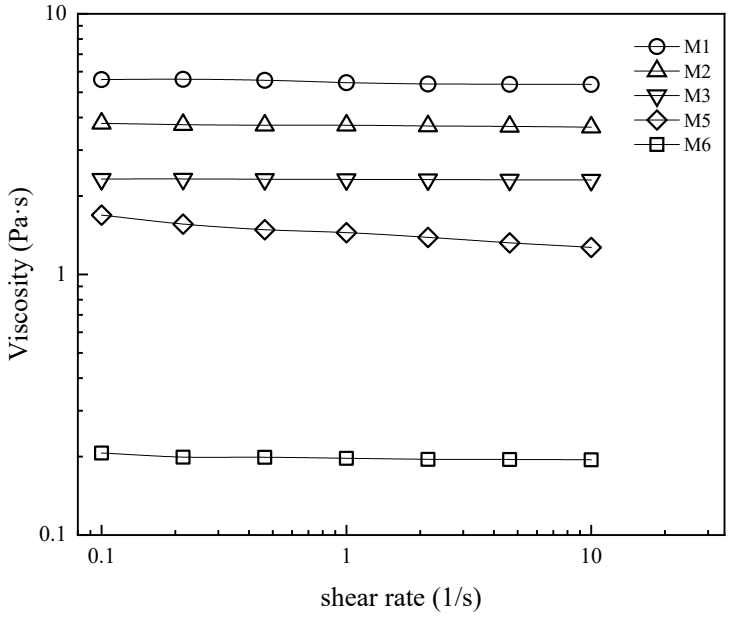

Figure 5.5 Viscosity changes as a function of shear rate

5.3.3 Morphology (SEM surface images)

In Figure 5.6, SEM images showed that from a large scale (50 μm), none of the membranes fabricated using the dope/solvent recipes shown in Table 3 showed any defects, which indicated that the solvents were effective to cast defect-free membranes. There were likely some impurities on the surfaces of M5 and M6 that were visible under SEM, but were deemed not to influence membrane properties. The topology was analyzed in detail using AFM. Pores were not observed on the images at this scale, which meant that the pores were likely less than 1 μm and were studied further using porometry.

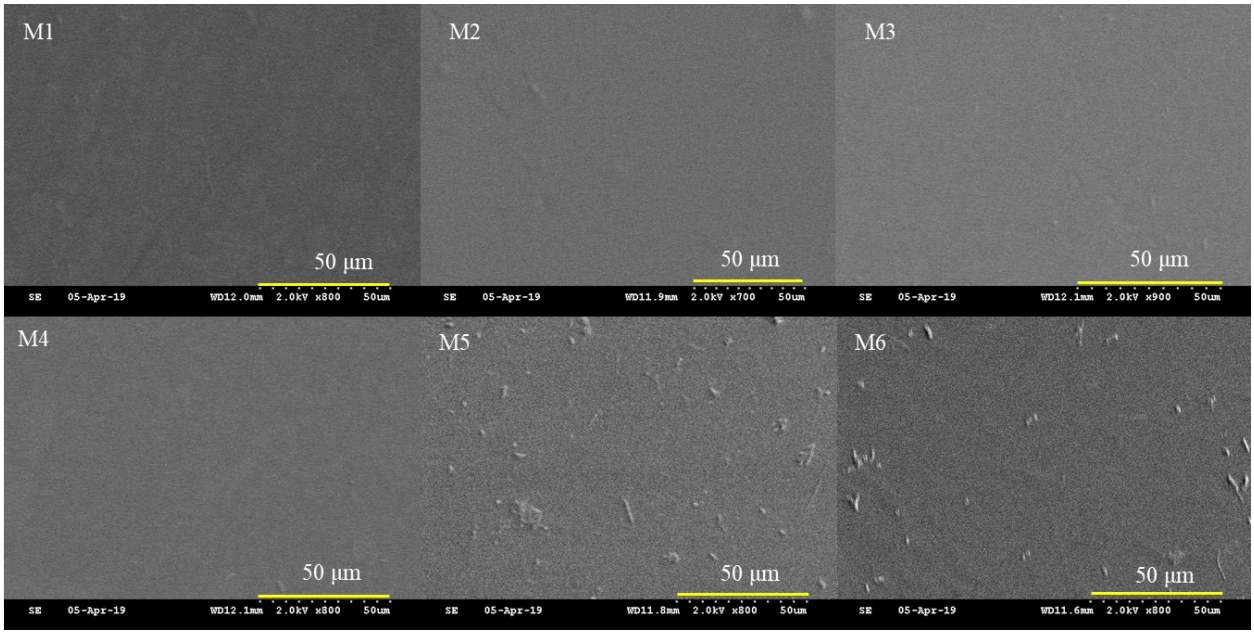

Figure 5.6 Surface SEM images of membranes

5.3.4 Pore size analysis

The bubble point pore diameter refers to the largest pore size on the membrane surface, while the mean pore diameter refers to the mean size of the pores on the surface. It was measured that the bubble point pore diameter of M5, the PSf/GVL membrane, was

less than the instrument limit of 1 nm. From M1 to M4, the mean pore diameter was measured to be 48.1, 21.8, 9.3 and 1.7 nm, respectively. The mean pore decreased as the weight percent of GVL in the dope solution increased; that is, as the viscosity of the dope solution decreased as compared to the PSf/PolarClean dope (Figure 5.3). When DMAc was used, the mean pore diameter was 3.8 nm, which was the least viscous dope solution (Figure 5.3). These results indicate that pore sizes were not a direct relation of dope solution viscosity, but instead polar interactions between the polymer and the solvent/co-solvent impacted the phase inversion and pore formation. The largest surface pores, measured by the bubble point pore diameters of M1-M6 were 58.2, 28.9, 17.4, 21.7, and 9.7 nm, respectively, which also mostly decreased as the viscosity of dope solutions decreased. Therefore again, viscosity alone was insufficient to explain surface pore sizes, and possibly hydrogen bonding (δ_h, Table 3) between sole-/co-solvents and polymer in combination with viscosity influenced the pore formation during the phase inversion process. For high viscosity dope solutions, water transport during phase inversion is retarded, so hydrogen bonding plays a greater role. From Table 3, hydrogen bonding decreased as the GVL fraction increased, which is the same trend as the mean pore sizes.

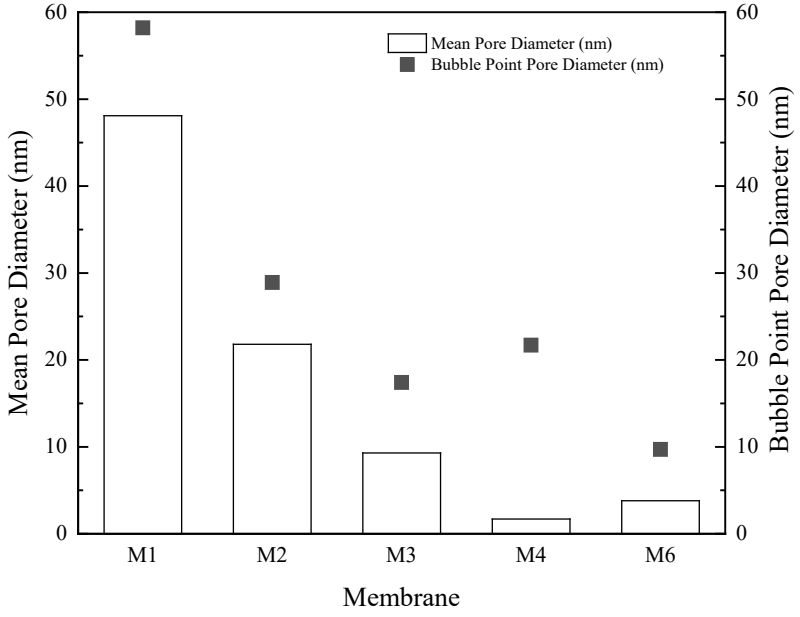

Figure 5.7 Pore analysis on the membrane surface

5.3.5 Topology (AFM)

The topologies of M1-M6 were determined using AFM, and the average RMS roughness of each membrane is shown quantitatively in Figure 5.8 and qualitatively in Figure 5.9. It was observed that the surface roughness was not significantly different when sole solvents, PolarClean (M1), GVL (M5) or DMAc (M6), were used to cast the membranes. The average RMS roughness of these membranes averaged between 30-40 nm. On the other hand, using the PolarClean/GVL as co-solvent systems led to different results. M2 showed an average RMS roughness of 9.0 nm with the deviation of 6.2 nm. M3 showed an average RMS roughness of 10.4 nm with the deviation of 4.8 nm. These two co-solvent recipes produced the smoothest membranes in this study. When GVL was the dominant solvent, M4 showed the average RMS roughness of 72.5 nm with deviation

of 28.5 nm. However, when standard deviations are considered, it is important to note that no significant differences were observed between the roughness values of different membranes.

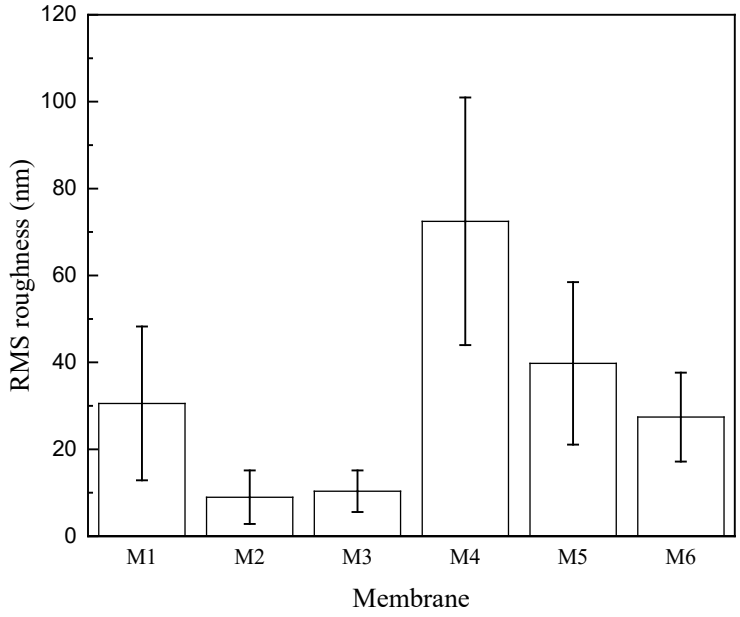

Figure 5.8 Surface roughness of different membranes

The topology profiles are presented in Figure 5.9. While there were no significant differences in the average RMS values among the membranes, there were visual differences among the membranes, as observed in Figure 5.9. M1 and M6 showed relative smooth surfaces with a few large peaks. The M5 image featured numerous hills and valleys on the membrane surface. For the co-solvent systems, M2 showed the smoothest surface with no obvious hills or valleys, while the majority of the M3 area was smooth with few hills. M4 was the roughest membrane and the topology image showed that multiple peaks provided the large roughness for the membrane. Based on the topology analysis, M4

showed the roughest (Figure 5.8) and most irregular surface (Figure 5.9). Thus, the recipe of 25wt% PolarClean/75wt% GVL was not recommended and was removed from further evaluation.

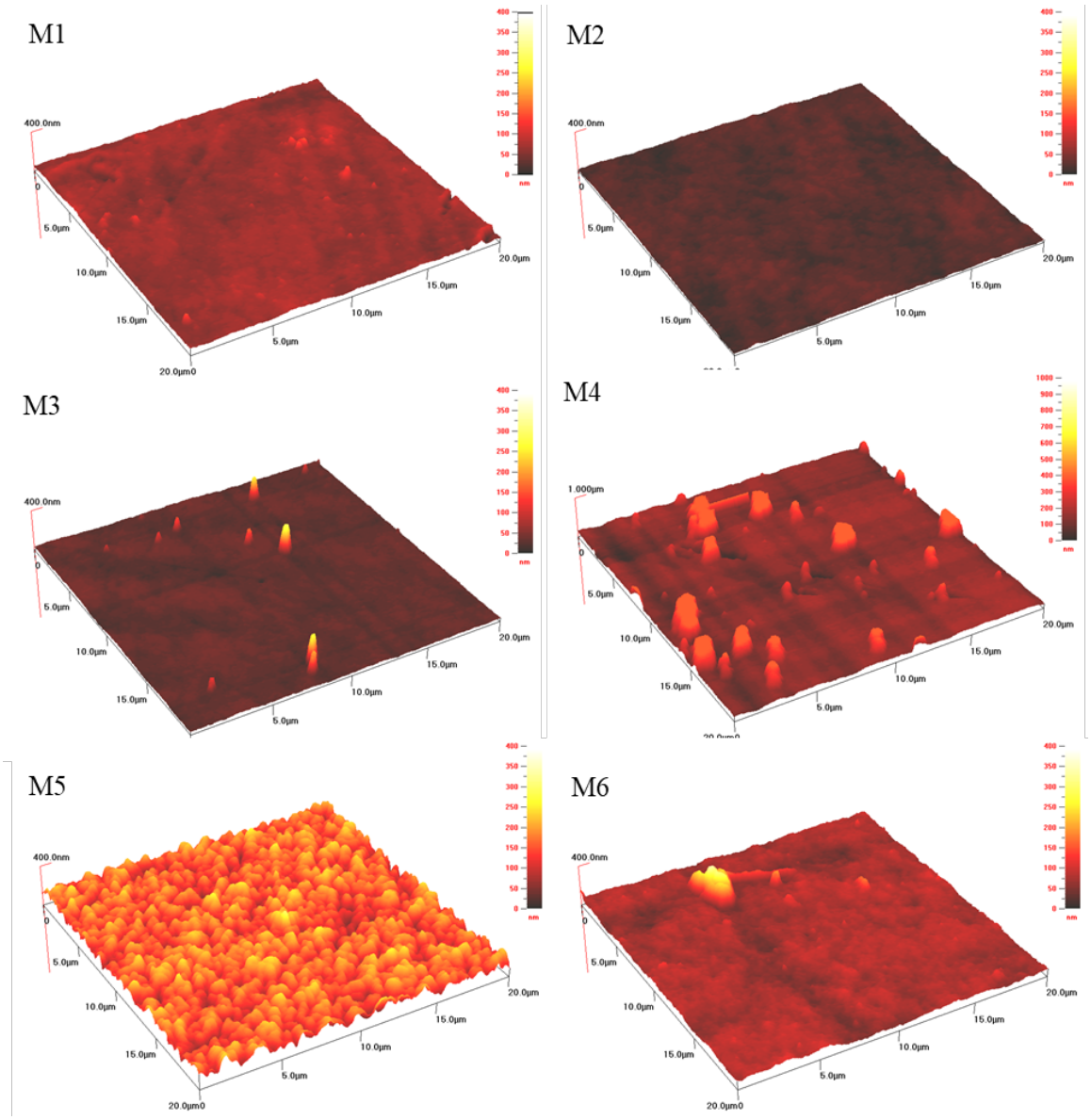

Figure 5.9 Topology images of PSf membrane

5.3.6 Hydrophilicity

The contact angle between water and the membrane surface is used to measure the hydrophility of the membranes (Figure 5.10). The contact angles of the membranes tested here varied from 68° to 72°. The contact angle slightly increased from M1 to M5, indicating that the hydrophilicity slightly decreased with more GVL in the co-solvent. However, the

difference of these contact angels was unnoticable because the material and weight percent of the polymer used in this study were the same.

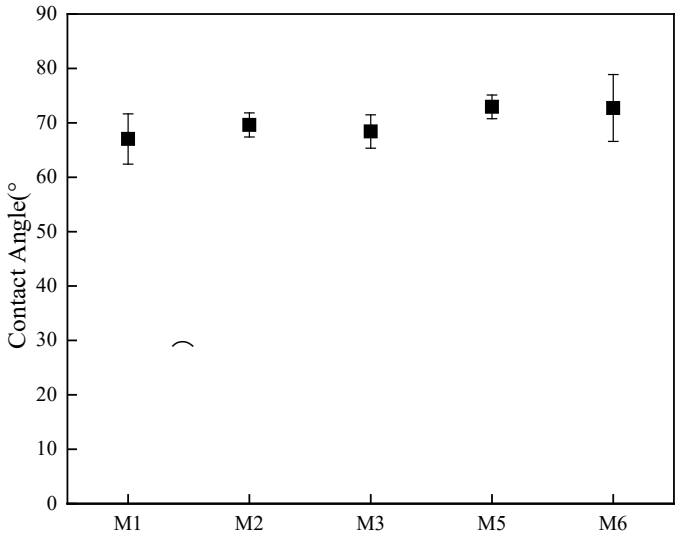

Figure 5.10 Contact angles of different membranes

5.3.7 FTIR

The polysulfone membranes prepared using different solvents were analyzed using FTIR. The primary structure of polysulfone has been previously investigated[258-260] and is listed in Table 4. Figure 5.11 shows the peaks associated with the primary structures of polysulfone present on the membrane surfaces. All of the FTIR spectra peaks match the peaks listed in Table 4. Therefore, the results also showed that the solvents used to fabricate the PSf membranes did not change the membrane chemistry.

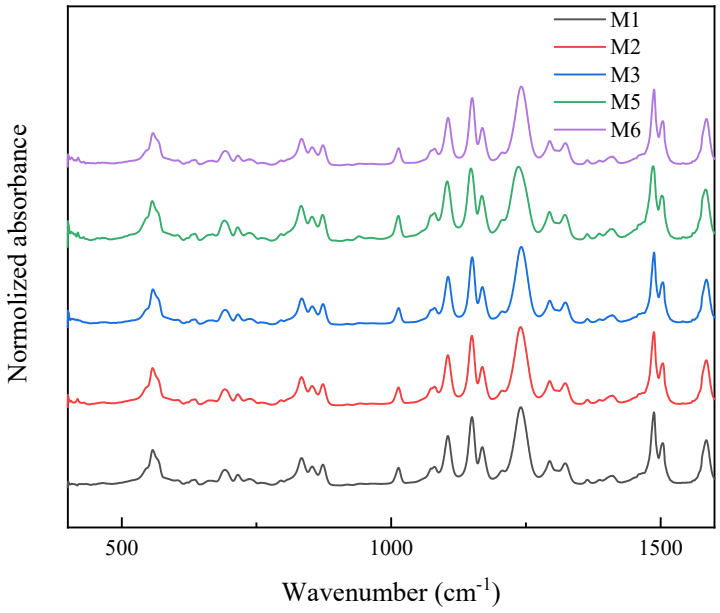

Figure 5.11 FTIR Spectrum of a polysulfone membrane in the wavenumber range of 1600-400 cm^{-1}

Table 5.4 FTIR spectra of Polysulfone

PSf spectra	Wavenumber (cm^{-1})
Aromatic C-H bending	871, 850, 831
C-SO_2-C symmetric stretch	1149
C-SO_2-C asymmetric stretch	1319, 1292
C-O asymmetric stretch	1238, 1012
C_6H_6 ring stretch	1587-1489

5.3.8 Permeability and separation performance

First of all, when M5 was used for pure water filtration, the pure water flux (PWF) was below 0.2 $L/m^2 \cdot h$ (LMH); therefore, M5 was not applicable to perform the filtration study. M5 was cast using the PSf/GVL dope solution, a Non-Newtonian fluid (Figure 5.5) that was found to be difficult to cast membranes manually. For M1-M3 and M6, the DI water flux values were 750, 300, 27 and 17 LMH, respectively; while for the 1 g/L BSA, flux values were 140, 115, 12 and 13 LMH, respectively. The hydrophilicity of membranes was similar, so flux curves observed were more related to the surface mean pore sizes, which for M1-M3 and M6, were 48.1, 21.8, 9.3 and 3.8 nm, respectively. When membranes M1, M2, M3 and M6 were used for BSA filtration, the flux of each membrane declined 82%, 62%, 56% and 24% during filtration. Based on the characteristics of membranes, two factors might lead to the differences in flux decline. First, the surface roughness of M1 was

significantly higher than M2 and M3, which may favor the cake formation during BSA filtration and lead to a higher decline. Second, BSA is a negative molecule in the aqueous solution and the surface of M6 was more negative-charged than M1-M3 (Figure 5.11), which also reduced BSA accumulation on membrane surface. After the reserve filtration using DI water to remove any reversibly attached foulants, the flux recovery percentages of M1, M2, M3 and M6 were 30%, 66%, 70% and 91%, respectively. It is important to note that after while M6 showed the highest flux recovery percentage, the absolute flux values of M1, M2 and M3 were larger than M6.

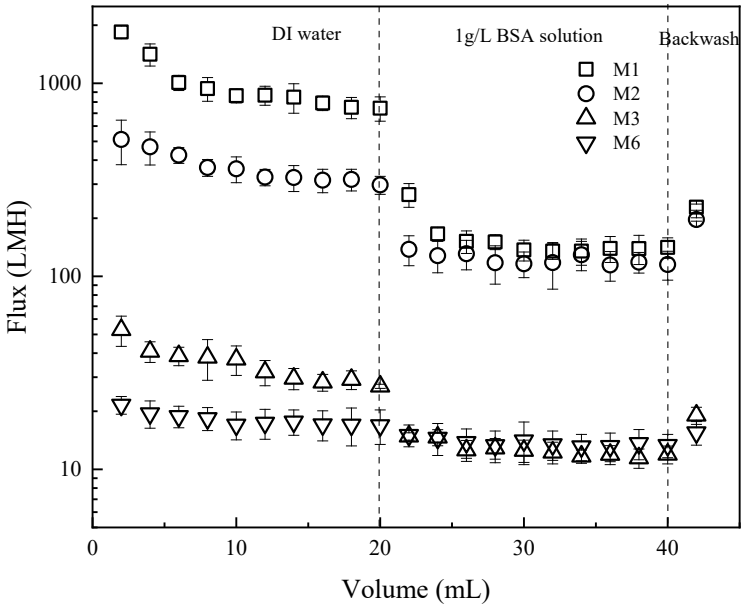

Figure 5.12 Filtration study for different membranes

BSA rejection using different membranes is shown in Figure 5.13. M1 rejected 89.5±1.0 % BSA in the aqueous solution, M2 rejected 99.2±0.1 %, M3 rejected 96.0±2.2 %, and M6 rejected 95.5±0.7%. BSA has a molecular weight of 66.5 kDa[261], and the

difference in BSA rejection is attributed first to the membrane active layer. The mean pore diameter of M1 surface was larger than M2, M3, and M6; thus, less BSA was rejected based on the mechanism of size exclusion. Second, the cross-sectional structures of these four membranes were different, as shown in Figure 5.14 M(a). M1(a) showed the spongy-like structure with microvoids in the supporting layer; M2(a) and M3(a) showed spongy-like structures without microvoids; M6(a) presented a finger-like supporting layer and microvoids. Besides the major influence of the dense layer on top of the membranes, the supporting layer also influenced the rejection rate of BSA because of the absorbance effect. Therefore, the spongy-like membrane without microvoids are able to absorb more solutes than the membranes with the finger-like structure and the spongy-like structure with microvoids.

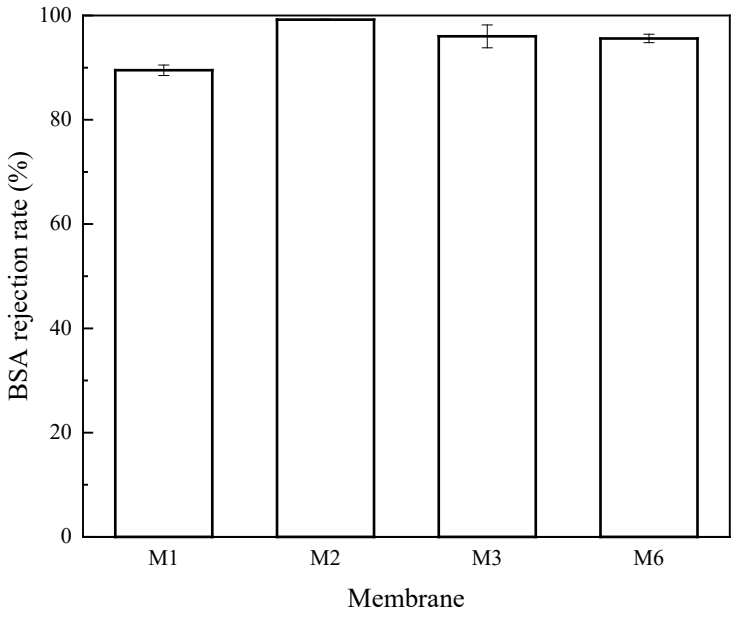

Figure 5.13 BSA rejection rates for different membranes

Figure 5.14 shows the evolution of the membranes from before filtration (labeled (a)), to after BSA filtration (labeled (b)) and ultimate reverse-flow filtration to emulate backwashing (labeled (c)). Figure 5.14 shows that using DMAc (M6) a finger-like support layer structure was developed, while using PolarClean and PolarClean/GVL as co-solvents, M1, M2 and M3 formed spongy-like support layer structures. This was likely due to the demixing speed of solvent and nonsolvent since that plays an important role in the formation of the structure of the support layers[232]. The fast exchange between solvent and nonsolvent results in the instantaneous demixing and a fast precipitation for the polymer film, which generally generates finger like structures. On the other hand, the slow exchange between solvent and nonsolvent generally leads to a delayed demixing and a slow precipitation, generating spongy like structures[252, 262-264]. Microvoids generally form

in a relative faster demixing process[262, 265], which indicates that PolarClean can diffuse in water faster than GVL, as shown in Figure 5.14 M1(a). Microvoids in the membranes disappeared with the addition of GVL, as shown in Figure 5.14 M2(a) and M3(a).

For M1, PolarClean as sole solvent, the original membranes presented a spongy-like structure with some microvoids, which is associated with membranes fabricated from dope solutions with high viscosities[266-268] (~ 5.50 Pa·s, Figure 5.3). The microvoids slightly collapsed after filtration and deformed after the backwash process, which was likely the cause for the low flux recovery percentage observed for M1 (30%, Figure 5.12). For M2 and M3, the original membranes showed spongy-like structures without microvoids, and thus, the membranes morphological structures did not experience deformation during filtration and backwash. These membranes were cast from dope solutions with viscosities lower than for PolarClean alone (Figure 5.3) to minimize the formation of microvoids, but still high enough to develop spongy structures. This might be the reason that these membranes showed higher rejection rates and higher flux recovery percentages as compared to M1. For M6, the membranes showed finger-like structures with microvoids, which is a characteristic of membranes formed from dopes with low viscosities (0.19 Pa·s for DMAc, Figure 5.3). During the filtration and backwash, the finger-like structures did not collapse but the microviods deformed significantly. However, the flux recovery percentage of M6 was high at 91%, which might have been due to the finger-like structures providing a more mechanically stable supportive layer[20, 232, 266].

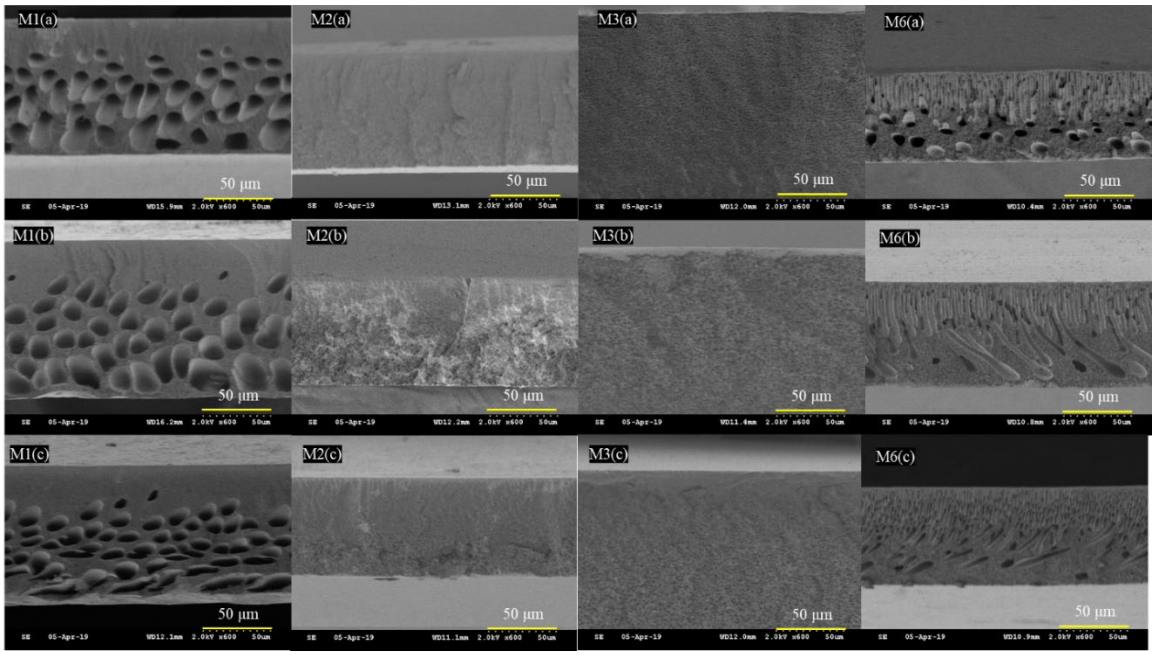

Figure 5.14 Cross-sectional images of membranes: (a) original (i.e. before filtration); (b) after BSA filtration; (c) after backwash

5.4 Conclusions

To address the problem of hazardous/toxic solvents involved in casting polymeric membranes, low-hazard solvents, PolarClean, GVL and PolarClean/GVL as co-solvents, were compared to a traditional solvent, DMAc, in fabricating PSf membranes via NIPS. Based on calculated Hansen solubility values, PolarClean/GVL co-solvents were determined to be better solvents than PolarClean and GVL as sole solvents. Furthermore, PolarClean/GVL as co-solvents showed Newtonian fluid behavior since their viscosities did not change as a function of shear rate. Viscosity was also used to quantify the time required for completely mixing of polymer/solvent and the normalized viscosity (NV) was used as an indicator for the homogeneity of a dope solution. After 24 h, all the dope solutions reached or surpassed NV values of 90%, indicating that these dope solutions

reached homogeneity. FTIR results showed that the use of different solvents produced membranes that were structurally identical. The mean pore diameter of fabricated membranes decreased as the weight percent of GVL increased from 0, 25%, 50% to 75% in the dope solution, and observed changes in mean pore size followed the same trend as a function of changes in dope viscosity. In filtration studies, it was observed that the membrane flux decreased as the mean pore size of membranes decreased, as expected, while all membranes showed nearly complete rejection of BSA. Long-term studies using the identified optimal solvent mixtures should be performed in the future. Since the starting goal of this study was to use low-hazard solvents/co-solvents to fabricate membranes with similar operation as membranes fabricated using DMAc, it was deemed that dope solutions using equal weight fractions of PolarClean and GVL produced the best membranes. Therefore, PolarClean/GVL co-solvents provided a promising solution to replace traditional solvents.

CHAPTER 6. LOW-HAZARD SOLVENTS AND THEIR MIXTURE FOR THE FABRICATION OF POLYSULFONE ULTRAFILTRATION MEMBRANES: AN INVESTIGATION OF DOCTOR BLADE AND SLOT DIE CASTING METHODS

The use of slot die in this chapter was co-supervised by Dr. Tequila Harris, and conducted in the Polymer Thin Film Processing (PTFP) group in the Georgia Institute of Technology.

This chapter has been published in the following report and adapted with permission from:

Dong, X.; Jeong, T.J.; Kline, E.; Banks, L.; Grulke, E.; Harris. T.; Escobar, I.C. Eco-friendly solvents and their mixture for the fabrication of polysulfone ultrafiltration membranes: An investigation of doctor blade and slot die casting methods. *Journal of Membrane Science*. 2020. (614) 118510 [269]

6.1 Introduction

Water treatment membranes are thin sheets of material that can be used to separate particles from water based on size exclusion, charge or aromaticity [270-272]. Nonsolvent phase induced separation (NIPS) is a common method for casting of polymeric membranes. In NIPS, polymer materials are first dissolved in a solvent/co-solvent mixture to produce a dope solution, which is then cast on a substrate as a liquid film. The liquid film is then immersed into a nonsolvent, often water, for phase inversion. During the phase inversion process, the solvents diffuse into water, and the polymer remains on the substrate as a membrane matrix.

As more applications are found for membranes, the environmental impacts of membrane production become more important to investigate. One associated concern is with respect to the solvents used to dissolve the polymers. Commonly used solvents, such as dimethylformamide (DMF), dimethylacetamide (DMAc), and N-Methyl-2-pyrrolidone (NMP), are generally toxic to humans and the environment [46], and regulations restricting their use during mass production are starting to appear. The European Legislation, Registration, Evaluation, Authorisation, and Restriction of Chemicals (REACH) has labeled DMF, DMAc and NMP as substances of very high concern (SVHC), and it bans the use of DMAc and NMP after May 2020 [273, 274]. Therefore, the need to find less hazardous alternatives for these solvents is imperative. Rhodiasolv® PolarClean (PC) and γ-valerolactone (GVL) are two solvents being researched because of their low levels of toxicity [46, 224].

Wang et al [38] prepared polyethersulfone (PES), polysulfone (PSf), and cellulose acetate (CA) membranes using PolarClean as the solvent which compare with membranes fabricated by traditional solvents. With PolarClean as the solvent, PES and PSf membranes formed surface pores suitable for ultrafiltration (UF), while CA membranes formed pores acceptable for nanofiltration (NF) [38]. The performance of these membranes was comparable to membranes created using traditional solvents. Marino et al [130] similarly worked with PolarClean in the fabrication of PES membranes. They found the cross-sectional structure of the membranes to be spongy, and that they performed well in permeability tests compared to membranes prepared with traditional solvents [2]. In addition to PolarClean, GVL is another low-toxicity solvent, and it is produced from biomass as a derivative of glucose [275, 276]. Rasool et al. [136] prepared membranes

using GVL and a variety of different polymers, most notably CA and cellulose triacetate (CTA). Specifically, 15% CA/GVL and 10% CTA/GVL dopes were used to cast nanofiltration (NF) that rejected 90% Rhodamine B, at permeances of 1.8 $Lm^{-2}h^{-1}bar^{-1}$ (LMH/bar) and 11.7 LMH/bar, respectively.

PolarClean and GVL have been previously used to dissolve PSf to fabricate ultrafiltration membranes both as sole solvents and as co-solvents. When PolarClean was used as a solvent, it produced membranes with spongy-like pore structures that were different from finger-like structures observed when DMAc was used to cast PSf membranes [20]. Furthermore, the PSf/PolarClean pore structure was observed to collapse upon backwashing. Conversely, GVL alone was found not to be suitable to fabricate PSf membranes because the dope formed gel-like films instead of solid films during NIPS with water as the nonsolvent [46]. Under equal amounts of PolarClean and GVL as a co-solvent mixture, it was observed that membranes had similar structural, morphological and operational properties compared to membranes made using DMAc [224].

At the laboratory scale, a doctor blade is a common tool to solution casting membranes; however, it is not scalable. In order to investigate the scale up abilities of the membranes cast using green solvent, slot die casting is introduced for this study, and used in combination with a roll-to-roll (R2R) system, which allows for continuous casting of polymeric membranes. An illustration of this system is shown in Figure 6.1.

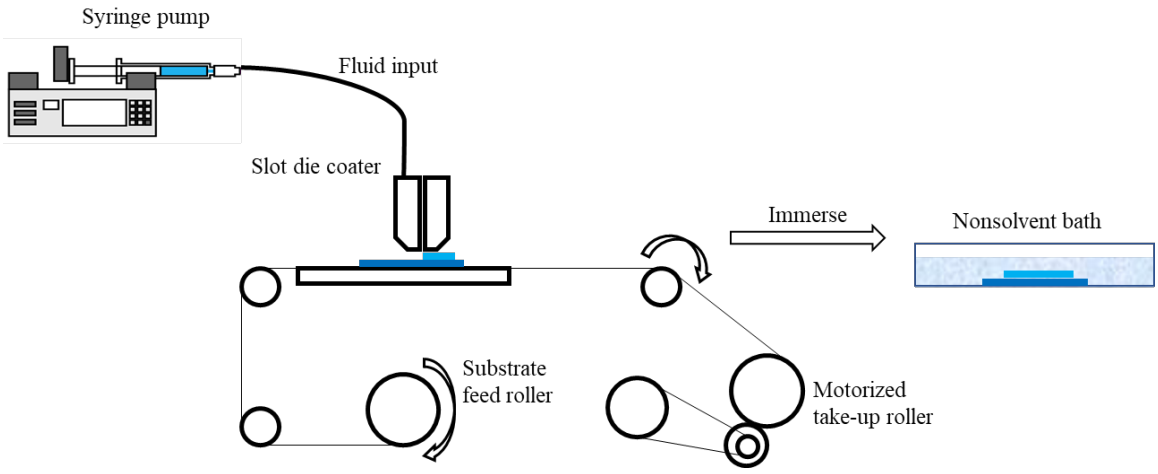

Figure 6.1 Schematic of the combination setup of a simple R2R system and a slot die coater [277]

Specifically, in this process, two die halves are set apart by a small gap (W) with a shim, and the fluid is pumped into the die at a chosen flow rate; then, the fluid is continuously cast onto a moving substrate. A zoomed in view of the casting region of the slot die coating process is shown in Figure 6.2. In this slot die process, the controlled casting thickness (h) is a function of the flow rate of solution per unit width ($Q^{'}$) and substrate speed (u_w) [48], which is $h= Q^{'}/ u_w$. Though to a lesser degree, the slot gap in the slot die (W) and the gap height (H) can also affect the quality of the films cast. In order to fabricate defect-free membranes, values of $Q^{'}$, u_w and H must be determined.

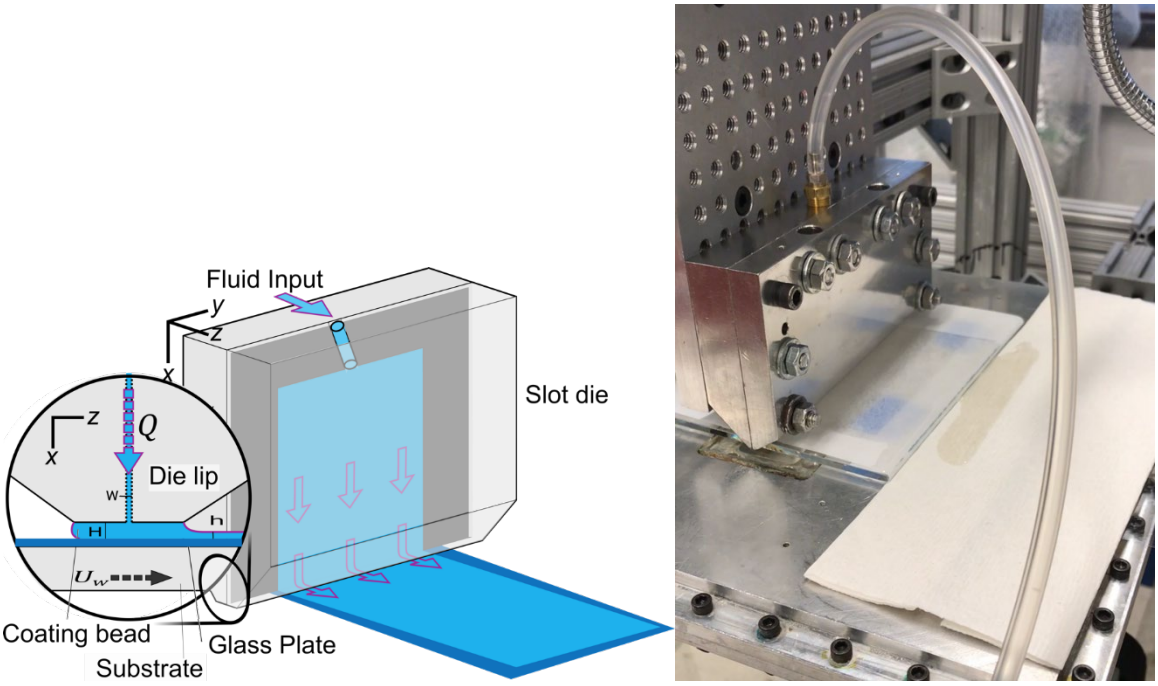

(a) (b)

Figure 6.2 (a) Schematic of the lower section of a slot die coater, (b) photo of the lower section of a slot die coater

In this study, low-hazard solvents, PolarClean and GVL, are investigated to dissolve PSf into a solution that can be cast into ultrafiltration membranes at the laboratory scale using a doctor blade and at the production scale using a slot die casting integrated into a R2R system. Different fabrication techniques may result in membranes with different properties; therefore, the membranes are characterized with respect to their chemical and morphological structures, and are used to filter different solutions for comparison. It is important to note that in the procedure described here, the membranes were cast directly

onto a glass plate using both methods, doctor blade extrusion and slot die coating. However, typically large-scale production membranes are cast onto a nonwoven fabric. A glass plate was used here instead of nonwoven fabric to minimize structural and operational interactions between the dope and the substrate from one processing method to another, so that the effects of scalability could be more comparably accessed.

6.2 Materials and Experimental:

6.2.1 Materials

PSf (flakes, ground material for Ultrason E. 6020P Q691) provided by BASF Performance Materials (Wyandotte, Michigan, United States) is used as the polymer. Three solvents are used to dissolve the polymer, (1) GVL, purchased from Acros Organics (Fair Lawn, New Jersey, United States); (2) Rhodiasolv® PolarClean provided by Solvay Novecare (Princeton, New Jersey, United States); and (3) DMAc purchased from Tokyo Chemical Industry Co., Ltd. (Tokyo, Japan). To study the filtration performance of the membranes, Grade I deionized (DI) water with a resistivity of 18.2 mΩ·cm at 25 °C provided by the Chemical Engineering Undergraduate Laboratory at University of Kentucky, and bovine serum albumin (BSA) purchased from VWR Life Science (Radnor, PA, USA), are used.

6.2.2 Thermodynamics study

6.2.2.1 Relative Energy Difference (RED)

The affinity of a polymer and a solvent is described as R_a was calculated by Hansen Solubility Parameter (HSP) theory, as equation 1:

$$R_a = \sqrt{4(\delta_{d2}-\delta_{d1})^2 + \left(\delta_{p2}-\delta_{p1}\right)^2 + (\delta_{h2}-\delta_{h1})^2} \quad (1)$$

Where δ_d is the dispersive force, $\delta_p$is the polar force, and δ_h is hydrogen bonding[141]. A solvent is considered as a good solvent for a polymer when the value of R_a is small [136, 141].

In this study, PSf was not only dissolved using single solvents, but also a binary solvent mixture. Therefore, the corresponding parameters of the binary solvent mixture were calculated according to following procedure: first, the volume fraction of each solvent was calculated by equations 2 and 3; second, the values of solubility parameters were then calculated using equation 4, 5, and 6[141]:

$$V_1 = \frac{W_1/\rho_1}{W_1/\rho_1+W_2/\rho_2} \quad (2)$$

$$V_2 = \frac{W_2/\rho_2}{W_1/\rho_1+W_2/\rho_2} \quad (3)$$

$$\delta_d = V_1\delta_{d1} + V_2\delta_{d2} \quad (4)$$

$$\delta_p = V_1\delta_{p1} + V_2\delta_{p2} \quad (5)$$

$$\delta_h = V_1\delta_{h1} + V_2\delta_{h2} \quad (6)$$

Where 1, 2 represents solvent 1 and solvent 2; V_i represents the volume fraction, and W_i represents the weight fraction.

Three parameters of a polymer or solvent can be used to form a polymer-solvent affinity sphere[141] in HSP theory, and the relative energy difference (RED) is then introduced to describe the interaction between a polymer and a solvent[45]. A good solvent for a polymer can be theoretically defined if the RED value is less than or equal to 1, calculated by equation 7[20, 141]:

$$\mathrm{RED} = \frac{R_a}{R_0} \qquad (7)$$

Where R_o represents the radius of the Hansen solubility parameter sphere for the polymer.

6.2.2.2 Cloud point curve

In order to determine the compatibility of a solvent to fabricate membranes by the nonsolvent phase inversion method, a cloud point curve must be obtained for solvent/nonsolvent/polymer trinary system [37]. For the solvent/water/PSf system, a cloud point curve is experimentally determined by titration [38]. During the experiments, dope solutions are prepared using 1, 3, 5, 10, 15, 20, 25 wt % concentrations of PSf in DMAc, PolarClean, GVL and the mixture of 50% PolarClean with 50% GVL. Each dope solution is mixed using a sonicator (Elmasonic P70H, from Elma Electronic Inc., Munich, Germany) at 65 °C (with frequency of 80 kHz, power of 900 W under pulse mode) for 24 h. All dope solutions are then cooled to room temperature, and DI water is gradually added into the dope solutions using a micropipette until the solutions visually became cloudy. The cloudy solution is then sonicated for one additional hour to determine if it returns to a clear state. If the solution remains cloudy, the composition of solvent/water/polymer is determined to be the cloud point.

6.2.3 Preparation of dope solutions

Three different PSf dope solutions are used in this study, 17 wt% PSf/DMAc, 17 wt% PSf/PolarClean, and 17 wt% PSf/50 wt% PolarClean-50 wt% GVL. These three dope solutions were chosen based on results from previous studies *[20, 46, 224]*. Since the purpose of this study is to investigate the scaled fabrication of membranes using slot die as compared to a laboratory doctor blade, all the dope solutions are prepared in large quantities, i.e., liters. Therefore, a kinetic study of polymer dissolution in different solvents is conducted after preparation.

6.2.4 Kinetic study of polymer dissolution

The polymer dissolution is studied in a high-pressure reactor (4540-600 mL, Parr Instrument, Moline, Illinois, United States). The reactor is equipped with a four-blade impeller. The dissolution process is conducted in a glass vessel under different rotation speeds of 300, 450, 600 rpm (revolutions per minute), separately. For each trial, 200 mL of solvent (DMAc, PolarClean, and the mixture of PolarClean and GVL with equal weight percent) is used and PSf flakes are mixed in the solvent, and time required for complete dissolution is measured. The flake form of PSf can minimize the influence of shape and size on the mixing process because compared to the common commercially available pellet form, the flake is thin and therefore provides more surface area to interact with the solvent.

6.2.5 Characteristics of dope solution

6.2.5.1 Viscosity

Polymer dissolution is conducted in a transparent vessel so that it can be visually monitored; moreover, viscosity is used as a quantitative indicator to monitor dope solution mixing until completion, and is measured as a homogenous solution [224]. After homogenous dope solutions are obtained, the viscosity of each solution sample is measured using a rheometer (AG-G2, TA instrument, Delaware, United States). Dope solution viscosity as a function of changing shear rate is used to demonstrate the fluid behavior of these solutions to determine if they can be cast using a doctor blade or slot die. The viscosity of each sample is recorded over the change of shear rate from 0.01-100/s.

6.2.5.2 Diffusion rate

The diffusion rate is measured in a cuvette cell, is then positioned in a VWR UV-6300PC spectrophotometer (Radnor, Pennsylvania, United States) [42]. 20 mL DI water is circulated in the spectrophotometer and the blank calibration is obtained. Then 1 mL dope solution is dropped into DI water and the light transmittance at 276 nm is recorded over 5 minutes. The light transmittance data is then normalized and compared among dope solutions of PSf/DMAc, PSf/PolarClean and PSf/50% PolarClean-50% GVL.

6.2.6 Membrane fabrication

To study the scale up of the membranes prepared using low-hazardous solvents, an aluminum doctor blade (AP-G10/10, Paul N. Gardner company, Florida, United States) is used to cast membranes in laboratory scale and an aluminum slot die is used to fabricate the membranes in a production scale, to understand the viability of scaling up the fabrication process. The dope solutions containing the three solvents in both casting scales are shown in Table 1. When the doctor blade method is used, the gap between the blade

and the glass plate is set at 200 μm. In the slot die casting method, the slot gap is set at 90 μm, and the coating gap is set at 200 μm above the glass plate substrate, which is placed on top of the poly(ethylene terephthalate) (PET) film. The PET film is the moving conveyor that is pulled at a speed of 1.3 mm/s from a feed roller to the take-up roller [253]. A syringe pump is used to set the flow rate of the dope solution dispensed from the slot die to fabricate defect free membranes. A different 2-D flow rate is used for each dope solution, for PSf/DMAc, 0.17 mm^2/s is used; for PSf/PolarClean, 0.75 mm^2/s is used, and 0.70 mm^2/s is used for PSf/50%PolarClean-50%GVL. All casting is performed at 25 ˚C and 48% humidity.

The glass substrates are cleaned with DI water and are then rinsed using isopropyl alcohol to guarantee no residual water on the surface before casting. After casting, the liquid films are inversed into a solid film via the NIPS method. Membranes pieces are then cast in the shape of 305×100 mm×mm (length×width).

Table 6.1 Recipes of PSf/solvent membranes (all dope solutions are made using 17% PSf and 83% solvent)

Weight percent (%)	M1	M2	M3	M4	M5	M6
PSf	17	17	17	17	17	17
DMAc	83	--	--	83	--	--
PolarClean	--	83	50%×83	--	83	50%×83
GVL	--	--	50%×83	--	--	50%×83
		Slot Die Casting		Lab casting		

6.2.7 Characterization of membranes

6.2.7.1 Attenuated total reflectance-Fourier transform infrared spectroscopy (ATR-FTIR)

ATR-FTIR (Thermo Nicolet iS50 FTIR Spectrometer, Thermo Scientific, Waltham, Massachusetts, USA) is performed to characterize the surface chemical structure of the six membranes and to determine if different solvents affect the surface chemical structure of membranes. A piece of each membrane sample is freeze-dried overnight to minimize the moisture in the membrane and is then placed on the ATR-FTIR crystal (diamond) for analysis. The absorbance spectra of these six different membranes are normalized [153-156] and are then adjusted in the same figure for comparison.

6.2.7.2 Scanning Electron Microscopy (SEM) morphology

Scanning electron microscope (SEM) images of the surface and cross sections can directly provide the morphology difference of the membranes fabricated using different solvents and methods. The surfaces and the cross sections of the six different PSf membranes are observed by two different SEMs (Hitachi S-4300 from Hitachi Group, Troy, MI, USA and FEI Quanta 250 from Thermo Scientific, Hillsboro, OR, USA). To prepare membrane samples for SEM imaging, the PSf membranes are immersed and fractured in liquid nitrogen, freeze-dried overnight and then sputtered with palladium for 4 minutes. All the images are presented as a scale bar of 50 μm.

6.2.7.3 Hydrophilicity and wettability

Membrane hydrophilicity represents the water affinity of the material. It affects its water permeability [278]. The contact angle is characterized to represent hydrophilicity of the membranes. It is measured by the sessile drop method using a drop shape analyzer connected to a high-definition camera (DSA 100S, Kruss Company, Hamburg, Germany). One drop 12 μL of DI water is deposited on the membrane surface. The interface between the water drop and the membrane surface is recorded by the camera and the contact angle is calculated according to the image. For each membrane sample, the water contact angle is recorded after five minutes. The measurement is repeated three times and then the average values and deviations are calculated.

6.2.7.4 Surface roughness and topology

The topography of membranes is measured at the atomic scale to characterize the roughness on the surface. Surface roughness provides quantitative information to

investigate the influence of different factors shaping the topography of the membrane surface, for instance, solvent evaporation, solvent-nonsolvent diffusion rate, etc. The surface roughness values of the six membranes (M1-M6) are measured using an atomic force microscope (AFM, Quesant Instrument Co., Agoura Hills, California, United States). The surface roughness is measured under the tapping mode and is then evaluated by root-mean-squared (RMS) roughness. Six areas of 20 × 20 μm on each membrane surface are randomly chosen and measured to calculate the average and standard deviation of the RMS roughness values.

6.2.8 Filtration performance

Filtration performance of membranes is characterized by using a crossflow apparatus Sterlitech HP4750 stirred cell (Kent, Washington, USA) to perform convective studies. The crossflow filtration cell is run at a flowrate of 1.2 L/min through the precompaction stage, fouling stage and tangential washing stage. DI water permeability is determined for each membrane by precompacting at 6.9 bar overnight and then measuring the volumetric flux of deionized ultrafiltered (DIUF) water at 1.4, 2.8, 4.1, 5.5, 6.9 bar, respectively. The linear correlations of membranes are analyzed accordingly. 50 mg/L BSA solution is then filtered through the membranes to investigate long-term filtration. At the fouling stage, the initial flux is measured. When the flux reached 70% of the initial value, the membrane surface is tangentially rinsed with DI water for 10 min. This process is repeated until the flux reaches 35% of the initial flux, and the overall filtration time is recorded. Then BSA solution is used to filter through the membrane again. This process is repeated three times. The permeate is collected and the BSA samples for the feed and permeate are analyzed using a VWR UV-6300PC Spectrophotometer (Radnor,

Pennsylvania, USA). The flux linearity study and the BSA filtration are duplicated for reproducibility.

6.3 Results and Discussion

6.3.1 Thermodynamics

6.3.1.1 Hansen solubility parameter calculation

Using the Hansen solubility parameter model, RED values were calculated and are shown in Table 2 to verify whether it was thermodynamically possible to use the low-hazardous solvents to dissolve PSf. As previously discussed, RED values are used as indicators to identify good solvents as defined by RED values between the polymer and solvent being close to or smaller than 1. Therefore, based on the calculated results of RED values, PolarClean, GVL, DMAc and the solvent mixture of 50% PolarClean and 50% GVL can all theoretically dissolve PSf. As shown in Table 2., the RED value of the solvent mixture of PolarClean and GVL was less than those of the individual solvents. This is because the dispersive force of the solvent mixture is closer to PSf than PolarClean, the polar force of the solvent mixture is closer to PSf than GVL, and the hydrogen bonding of the solvent mixture is the same to PSf. Therefore, from equation (1), the RED value of the solvent mixture is less than the two solvents individually, which makes it a potential solvent for PSf.

Table 6.2 RED values between PSf and different solvents/ water

Polymer	δ_d ($MPa^{1/2}$)	δ_p ($MPa^{1/2}$)	δ_h ($MPa^{1/2}$)	R_o ($MPa^{1/2}$)	
PSf	19.7	8.3	8.3	8.0	
Solvent	δ_d ($MPa^{1/2}$)	δ_p ($MPa^{1/2}$)	δ_h ($MPa^{1/2}$)	R_a ($MPa^{1/2}$)	RED
PolarClean	15.8	10.7	9.2	8.2	1.03
50% PolarClean-50% GVL	17.4	13.6	8.3	7.1	0.88
GVL	19.0	16.6	7.4	8.5	1.06
DMAc	16.8	11.5	10.2	6.9	0.86
Water	15.5	16.0	42.4	36.0	4.49

6.3.1.2 Ternary phase diagram

The cloud point curve has been recognized as an important factor to determine the cross-sectional morphology of a polymeric membranes. More specifically, the curve represents the capacity that a dope solution has to absorb water. With 20% and 25% of PSf in the dope solutions, the capacities of the dope solutions to absorb water are similar. With lower contents of polymers, the curve of PSf/GVL/water was closest to the axis, as shown in Figure 6.3, meaning that even a small amount of water could lead to phase separation.

This observation agreed with previous studies that GVL might not be an ideal solvent for fabricating PSf membranes [46, 224]. The curve of PSf/DMAc/water shows the largest capacity to absorb water, which supports the ability of DMAc to dissolve PSf polymer. PSf/PolarClean/water is in between PSf/GVL/water and PSf/DMAc/water. The curve of PSf/50%PolarClean-50%GVL/water is in between PSf/GVL/water and PSf/PolarClean/water, but with no significant difference between the curves of PSf/50%PolarClean-50%GVL/water and PSf/PolarClean/water. Therefore, thermodynamically, the cross-sectional structures of these two membranes are expected to be similar; however, the diffusion rate of PolarClean and the solvent mixture should also be considered.

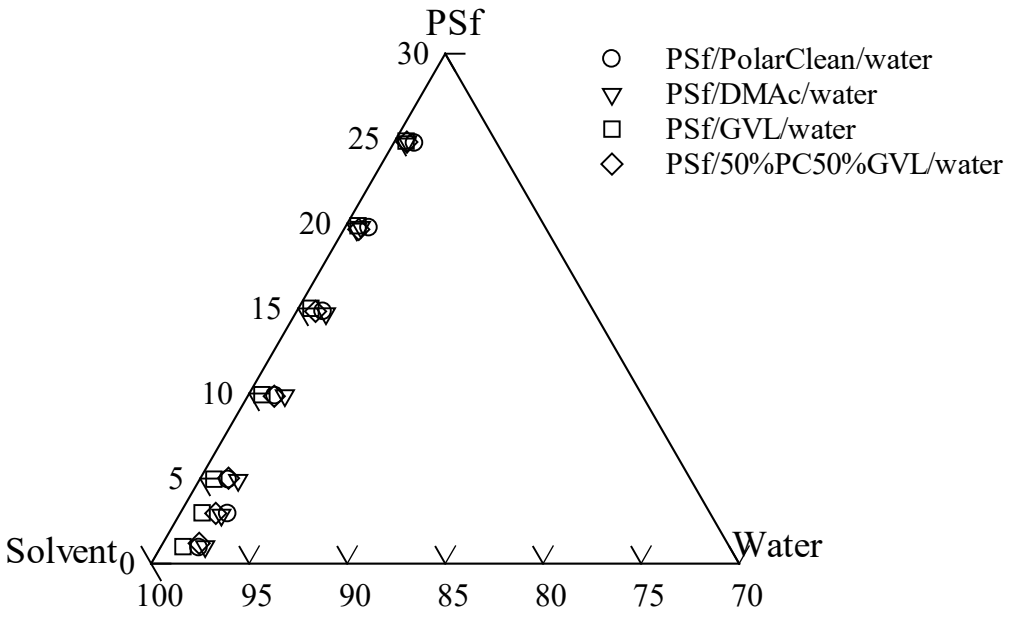

Figure 6.3 Cloud point curves of PSf/solvent/water: PSf/DMAc/water and PSf/GVL/water are on the opposite, curves of PSf/PolarClean/water and PSf/solvent mixture/water are in between

6.3.2 Characteristics of dope solution

6.3.2.1 Diffusion rate of solvents into nonsolvents

During phase separation, the solvent diffuses into the nonsolvent, which is DI water, and the solid polymeric film remains. The diffusion rate from solvent into nonsolvent is a direct factor that influences the cross-sectional morphology of the membranes. The diffusion into water curves for DMAc and PolarClean pure solvents and of PolarClean/GVL solvent mixture are shown in Figure 6.4. DMAc diffused into water at a linear speed until 90% of the DMAc had diffused, which occurred in 180 seconds.

PolarClean gradually diffused into water, and it took approximately 225 seconds for 90% of PolarClean to diffuse into water. It is hypothesized that the curve representing the solvent mixture of PolarClean/GVL diffusion into water can be discussed in two stages. First, GVL diffuses into water at a faster speed than PolarClean, and 50% of the solvent diffuses into water during the first 30 seconds. Then, the leftover solvent, mostly PolarClean, diffuses into water at a slower speed, and 90% of the solvent diffuses into the water within 150 seconds. The different diffusion rates between solvents and nonsolvent might lead to different cross-sectional morphologies of membranes.

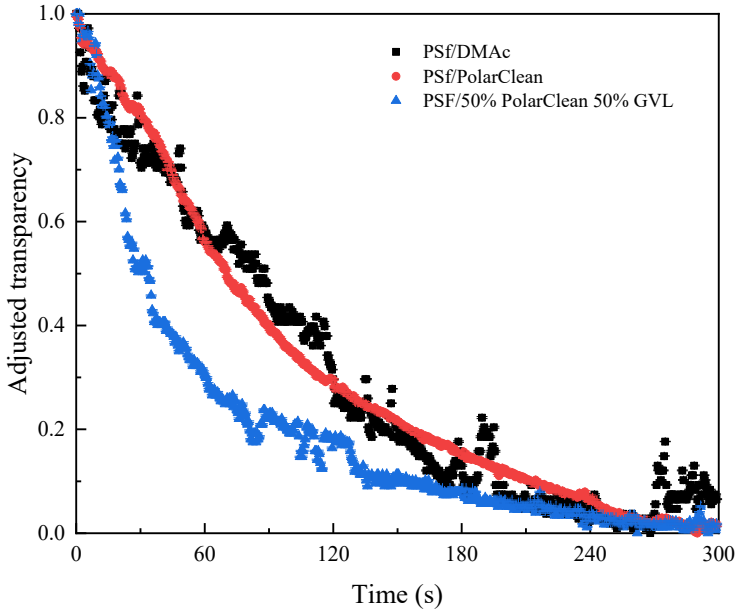

Figure 6.4 The kinetics study of dope solutions diffusion into DI water: light transmittance was measured at 276 nm over 5 minutes

6.3.2.2 Dissolution kinetics

The mixing time required to fully dissolve PSf into different solvents on a large-scale was measured individually and is shown in Figure 6.5. An impeller was used to continuously mix the solvent and polymer at room temperature. For DMAc, 4.67 hours were required to fully dissolve PSf at a rotation speed of 300 RPM, 4.42 hours to dissolve PSf at 450 RPM, and 3.83 hours to dissolve the polymer at 600 RPM. Due to the higher viscosity of PolarClean (9.78 mPa.s at 25 °C) in comparison to DMAc (0.92 mPa.s at 25 °C), the rotation speed of 300 RPM was not sufficient to fully disperse the polymer in solvent because there was a dead zone observed during mixing. The polymer flakes piled at the bottom of the reaction vessel, and the rotating impeller was used to produce turbulence to fully suspend the flakes in the vessels. If the rotation speed was not fast enough for full suspension, a dead zone forms at the center of the bottom of the vessel. At the rotation speed of 450 RPM, 22 hours was needed to fully dissolve the PSf; and for 600 RPM, 20 hours was needed to dissolve PSf, meaning that the rotation speed of the impeller was able to speed up the process. Adding GVL to the dope solution to replace half of the PolarClean was able to significantly decrease the viscosity of the dope solution, and therefore also sped up the mixing process. For the recipe using 50% PolarClean and 50% GVL, 300 RPM was again not sufficient to fully disperse the polymer into the solvent, 7.2 hours were needed to dissolve at 450 RPM and 4.8 hours to dissolve at 600 RPM. At 600 RPM, similar times to dissolve PSf were needed for both the solvent mixture of 50% PolarClean and 50% GVL, and for the pure DMAc solvent. Qualitatively, decreasing the viscosity of the solvent and increasing the rotation speed of the impeller was able to speed up the required mixing time to fully dissolve the polymer.

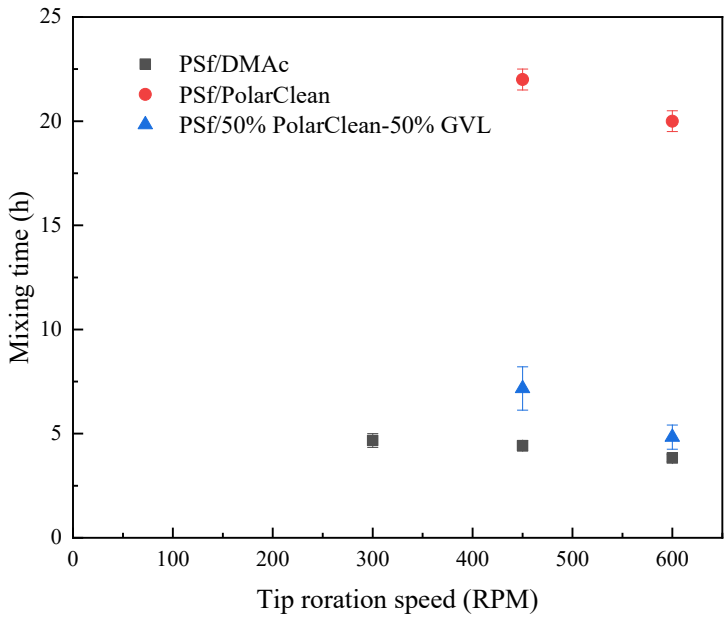

Figure 6.5 Kinetic study of dissolution PSf using different solvents under different rotation speeds of the impeller: Using DMAc requires least time while PolarClean requires longest time, adding GVL can decrease the time required

6.3.2.3 Viscosity

The viscosity data of the three dope solutions are presented in Figure 6.6. In the range of shear rate from 0.01-100 s^{-1}, the viscosity did not change significantly, which means the dope solutions showed Newtonian fluid behavior. Though Newtonian fluids are more ideal for fabrication, casting non-Newtonian solutions is more amenable for slot die casting versus doctor blade extrusion. The viscosity of PSf/DMAc and PSf/PolarClean dope solutions are approximately 0.37 Pa.s and 13.6 Pa.s, respectively. The addition of GVL in the PSf/50%PolarClean-50%GVL decreases the viscosity to approximately 4.6 Pa.s.

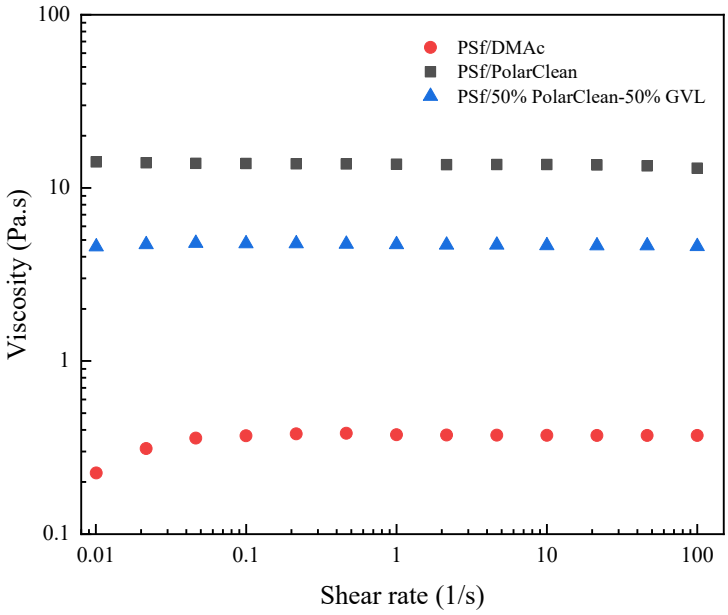

Figure 6.6 Viscosity of dope solutions change over shear rate: all the solutions showed Newtonian fluid behavior

6.3.3 Characterization of membranes

6.3.3.1 FTIR

Six membranes were characterized using FTIR and are shown in Figure 6.7. The peaks of the primary microstructures of PSf are listed in Table 3. The spectrum in Figure 6.7 shows that the peaks of PSf membranes M1- M6 match the peaks listed in Table 3. Therefore, during the membrane fabrication process, different solvents do not affect the chemistry of membrane surface.

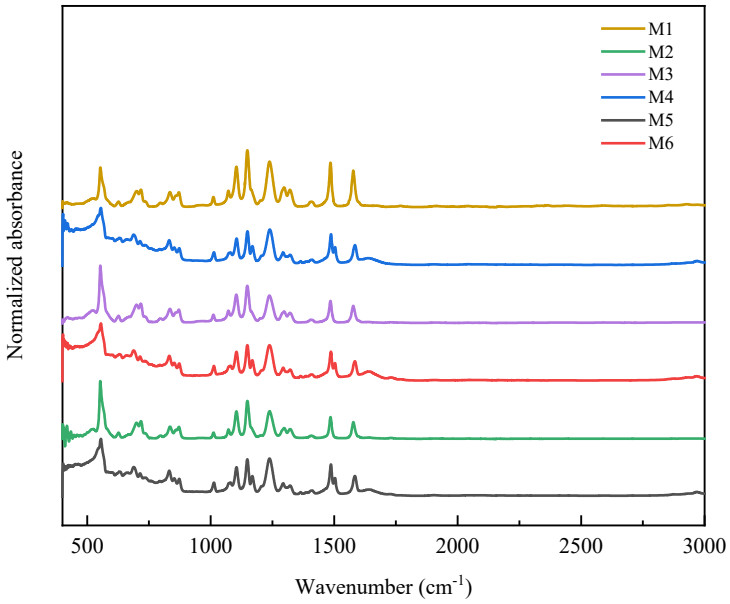

Figure 6.7 FTIR spectrum of PSf membranes M1- M6

Table 6.3 FTIR spectra of Polysulfone

PSf spectra	Wavenumber (cm^{-1})
Aromatic C-H bending	871, 850, 831
C-SO_2-C symmetric stretch	1149
C-SO_2-C asymmetric stretch	1319, 1292
C-O asymmetric stretch	1238, 1012
C_6H_6 ring stretch	1587-1489

6.3.3.2 Surface and cross-sectional morphology

SEM images of surface and cross-sectional morphology of PSf membranes made using different solvents and different casting methods are shown in Figures 6.8 and 6.9, respectively. The surface images show that all three dope solutions can be used to fabricate membranes without significant defects on the surface, both using the doctor blade and the slot die techniques. There were likely some impurities on the surface of membranes, but these did not affect the membrane properties.

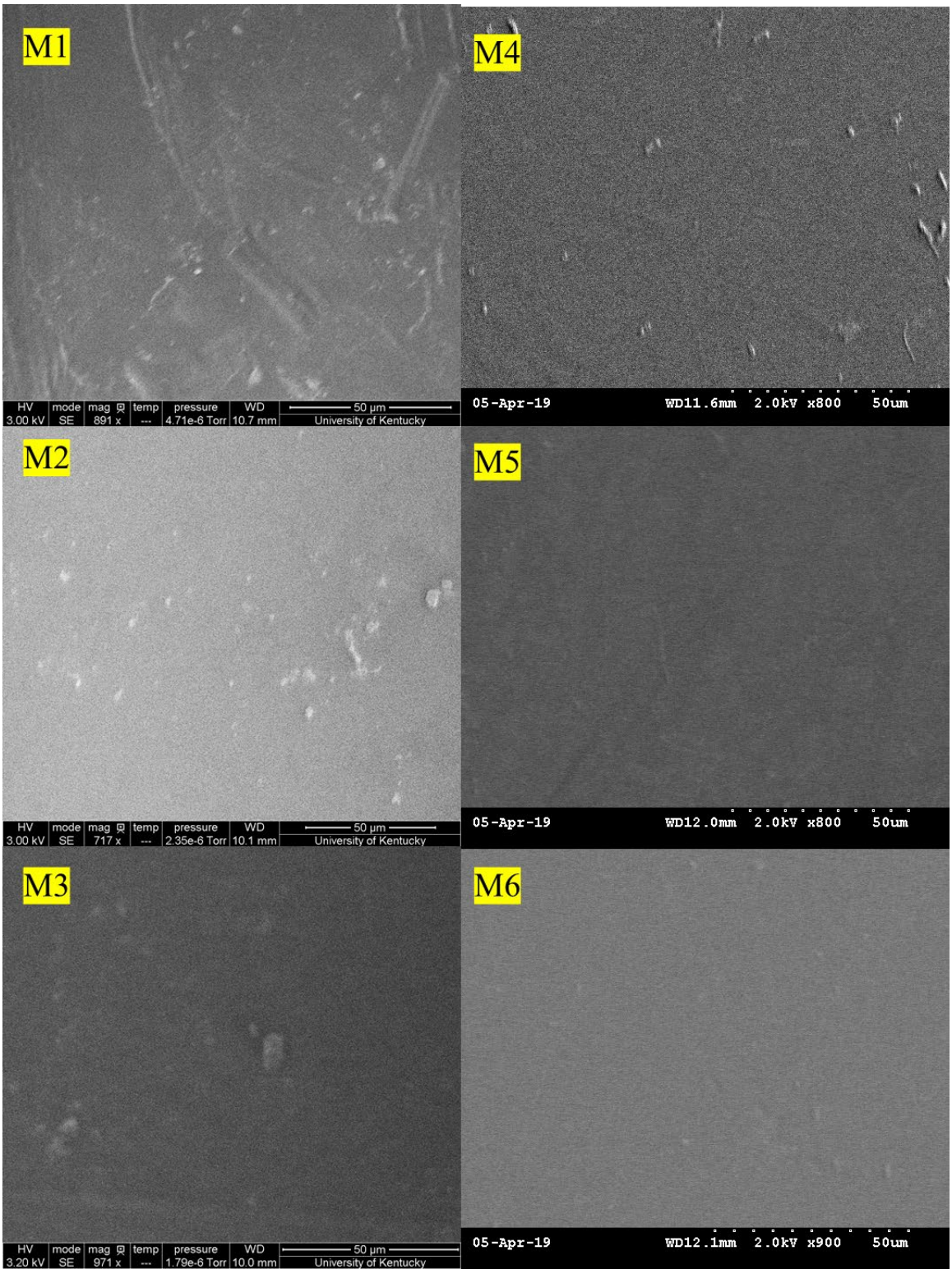

Figure 6.8 Surface images of PSf membranes casting using different solvents and different methods: No obvious deficits observed

In Figure 6.9, it is shown that the thickness of membranes fabricated using the three recipes, which ranges from 125-150 μm. The thickness of the liquid films should have been similar for the different dope solutions. However, considering the wetting property, solvent evaporation, and the demixing process in the nonsolvent bath are different for these three dope solutions, thus the thickness values of formed membranes were not the same.

Furthermore, it is shown in Figure 6.9 that the cross-section morphologies of membranes are different based on different fabrication methods and different solvents used. As observed, all six cross-sectional images of membranes are different. Using the traditional solvent DMAc, both M1 and M4, doctor blade and slot die, respectively, show similar cross-sectional structures with finger-like pores close to the active layer, and irregular microvoids in the supportive layer. When PolarClean is used, the membranes show different morphologies under the different casting methods. Using the slot die technique, the membrane exhibits patterned finger-like structures throughout the supportive layer of the membrane; on the other hand, while using the doctor blade, the membrane exhibits sponge-like structures. The solvent mixture of PolarClean and GVL also produced membranes with different morphologies under different casting techniques. Using slot die, M3 shows a unique structure, composed of a dense active layer on top, followed by a layer of finger-like microvoids and a sponge-like supportive layer. Using the doctor blade, M6 shows only a sponge-like structure in the supportive layer.

Considering the demixing process thermodynamically and kinetically, the demixing path of the dope solutions in the nonsolvent bath is the dominant factor to shape the cross-section morphology [232, 279]. Specifically, an instantaneous demixing process can form finger-like structures while a delayed demixing process can form sponge-like

structures [232]. For the slot die membranes, M1 shows larger microvoids than M2 and M3 in the cross-section structures, while for the doctor blade membranes, M4 also shows finger-like structures while M5 and M6 show spongey-like structures. This might be due that the low viscosity of PSf/DMAc dope solution that caused an instantaneous demixing process in the nonsolvent bath, while the PSf/PolarClean and PSf/50% PolarClean-50%GVL dope solutions had higher viscosity and hence caused a delayed demixing process.

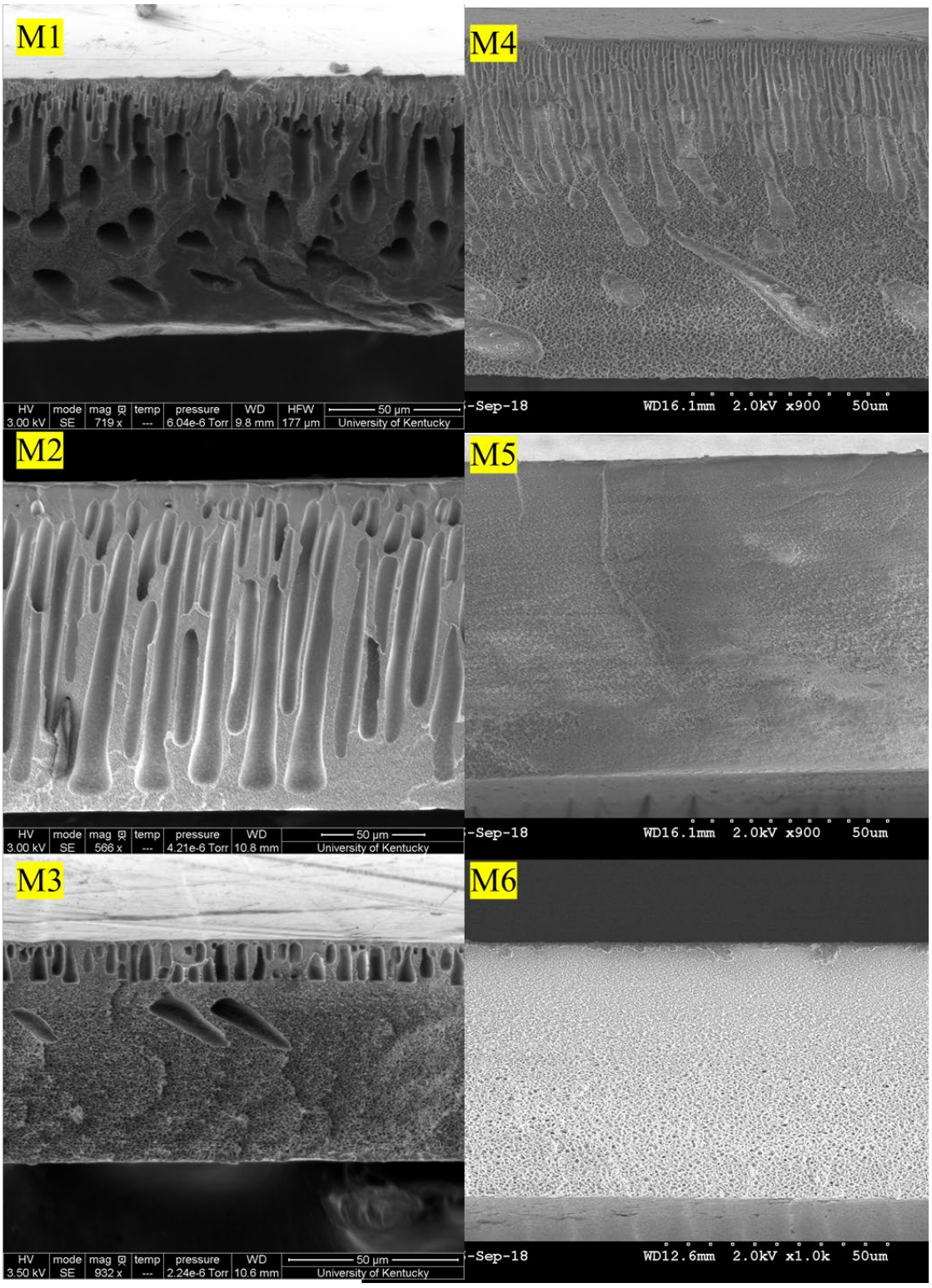

Figure 6.9 Cross sectional SEM images of PSf membranes cast using different solvents and methods

6.3.3.3 Surface roughness and topology

The average root mean square (RMS) roughness values of the six membranes are shown in Figure 6.10. Using slot die coating, the RMS roughness values of M1, M2 and M3 are 103±22 nm, 129±20 nm, and 89±17 nm, respectively. On the other hand, when using the doctor blade, the RMS roughness values of M4, M5, M6 are 27±10 nm, 31±18 nm, 10±5 nm, respectively. The membranes cast using pure solvents are rougher than the membranes fabricated using the solvent mixtures, and it could be due to membrane formation being mostly dominated by the demixing process of dope solutions, which could be quantified by the diffusion rates of the solvent into the nonsolvent, water [46]. Considering the diffusion rate of different solvents, pure PolarClean diffuses into water slower than DMAc and PolarClean/GVL, resulting in the rougher surfaces of M2 and M5. It is also noticeable that when using slot die coating, the membranes are rougher than those cast using a doctor blade extrusion. This could be due to differences between these two manufacturing processes and different noise in the systems: for the doctor blade process, a blade is run over the top of the substrate to form a liquid film on a rigid countertop, while slot die coating is conducted on a roll-to-roll system. The during the slot die coating process, the liquid film is pumped onto a moving substrate, which will be subjected to small vibration due to the motors [49, 280]. The smoother surface of M6 is due to both the doctor blade process and the instantaneous demixing process of the dope solution.

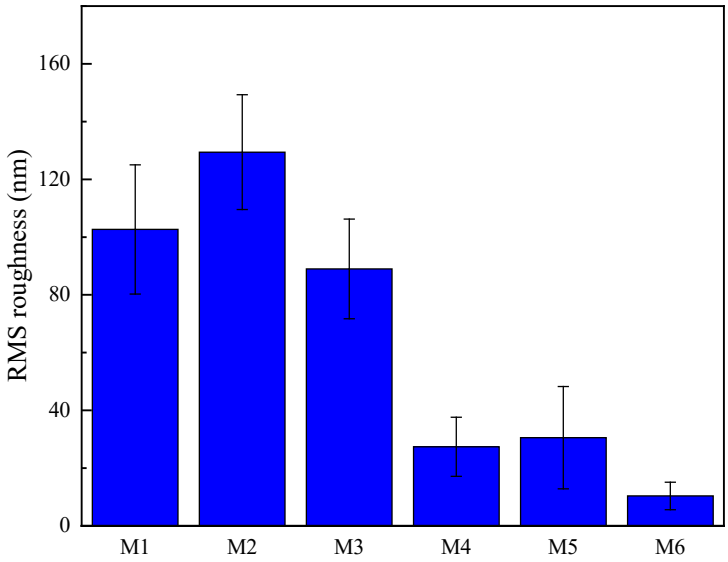

Figure 6.10 RMS roughness of membranes of M1- M6: Membranes cast using the slot die method are significantly rougher than those cast using lab casting

6.3.3.4 Hydrophilicity and wettability

The contact angle values of all six membranes were measured and monitored for five minutes and the results are shown in Figure 6.11. At 15 seconds, the average contact angle values of these membranes were in the range of 60-75 °. Theoretically, with the same membrane material, the contact angle should be in the same range. The contact angle values of M1 and M4 are slightly smaller than M3 and M6, and the values of M1 and M3 are smaller than M4 and M6, indicating that the contact angle might be correlated to the surface roughness, which would be expected. The smoother surfaces might lead to more hydrophobic membrane surfaces when the same membrane material is used. The M2 membrane, the slot die membrane fabricated using PolarClean, is an outlier.

Wettability was evaluated as the contact angle dropped over the time. M2 was the most hydrophobic at the beginning and then the contact angle drastically dropped over 5 minutes, which also eventually led to the highest wettability. The reason for this might have been the slot die membranes fabricated using PolarClean form a regular finger-like water channel. The contact angle values of other membranes gradually decreased over time; therefore, the wettability of these membranes is similar.

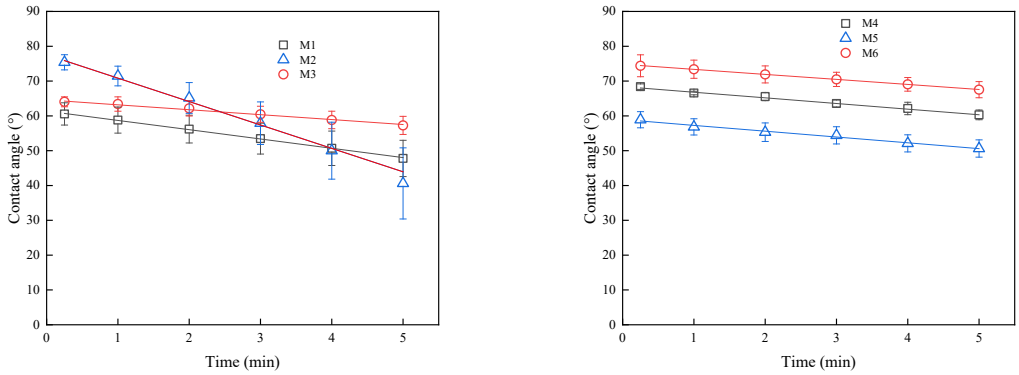

Figure 6.11 Contact angels and wettability of PSf membranes M1- M6

6.3.4 Filtration performance

6.3.4.1 Filtration linear relations

The flux linearity of these six membranes under crossflow filtration is shown in Figure 6.12. After 20 hours of precompaction, all the membranes were assumed to be fully compacted, and the flux of membranes changed linearly over the pressure applied on the membranes. From Figure 6.12, the membranes fabricated using slot die casting and doctor blade extrusion show strong linear correlations between DI water flux and applied pressure. Moreover, all of the membranes show good reproducibility except M5. The DI water

permeability of M5 is linear to the applied pressure on the membrane in both trials, but the permeability values are different. It is observed that one of the M5 trials had a slightly lower flux, which might be due to the spongy-like pore structures of this membrane collapsing during precompaction, which affects the water channels of this membranes. It has been reported previously that when pure PolarClean was used to fabricate polymeric membranes, the sponge-like pore structures collapsed during filtration and cleaning process [20, 281], and the addition of GVL can increase the stability of the pore structures [281]. It was proved by the filtration data of M3 and M6 in Figure 6.12.

Another finding here is that the flux values of membranes fabricated using PolarClean (M2 and M5) are larger than those of membranes made of DMAc (M1 and M4), and the flux values of membranes made of the PolarClean/GVL mixture are the smallest. The flux values also match the contact angle values of these membranes; that is, the more hydrophilic the membranes are the higher water permeability values the membranes can obtain.

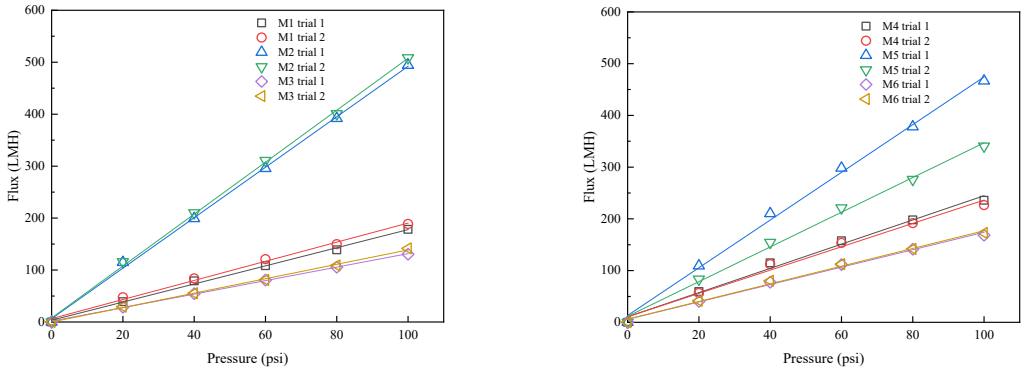

Figure 6.12 DI water flux of PSf membranes over pressure: all the precompacted membranes showed linear correlations

6.3.4.2 BSA Crossflow filtration

The six membranes were evaluated for BSA filtration. The initial flux was recorded, and then the membrane sample was tangentially washed using DI water when the flux reached 70% of the previous starting flux. This continued until the final flux of membranes reached 35% of the initial flux value at the start of filtration. The flux of BSA solutions and BSA rejection are presented in Figure 6.13. For membranes fabricated using DMAc, the slot die membranes lasted for 10 hours and the rejection of BSA is maintained at a level of 85%-95%, while the membranes cast using the doctor blade lasted approximately 6 hours with a slight higher, but not significantly different, rejection of 90%-95%. For membranes fabricated using PolarClean, the curves of M2 and M5 are compared. The initial flux values of M2 and M5 are higher than those of the other membranes, and the slot die membranes lasted for approximately 6.5 hours while the doctor blade membranes lasted for approximately 4.5 hours. The rejection of BSA for M2 membranes fluctuates between 80%-90%, while that of M5 is significantly higher at a range of 90%-

95%. Using PolarClean/GVL mixture, both membranes (M3 and M6) fabricated using slot die and the doctor blade operates for over 8 hours, and the BSA rejection of M3 and M6 gradually increases until the rejection of M6 achieved over 95% and of M3 achieved around 85%.

The crossflow filtration shows that the membranes cast using the slot die technique perform better or have at least equivalent flux to those cast using the doctor blade. However, it is observed that all the membranes cast using the doctor blade show higher BSA rejections than the slot die membranes, mostly due to the sponge-like support layers in the cross-sectional structures of the membranes, which were discussed previously (Figure 6.9).

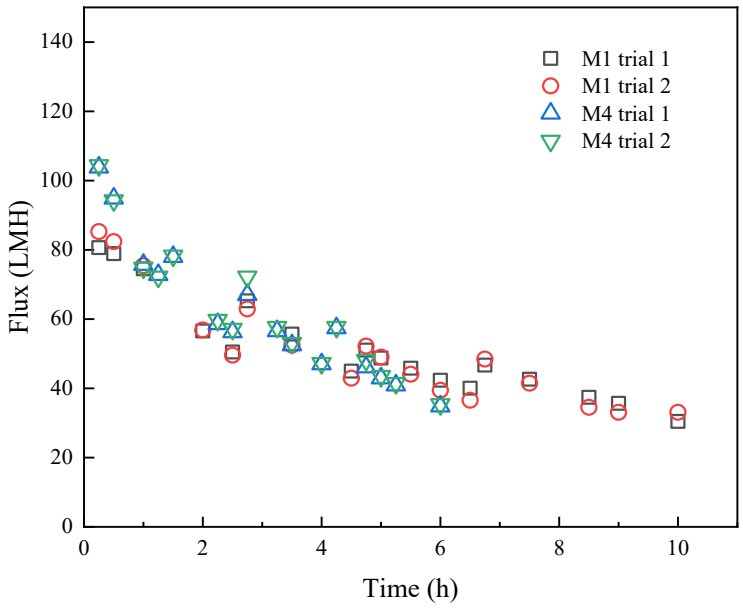

(a)

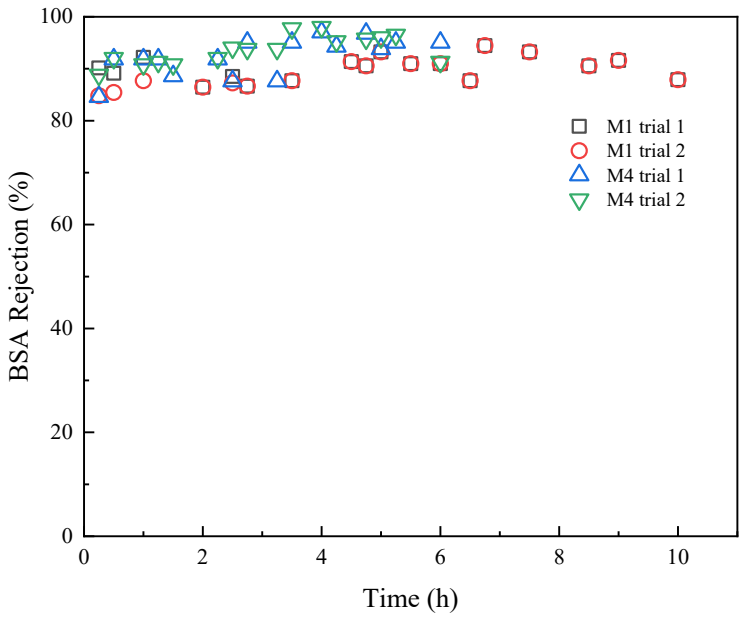
BSA Rejection (%)
Time (h)
M1 trial 1
M1 trial 2
M4 trial 1
M4 trial 2

(b)

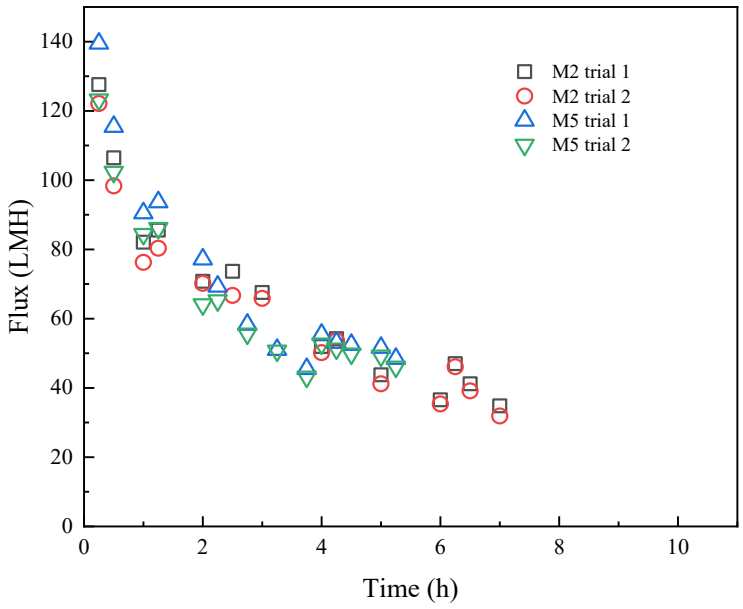
Flux (LMH)
Time (h)
M2 trial 1
M2 trial 2
M5 trial 1
M5 trial 2

(c)

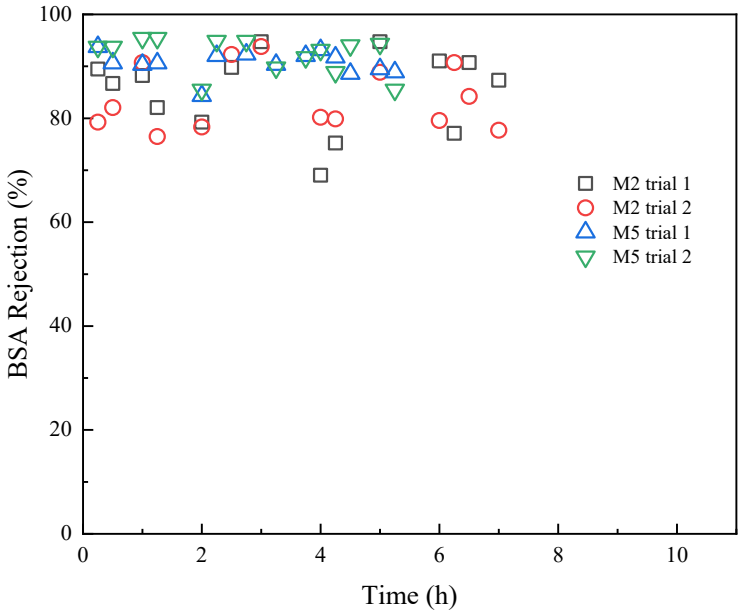
BSA Rejection (%)
Time (h)
M2 trial 1
M2 trial 2
M5 trial 1
M5 trial 2

(d)

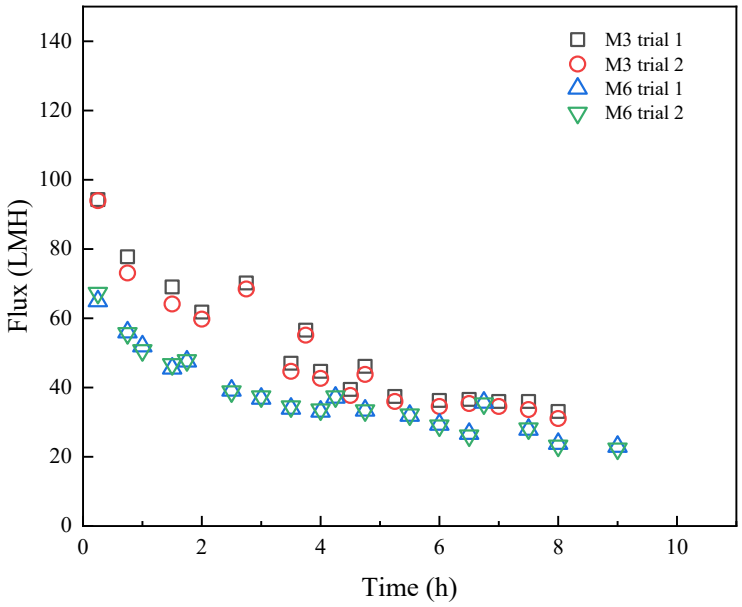
Flux (LMH)
Time (h)
M3 trial 1
M3 trial 2
M6 trial 1
M6 trial 2

(e)

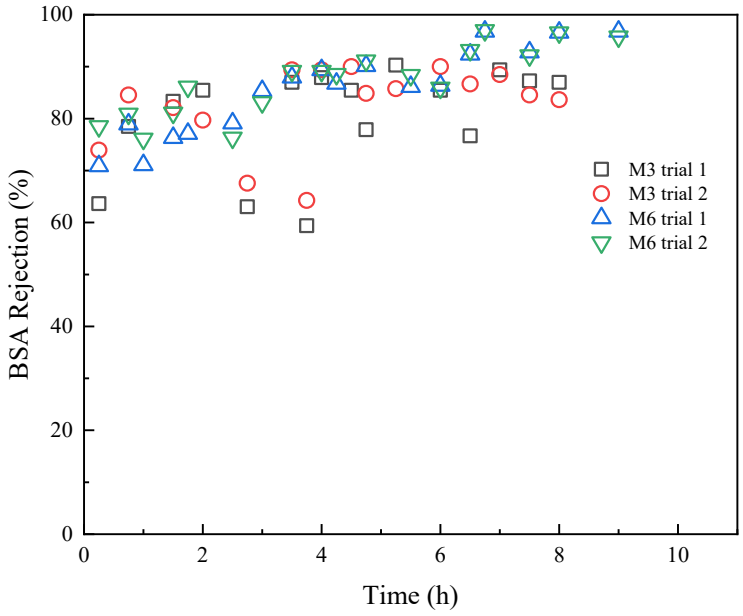

(f)

Figure 6.13 BSA filtration tests of PSf membranes: (a)flux of M1 and M4; (b) BSA rejection of M1 and M4; (c)flux of M2 and M5; (b) BSA rejection of M2 and M5; (a)flux of M3 and M6; (b) BSA rejection of M3 and M6.

6.4 Conclusions

In this study, a doctor blade extrusion at the laboratory scale and slot die casting on a R2R system (production scale) were used to fabricate PSf ultrafiltration membranes using low-hazard solvents. The properties and structure of the membranes were compared. Thermodynamically, the RED values showed that PolarClean and the solvent mixture of PolarClean/GVL were theoretically able to fully dissolve PSf. Furthermore, cloud point

curves showed that all solvents and co-solvents were fit for membrane fabrication through NIPS with water as the nonsolvent. In mixing dope solutions, dissolution kinetics studies showed that the addition of GVL to PolarClean decreased the required mixing time regardless of RPM speed, and all dope solutions showed Newtonian fluid behavior. With respect to characterization, the FTIR spectra of the membranes were similar, and membrane roughness values did not show significant changes with respect to solvent/co-solvent and casting scale. On the other hand, cross-sectional images showed that the structures of the membranes were different, due to differences in the cloud point curves for the solvent/water/PSf and in the diffusion rate of solvents/co-solvents into nonsolvents. With respect to operation, all membranes fabricated using the slot die and doctor blade showed flux linearity, and during BSA filtration, all membranes performed similarly with respect to permeability and BSA rejection. Therefore, this study not only shows that co-solvent mixtures of PolarClean and GVL were able to produce membranes with similar operational characteristics as a traditional solvent, but also that these membranes could be fabricated using slot die casting integrated into a production scale R2R system.

CHAPTER 7. CONCLUSIONS AND RECOMMENDATIONS

7.1 Conclusions

The overarching goal of this dissertation was to investigate greener/less toxic solvents, PolarClean and GVL, as sole solvents and as solvent mixtures to replace traditional petroleum-derived solvents, in this case DMAc, in fabrication of PSf membranes, along with the ability of scaling up the membranes using slot die-R2R systems. Objectives 1 and 2 focused on investigating PolarClean as a solvent to replace DMAc to cast PSf membranes, followed by characterizing the membranes and then comparing to membranes prepared with DMAc. PSf/PolarClean membranes were found to have sponge-like pores that would collapse upon reverse-flow filtration. To address this drawback, Objectives 3 and 4 investigated PolarClean and GVL as cosolvents to replace DMAc in casting PSf membranes. Objective 5 used dope solution viscosity as an indicator to quantify the kinetics of dope solution mixing and to characterize the homogeneity of the dope solutions. Finally, in Objective 6, a slot die-R2R system was used to scale up the PSf membranes prepared using PolarClean and GVL sole solvents and cosolvents to show if membranes with similar morphological and operational properties to those made using DMAc would be fabricated.

First, PolarClean was used as a NIPS solvent to cast PSf membranes and then compared with DMAc. Based on the trinary phase diagram, the cloud point curve of PSf/PolarClean/water was similar to that of PSf/DMAc/water. Dope solutions for PSf/PolarClean and PSf/DMAc were prepared at 65 °C and membranes were cast and characterized afterwards. The overall porosity, MWCO and hydrophobicity of membranes made using PolarClean and DMAc were not significantly different. However, the cross-

sections images of the membranes were different, with PSf/DMAc membranes showing finger-like structures and PSf/PolarClean membranes showing sponge-like structures. Regarding membranes performance, PSf/PolarClean membranes showed slightly higher BSA rejection rates (99 ± 0.51%) as compared to PSf/DMAc membranes (96 ± 2.00%), which agreed with their sponge-like pores structures. Furthermore, PSf/PolarClean membranes also showed higher flux values (176.0 ± 8.8 LMH) than PSf/DMAc membranes (63.1 ± 12.4 LMH), which disagreed with the sponge-like structure theory and might have been due to evaporation time. However, pore collapsing was observed in the study, which means the stability of PolarClean membranes is uncertain.

To address the pore collapse of PSf/PolarClean membranes during membrane cleaning, GVL was introduced as a cosolvent of PolarClean to fabricate PSf membranes via NIPS. Based on calculated Hansen solubility values, PolarClean/GVL co-solvents were determined to be better solvents than PolarClean and GVL as sole solvents. Furthermore, PolarClean/GVL as co-solvents showed Newtonian fluid behavior since their viscosities did not change as a function of shear rate. The mean pore diameter of fabricated membranes decreased as the weight percent of GVL increased from 0, 25%, 50% to 75% in the dope solution, and observed changes in isoelectric points followed the same trend as mean pore size as a function of changes in dope viscosity. In filtration studies, it was observed that the membrane flux decreased as the mean pore size of membranes decreased, as expected, while all membranes showed nearly complete rejection of BSA. Since the starting goal of this study was to use low-hazard solvents/co-solvents to fabricate membranes with similar operation as membranes fabricated using DMAc, it was deemed that dope solutions using equal weight fractions of PolarClean and GVL produced the best membranes. Therefore,

PolarClean/GVL co-solvents provided a promising solution to replace traditional solvents. Furthermore, PolarClean and GVL as sole solvents and cosolvents were used to dissolve PSf, and viscosity was used to quantify the time required for completely mixing of polymer/solvent and the related viscosity (RV) was used as an indicator for the homogeneity of a dope solution. After 24 h, all the dope solutions reached or surpassed RV values of 90%, indicating that these dope solutions reached homogeneity.

Finally, a slot die-R2R system was used to fabricate PSf ultrafiltration membranes using low-hazard solvents at a production scale and compared to a doctor's blade at the laboratory scale. Dope solutions were prepared in a large amount. In mixing dope solutions, dissolution kinetics studies showed that the addition of GVL to PolarClean decreased the required mixing time regardless of RPM speed. With respect to characterization, the FTIR spectra of the membranes were similar, and membrane roughness values did not show significant changes with respect to solvent/co-solvent and casting scale. On the other hand, cross-sectional images showed that the structures of the membranes were different and likely due to differences in the cloud point curves for the PSf/solvent/water and in the diffusion rate of solvents/co-solvents into nonsolvents. With respect to operation, all membranes fabricated using the slot die and doctor blade showed flux linearity, and during BSA filtration, all membranes performed similarly with respect to permeability and BSA rejection. Therefore, this study not only shows that co-solvent mixtures of PolarClean and GVL were able to produce membranes with similar operational characteristics as a traditional solvent, but also that these membranes could be scaled using slot die-R2R systems.

Overall, the solvent mixture of equal amounts of PolarClean and GVL was shown to be an alternative for DMAc to fabricate PSf membranes. Moreover, a slot die-R2R system could be used to scale up PSf membranes prepared with PolarClean/GVL cosolvent. The membranes prepared using the greener solvent mixture were comparable to the membrane prepared using DMAc in terms of structural and morphological characteristics and of filtration performance.

7.2 Recommendations

This work investigated the use of greener solvents, PolarClean and GVL, to replace a traditional petroleum-derived and toxic solvent, namely DMAc, in PSf membrane fabrication. It also used a slot die-R2R system to scale up the membranes. To continue on the study, suggestions follow to make the membrane fabrication process more environmentally friendly:

1. Although both PolarClean and GVL have been investigated as greener solvents with respect to biodegradability, their actual biodegradability in the NIPS waste after membrane fabrication is unknown since the waste mixture contains a non-negligible concentration of solvent. Therefore, their actual biodegradability of these two solvents should be investigated.
2. Besides the biodegradability of these solvents, recyclability and reusability of the solvents are unknown. Absorbents should be investigated to determine the feasibility of recycling the organic solvents. Distillation could be another method to recycle the solvents. Moreover, an economic analysis should also be performed to determine if the recycling is economically acceptable.

3. In this study, the pores of PSf/PolarClean membranes collapsed during membrane cleaning. The mechanical strengthen of the membranes should be studied further. The analysis of mechanical properties has the potential to guide future membrane fabrication.
4. In this study, only the polymer and solvents were considered to minimize variables. With this work as a foundation, other factors can take into consideration. Additives should be studied to enhance the selectivity of membranes or improve the antifouling properties of the membranes. Casting conditions, for example, humidity, temperature, nonsolvent composition, should also be studied in the future.

APPENDICES

APPENDIX 1 FILTRATION DATA

Table A1. The original filtration data in Chapter 3, a comparison between PSf/DMAc membranes and PSf/PolarClean membranes. All the dead-end filtration experiments were performed at room temperature, at pressure of 4.14 bar (60 psi).

		17 PSf/DMAc		17 PSf/PolarClean	
	Permeate volume (mL)	Flux (LMH)	STD	Flux (LMH)	STD
DI Water	2	73.22	11.30	3466.70	306.24
	4	72.08	10.31	3066.23	82.13
	6	74.86	8.06	2649.52	137.39
	8	81.72	10.24	2605.74	31.78
	10	82.27	9.98	2578.88	26.37
	12	83.26	11.18	2543.66	92.24
	14	84.68	8.92	2569.48	90.46
	16	84.95	9.07	2400.49	72.65
	18	84.98	9.97	2462.80	215.57
	20	83.96	8.46	2423.19	124.88
BSA	22	63.14	12.43	176.49	8.84
	24	57.85	16.47	132.53	41.10
	26	52.10	13.19	144.89	5.76
	28	46.80	21.84	135.37	7.68
	30	48.37	21.12	138.15	7.04
	32	44.64	16.95	134.28	6.65
	34	42.24	15.43	125.16	7.81
	36	43.49	14.18	109.73	29.41
	38	40.61	13.77	104.67	31.89
	40	39.93	13.61	125.25	4.52
back wash	42	56.63	15.72	740.42	54.39

Table A2. The original filtration data in Chapter 5, a comparison among PSf membranes, M1 (PSf/PolarClean), M2 (PSf/75% PolarClean), M3 (PSf/50% PolarClean 50% GVL), M6 (PSf/DMAc). All the dead-end filtration experiments were performed at room temperature, at pressure of 4.14 bar (60 psi).

		M1		M2		M3		M6	
	Permeate volume (mL)	Flux (LMH)	STD	Flux (LMH)	STD	Flux (LMH)	STD	Flux (LMH)	STD
DI Water	2	1842.9	140.1	511.6	132.7	52.8	9.4	21.6	2.3
	4	1414.0	186.4	468.3	91.0	40.8	5.0	19.5	3.1
	6	1008.4	91.7	424.3	39.7	38.7	4.2	18.8	2.4
	8	938.6	131.7	366.0	36.5	38.0	9.0	18.4	2.5
	10	861.8	70.6	360.5	55.1	37.1	6.5	17.0	2.8
	12	867.2	98.4	326.4	31.7	31.9	4.8	17.4	3.1
	14	847.1	147.9	324.9	50.0	29.6	3.7	17.7	2.6
	16	790.1	67.7	315.0	43.7	28.2	2.8	17.1	3.0
	18	750.5	94.6	317.5	40.8	29.1	3.2	17.0	3.8
	20	743.2	107.3	297.7	32.0	26.9	0.7	16.9	3.4
BSA	22	265.1	37.4	137.8	24.4	14.8	0.7	15.0	1.9
	24	165.9	12.9	127.9	23.7	14.7	1.4	14.5	2.7
	26	151.6	20.3	130.8	22.7	12.6	1.6	13.8	2.4
	28	150.8	13.3	117.5	26.4	12.9	1.6	13.3	2.5
	30	136.9	16.9	116.0	17.7	12.5	1.7	14.1	3.5
	32	135.0	12.6	117.7	31.9	12.2	1.6	13.5	2.3
	34	135.0	20.9	129.3	22.3	11.7	0.9	13.1	2.0
	36	139.3	21.3	114.4	20.0	11.9	1.3	13.2	2.2
	38	139.1	23.9	118.5	14.5	11.4	1.3	13.6	2.4
	40	141.0	17.1	115.1	19.6	11.9	1.3	13.3	1.8
back wash	42	228.3	8.6	196.9	4.0	19.0	1.9	15.5	2.2

Table A3. The original crossflow filtration data in Chapter 6. The flux linearity data of membranes prepared using DMAc, PolarClean, and 50% PolarClean/ 50% GVL, and using the slot die and doctor blade were compared.

	Slot die					
	PSf/DMAc (LMH)		PSf/PC (LMH)		PSf/50PolarClean 50GVL (LMH)	
△P (psi)	Trail 1	Trail 2	Trail 1	Trail 2	Trail 1	Trail 2
0	0.00	0.00	0.00	0.00	0.00	0.00
20	39.03	47.48	114.76	115.92	28.54	29.42
40	79.22	83.88	199.22	210.00	54.47	55.34
60	108.35	120.87	295.63	310.78	80.68	80.97
80	138.93	149.71	392.04	400.78	105.44	108.93
100	178.25	188.74	494.27	508.54	130.49	141.55
	Doctor blade					
	PSf/DMAc (LMH)		PSf/PC (LMH)		PSf/50PolarClean 50GVL (LMH)	
△P (psi)	Trail 1	Trail 2	Trail 1	Trail 2	Trail 1	Trail 2
0	0.00	0.00	0.00	0.00	0.00	0.00
20	59.42	56.80	109.22	83.30	40.49	41.65
40	115.05	112.43	210.29	154.37	77.48	80.39
60	157.57	153.50	298.25	221.07	111.55	112.43
80	198.06	191.65	378.06	276.12	141.26	141.84
100	235.92	226.60	466.60	340.49	168.35	172.72

Table A4. The original crossflow filtration data in Chapter 6. The flux data of membranes prepared using DMAc, PolarClean, and 50% PolarClean/ 50% GVL, and using the slot die and doctor blade were compared. The pressure applied on membranes used was constant at 100 psi (6.9 bar). The membranes were cleaned using DI water when the flux hits the 70% of the original flux, and this procedure repeated until the flux reached at 35% of the starting original flux.

Slot die membranes:

PSf/DMAc			PSf/ 50PC 50GVL			PSf/ PolarClean		
Time (h)	Cell 1 (LMH)	Cell 2 (LMH)	Time (h)	Cell 1 (LMH)	Cell 2 (LMH)	Time (h)	Cell 1 (LMH)	Cell 2 (LMH)
0.25	80.62	85.26	0.25	94.25	93.96	0.25	127.6	122.09
0.5	78.88	82.36	0.75	77.72	73.08	0.5	106.43	98.31
1	74.53	75.4	1.5	69.02	64.09	1	82.07	76.27
2	56.55	56.84	2	61.77	59.74	1.25	85.55	80.33
2.5	50.46	49.59	2.75	70.18	68.44	2	70.76	70.18
2.75	65.25	62.93	3.5	46.98	44.66	2.5	73.66	66.7
3.5	55.68	52.49	3.75	56.55	55.1	3	67.57	65.83
4.5	44.95	42.92	4	44.66	42.63	4	51.91	50.17
4.75	51.04	52.2	4.5	39.44	37.7	4.25	54.23	53.65
5	48.72	49.01	4.75	46.11	43.79	5	43.79	41.18
5.5	45.82	44.08	5.25	37.41	35.96	6	36.54	35.38
6	42.34	39.44	6	36.25	34.51	6.25	46.98	46.11
6.5	40.02	36.54	6.5	36.54	35.38	6.5	41.18	39.15
6.75	46.69	48.43	7	35.96	34.51	7	34.8	31.9
7.5	42.63	41.47	7.5	35.96	33.64			
8.5	37.41	34.51	8	33.06	31.03			
9	35.67	33.06						
10	30.45	33.06						

Doctor blade casting membranes:

	PSf/DMAc			PSf/50PC 50GVL			PSf/PolarClean	
Time (h)	Cell 1 (LMH)	Cell 2 (LMH)	Time (h)	Cell 1 (LMH)	Cell 2 (LMH)	Time (h)	Cell 1 (LMH)	Cell 2 (LMH)
0.25	103.82	104.4	0.25	64.96	67.28	0.25	139.49	123.25
0.5	94.83	94.25	0.75	55.97	55.68	0.5	115.42	102.37
1	75.69	74.82	1	51.91	50.75	1	90.48	84.39
1.25	72.79	72.21	1.5	45.53	46.69	1.25	93.67	86.13
1.5	78.01	78.3	1.75	47.56	47.85	2	77.14	64.09
2.25	58.58	59.74	2.5	39.15	38.86	2.25	69.31	65.25
2.5	56.26	57.13	3	36.83	37.41	2.75	58.29	55.68
2.75	66.99	72.21	3.5	33.93	34.51	3.25	51.04	50.75
3.25	56.55	57.71	4	33.06	33.64	3.75	45.53	43.21
3.5	52.49	53.07	4.25	37.12	37.41	4	55.39	52.78
4	46.98	47.27	4.75	33.35	33.35	4.25	53.07	51.33
4.25	57.42	57.71	5.5	31.9	32.19	4.5	52.49	49.88
4.75	46.11	48.14	6	29.29	29	5	51.62	49.3
5	42.92	43.5	6.5	26.68	26.1	5.25	48.43	46.11
5.25	40.89	41.47	6.75	35.67	35.38			
6	34.8	35.38	7.5	27.84	28.13			
			8	23.78	23.2			
			9	22.91	22.33			

Table A5. The original crossflow filtration data in Chapter 6. The BSA rejection of membranes prepared using DMAc, PolarClean, and 50% PolarClean/ 50% GVL, and using the slot die and doctor blade were compared. The pressure applied on membranes used was constant at 100 psi (6.9 bar). The membranes were cleaned using DI water when the flux hits the 70% of the original flux, and this procedure repeated until the flux reached at 35% of the starting original flux.

Slot die membranes:

PSf/DMAc			PSf/ 50PC 50GVL			PSf/ PolarClean		
Time (h)	Cell 1 (LMH)	Cell 2 (LMH)	Time (h)	Cell 1 (LMH)	Cell 2 (LMH)	Time (h)	Cell 1 (LMH)	Cell 2 (LMH)
0.25	90.1%	84.8%	0.25	63.6%	73.9%	0.25	89.5%	79.3%
0.5	89.1%	85.4%	0.75	78.5%	84.5%	0.5	86.7%	82.0%
1	92.2%	87.7%	1.5	83.3%	82.1%	1	88.2%	90.7%
2	86.4%	86.4%	2	85.5%	79.7%	1.25	82.0%	76.5%
2.5	88.5%	87.3%	2.75	63.0%	67.6%	2	79.3%	78.3%
2.75	86.7%	86.7%	3.5	87.0%	89.4%	2.5	89.8%	92.3%
3.5	87.7%	87.7%	3.75	59.4%	64.2%	3	94.7%	93.8%
4.5	91.4%	91.4%	4	87.9%	89.4%	4	69.0%	80.2%
4.75	90.6%	90.6%	4.5	85.5%	90.0%	4.25	75.2%	79.9%
5	93.2%	93.2%	4.75	77.9%	84.8%	5	94.7%	88.9%
5.5	91.0%	91.0%	5.25	90.3%	85.8%	6	91.0%	79.6%
6	91.0%	91.0%	6	85.5%	90.0%	6.25	77.1%	90.7%
6.5	87.7%	87.7%	6.5	76.7%	86.7%	6.5	90.7%	84.2%
6.75	94.5%	94.5%	7	89.4%	88.5%	7	87.3%	77.7%
7.5	93.2%	93.2%	7.5	87.3%	84.5%			
8.5	90.6%	90.6%	8	87.0%	83.6%			
9	91.6%	91.6%						
10	87.9%	87.9%						

Doctor blade casting membranes:

PSf/DMAc			PSf/50PC 50GVL			PSf/PolarClean		
Time (h)	Cell 1(LMH)	Cell 2 (LMH)	Time (h)	Cell 1(LMH)	Cell 2 (LMH)	Time (h)	Cell 1(LMH)	Cell 2 (LMH)
0.25	84.6%	88.8%	0.25	70.9%	78.5%	0.25	93.7%	93.7%
0.5	91.8%	92.1%	0.75	78.9%	80.9%	0.5	90.6%	93.7%
1	91.8%	90.8%	1	71.1%	76.1%	1	90.3%	95.4%
1.25	91.8%	91.3%	1.5	76.3%	81.1%	1.25	90.6%	95.4%
1.5	88.6%	90.8%	1.75	77.1%	86.1%	2	84.3%	85.5%
2.25	91.8%	92.1%	2.5	79.1%	76.3%	2.25	92.0%	94.9%
2.5	87.6%	94.0%	3	85.3%	83.1%	2.75	92.3%	94.9%
2.75	95.0%	93.8%	3.5	88.0%	89.2%	3.25	90.3%	89.7%
3.25	87.6%	93.8%	4	89.4%	89.2%	3.75	92.0%	91.7%
3.5	95.0%	97.8%	4.25	86.7%	88.6%	4	93.2%	93.2%
4	97.0%	98.0%	4.75	90.2%	91.2%	4.25	91.7%	88.9%
4.25	94.3%	95.3%	5.5	86.1%	88.4%	4.5	88.6%	94.0%
4.75	96.8%	95.8%	6	86.3%	85.9%	5	89.5%	94.3%
5	93.8%	96.0%	6.5	92.4%	93.2%	5.25	88.9%	85.5%
5.25	95.0%	96.5%	6.75	96.8%	97.0%			
6	95.0%	91.3%	7.5	92.8%	92.2%			
			8	96.6%	96.6%			
			9	96.8%	95.8%			

APPENDIX 2. DISSOLUTION DYNAMIC STUDY RAW DATA

In Chapter 5, the viscosity was used as a parameter to determine if the dope solutions are homogenous. The change of viscosity over time was recorded for 72 hours.

Table B1. Viscosity of dope solutions change over time. Five different dope solutions were compared.

	Average Viscosity (Pa.s)								
	1h	2h	3h	4h	6h	8h	16h	24h	72h
DMAc	0.069	0.156	0.176	0.179	0.182	0.196	0.181	0.190	0.193
PolarClean	0.048	0.052	0.096	0.130	0.320	0.452	1.594	5.496	5.834
75PC25GVL	0.253	0.102	0.116	0.302	0.526	0.747	1.929	3.430	3.983
50PC50GVL	0.175	0.137	0.197	0.313	0.500	0.856	1.677	2.569	2.673
GVL	0.143	0.116	0.458	0.674	1.181	1.120	1.466	1.487	1.551
	Standard Diviation								
	1h	2h	3h	4h	6h	8h	16h	24h	72h
DMAc	0.036	0.022	0.007	0.008	0.010	0.011	0.016	0.008	0.011
PolarClean	0.023	0.007	0.038	0.021	0.138	0.124	0.423	0.260	0.372
75PC25GVL	0.362	0.050	0.005	0.096	0.093	0.208	0.084	0.242	0.310
50PC50GVL	0.247	0.045	0.102	0.089	0.098	0.197	0.196	0.152	0.323
GVL	0.153	0.052	0.115	0.079	0.225	0.094	0.042	0.021	0.093

Table B2. Normalized viscosity was introduced as a parameter to represent the homogeneity of dope solutions.

	Normalized viscosity								
	1h	2h	3h	4h	6h	8h	16h	24h	72h
DMAc	0.359	0.807	0.912	0.924	0.942	1.014	0.938	0.984	1.000
PolarClean	0.008	0.009	0.017	0.022	0.055	0.077	0.273	0.942	1.000
75PC25GVL	0.064	0.026	0.029	0.076	0.132	0.188	0.484	0.861	1.000
50PC50GVL	0.065	0.051	0.074	0.117	0.187	0.320	0.627	0.961	1.000
GVL	0.092	0.075	0.295	0.435	0.761	0.722	0.946	0.959	1.000
	Standard Diviation								
	1h	2h	3h	4h	6h	8h	16h	24h	72h
DMAc	0.188	0.113	0.035	0.041	0.051	0.058	0.083	0.042	0.059
PolarClean	0.004	0.001	0.006	0.004	0.024	0.021	0.073	0.045	0.064
75PC25GVL	0.091	0.013	0.001	0.024	0.023	0.052	0.021	0.061	0.078
50PC50GVL	0.092	0.017	0.038	0.033	0.037	0.074	0.073	0.057	0.121
GVL	0.099	0.034	0.074	0.051	0.145	0.061	0.027	0.014	0.060

REFERENCES

[1] A. Figoli, T. Marino, S. Simone, E. Di Nicolò, X.M. Li, T. He, S. Tornaghi, E. Drioli, Towards non-toxic solvents for membrane preparation: a review, Green Chemistry, 16 (2014) 4034-4059.

[2] J.H. Clark, S.J. Tavener, Alternative Solvents: Shades of Green, Organic Process Research & Development, 11 (2007) 149-155.

[3] P.G. Jessop, Searching for green solvents, Green Chemistry, 13 (2011) 1391-1398.

[4] C. Capello, U. Fischer, K. Hungerbuhler, What is a green solvent? A comprehensive framework for the environmental assessment of solvents, Green Chemistry, 9 (2007) 927-934.

[5] J.H. Clark, T.J. Farmer, A.J. Hunt, J. Sherwood, Opportunities for Bio-Based Solvents Created as Petrochemical and Fuel Products Transition towards Renewable Resources, International Journal of Molecular Sciences, 16 (2015) 17101-17159.

[6] Y. Gu, F. Jerome, Bio-based solvents: an emerging generation of fluids for the design of eco-efficient processes in catalysis and organic chemistry, Chemical Society Reviews, 42 (2013) 9550-9570.

[7] Y. Medina-Gonzalez, P. Aimar, J.F. Lahitte, J.C. Remigy, Towards green membranes: preparation of cellulose acetate ultrafiltration membranes using methyl lactate as a biosolvent, International Journal of Sustainable Engineering, 4 (2011) 75-83.

[8] C.Y. Wong, W.Y. Wong, K.S. Loh, W.R.W. Daud, K.L. Lim, M. Khalid, R. Walvekar, Development of poly (vinyl alcohol)-based polymers as proton exchange membranes and challenges in fuel cell application: a review, Polymer Reviews, 60 (2020) 171-202.

[9] N.A.H. Rosli, K.S. Loh, W.Y. Wong, R.M. Yunus, T.K. Lee, A. Ahmad, S.T. Chong, Review of Chitosan-Based Polymers as Proton Exchange Membranes and Roles of Chitosan-Supported Ionic Liquids, International journal of molecular sciences, 21 (2020) 632.

[10] M. Chen, L. Zhu, J. Chen, F. Yang, C.Y. Tang, M.D. Guiver, Y. Dong, Spinel-based ceramic membranes coupling solid sludge recycling with oily wastewater treatment, Water research, 169 (2020) 115180.

[11] N. Gao, W. Fan, Z.-K. Xu, Ceramic membrane with protein-resistant surface via dopamine/diglycolamine co-deposition, Separation and Purification Technology, 234 (2020) 116135.

[12] J.Y. Chong, B. Wang, K. Li, High performance stainless steel-ceramic composite hollow fibres for microfiltration, Journal of Membrane Science, 541 (2017) 425-433.

[13] X. Gao, B. Gao, H. Liu, C. Zhang, Y. Zhang, J. Jiang, X. Gu, Fabrication of stainless steel hollow fiber supported NaA zeolite membrane by self-assembly of submicron seeds, Separation and Purification Technology, 234 (2020) 116121.

[14] G.R. Guillen, Y. Pan, M. Li, E.M.V. Hoek, Preparation and Characterization of Membranes Formed by Nonsolvent Induced Phase Separation: A Review, Industrial & Engineering Chemistry Research, 50 (2011) 3798-3817.

[15] R. Hausman, B. Digman, I.C. Escobar, M. Coleman, T.S. Chung, Functionalization of polybenzimidizole membranes to impart negative charge and hydrophilicity, Journal of Membrane Science, 363 (2010) 195-203.

[16] P. Staiti, F. Lufrano, A.S. Arico, E. Passalacqua, V. Antonucci, Sulfonated polybenzimidazole membranes - preparation and physico-chemical characterization, J. Membr. Sci., 188 (2001) 71-78.

[17] J. Kim, B. Van der Bruggen, The use of nanoparticles in polymeric and ceramic membrane structures: Review of manufacturing procedures and performance improvement for water treatment, Environmental Pollution, 158 (2010) 2335-2349.

[18] J. Mallevialle, J.L. Bersillon, C. Anselme, P. Aptel, MEMBRANE FILTRATION IN DRINKING-WATER TREATMENT - A CASE STORY, 1992.

[19] M. Pagliero, A. Bottino, A. Comite, C. Costa, Novel hydrophobic PVDF membranes prepared by nonsolvent induced phase separation for membrane distillation, Journal of Membrane Science, 596 (2020) 117575.

[20] X. Dong, A. Al-Jumaily, I.C. Escobar, Investigation of the Use of a Bio-Derived Solvent for Non-Solvent-Induced Phase Separation (NIPS) Fabrication of Polysulfone Membranes, Membranes (Basel), 8 (2018) 23.

[21] J.F. Kim, J.H. Kim, Y.M. Lee, E. Drioli, Thermally induced phase separation and electrospinning methods for emerging membrane applications: A review, AIChE Journal, 62 (2016) 461-490.

[22] B. Lei, K.-H. Shin, D.-Y. Noh, I.-H. Jo, Y.-H. Koh, W.-Y. Choi, H.-E. Kim, Nanofibrous gelatin–silica hybrid scaffolds mimicking the native extracellular matrix (ECM) using thermally induced phase separation, Journal of Materials Chemistry, 22 (2012) 14133-14140.

[23] O. M'barki, A. Hanafia, D. Bouyer, C. Faur, R. Sescousse, U. Delabre, C. Blot, P. Guenoun, A. Deratani, D. Quemener, C. Pochat-Bohatier, Greener method to prepare porous polymer membranes by combining thermally induced phase separation and crosslinking of poly(vinyl alcohol) in water, Journal of Membrane Science, 458 (2014) 225-235.

[24] M. Zahid, A. Rashid, S. Akram, Z. Rehan, W. Razzaq, A comprehensive review on polymeric nano-composite membranes for water treatment, J. Membr. Sci. Technol, 8 (2018) 1-20.

[25] Q. Zhao, R. Xie, F. Luo, Y. Faraj, Z. Liu, X.-J. Ju, W. Wang, L.-Y. Chu, Preparation of high strength poly(vinylidene fluoride) porous membranes with cellular structure via vapor-induced phase separation, Journal of Membrane Science, 549 (2018) 151-164.

[26] R. Pervin, P. Ghosh, M.G. Basavaraj, Tailoring pore distribution in polymer films via evaporation induced phase separation, RSC Advances, 9 (2019) 15593-15605.

[27] A.Z. Samuel, S. Umapathy, S. Ramakrishnan, Functionalized and Postfunctionalizable Porous Polymeric Films through Evaporation-Induced Phase Separation Using Mixed Solvents, ACS Applied Materials & Interfaces, 3 (2011) 3293-3299.

[28] N. Ismail, A. Venault, J.-P. Mikkola, D. Bouyer, E. Drioli, N. Tavajohi Hassan Kiadeh, Investigating the potential of membranes formed by the vapor induced phase separation process, Journal of Membrane Science, 597 (2020) 117601.

[29] W. Lu, Z. Yuan, Y. Zhao, H. Zhang, H. Zhang, X. Li, Porous membranes in secondary battery technologies, Chemical Society Reviews, 46 (2017) 2199-2236.

[30] V.P. Khare, A.R. Greenberg, W.B. Krantz, Vapor-induced phase separation—effect of the humid air exposure step on membrane morphology: Part I. Insights from mathematical modeling, Journal of Membrane Science, 258 (2005) 140-156.

[31] J. Barzin, B. Sadatnia, Theoretical phase diagram calculation and membrane morphology evaluation for water/solvent/polyethersulfone systems, Polymer, 48 (2007) 1620-1631.

[32] Y.-M. Wei, Z.-L. Xu, X.-T. Yang, H.-L. Liu, Mathematical calculation of binodal curves of a polymer/solvent/nonsolvent system in the phase inversion process, Desalination, 192 (2006) 91-104.

[33] D.M. Koenhen, M.H.V. Mulder, C.A. Smolders, Phase separation phenomena during the formation of asymmetric membranes, Journal of Applied Polymer Science, 21 (1977) 199-215.

[34] F.W. Altena, C.A. Smolders, Calculation of liquid-liquid phase separation in a ternary system of a polymer in a mixture of a solvent and a nonsolvent, Macromolecules, 15 (1982) 1491-1497.

[35] L. Keshavarz, M.A. Khansary, S. Shirazian, Phase diagram of ternary polymeric solutions containing nonsolvent/solvent/polymer: Theoretical calculation and experimental validation, Polymer, 73 (2015) 1-8.

[36] W.R. Krigbaum, Polymer Solutions. H. Tompa, Academic Press, New York, 1956. 325 pp. $8.50, Journal of Polymer Science, 25 (1957) 354-354.

[37] L. Yilmaz, A.J. McHugh, Analysis of nonsolvent–solvent–polymer phase diagrams and their relevance to membrane formation modeling, Journal of Applied Polymer Science, 31 (1986) 997-1018.

[38] H.H. Wang, J.T. Jung, J.F. Kim, S. Kim, E. Drioli, Y.M. Lee, A novel green solvent alternative for polymeric membrane preparation via nonsolvent-induced phase separation (NIPS), Journal of Membrane Science, 574 (2019) 44-54.

[39] S. Mazinani, S. Darvishmanesh, A. Ehsanzadeh, B. Van der Bruggen, Phase separation analysis of Extem/solvent/non-solvent systems and relation with membrane morphology, Journal of Membrane Science, 526 (2017) 301-314.

[40] C. Kahrs, T. Gühlstorf, J. Schwellenbach, Influences of different preparation variables on polymeric membrane formation via nonsolvent induced phase separation, Journal of Applied Polymer Science, 137 (2020) 48852.

[41] D.S. Lakshmi, T. Cundari, E. Furia, A. Tagarelli, G. Fiorani, M. Carraro, A. Figoli, Preparation of Polymeric Membranes and Microcapsules Using an Ionic Liquid as Morphology Control Additive, Macromolecular Symposia, 357 (2015) 159-167.

[42] J. Chang, J. Zuo, L. Zhang, G.S. O'Brien, T.-S. Chung, Using green solvent, triethyl phosphate (TEP), to fabricate highly porous PVDF hollow fiber membranes for membrane distillation, Journal of Membrane Science, 539 (2017) 295-304.

[43] T. Marino, E. Blasi, S. Tornaghi, E. Di Nicolò, A. Figoli, Polyethersulfone membranes prepared with Rhodiasolv® Polarclean as water soluble green solvent, Journal of membrane science, 549 (2018) 192-204.

[44] D.Y. Xing, S.Y. Chan, T.-S. Chung, Fabrication of porous and interconnected PBI/P84 ultrafiltration membranes using [EMIM] OAc as the green solvent, Chemical engineering science, 87 (2013) 194-203.

[45] W. Xie, T. Li, C. Chen, H. Wu, S. Liang, H. Chang, B. Liu, E. Drioli, Q. Wang, J.C. Crittenden, Using the Green Solvent Dimethyl Sulfoxide To Replace Traditional Solvents Partly and Fabricating PVC/PVC-g-PEGMA Blended Ultrafiltration Membranes with High Permeability and Rejection, Industrial & Engineering Chemistry Research, 58 (2019) 6413-6423.

[46] X. Dong, H.D. Shannon, I.C. Escobar, Investigation of PolarClean and Gamma-Valerolactone as Solvents for Polysulfone Membrane Fabrication, in: Green Polymer Chemistry: New Products, Processes, and Applications, American Chemical Society, 2018, pp. 385-403.

[47] T. Bucher, V. Filiz, C. Abetz, V. Abetz, Formation of Thin, Isoporous Block Copolymer Membranes by an Upscalable Profile Roller Coating Process-A Promising Way to Save Block Copolymer, Membranes (Basel), 8 (2018) 57.

[48] K. Bhamidipati, S. Didari, T.A.L. Harris, Experimental Study on Air Entrainment in Slot Die Coating of High-Viscosity, Shear-Thinning Fluids, Chemical Engineering Science, 80 (2012) 195-204.

[49] K.L. Bhamidipati, S. Didari, T.A.L. Harris, Slot die coating of polybenzimiazole based membranes at the air engulfment limit, Journal of Power Sources, 239 (2013) 382-392.

[50] X. Ding, J. Liu, T.A.L. Harris, A review of the operating limits in slot die coating processes, AIChE Journal, 62 (2016) 2508-2524.

[51] B.-J. Huang, C.-K. Guan, S.-H. Huang, W.-F. Su, Development of once-through manufacturing machine for large-area Perovskite solar cell production, Solar Energy, 205 (2020) 192-201.

[52] A. Berni, M. Mennig, H. Schmidt, Doctor blade, in: Sol-gel technologies for glass producers and users, Springer, 2004, pp. 89-92.

[53] A.d. Kergommeaux, A. Fiore, J. Faure-Vincent, A. Pron, P. Reiss, Colloidal CuInSe 2 nanocrystals thin films of low surface roughness, Advances in Natural Sciences: Nanoscience and Nanotechnology, 4 (2013) 015004.

[54] R. Patidar, D. Burkitt, K. Hooper, D. Richards, T. Watson, Slot-die coating of perovskite solar cells: An overview, Materials Today Communications, 22 (2020) 100808.

[55] G.L. Jin, W.-G. Ahn, S.J. Kim, J. Nam, H.W. Jung, J.C. Hyun, Effect of shim configuration on internal die flows for non-Newtonian coating liquids in slot coating process, Korea-Australia Rheology Journal, 28 (2016) 159-164.

[56] C.F. Wang, Y. An, Q.H. Li, S.J. Wan, W.X. Chen, X.D. Liu, Nonsolvent Effects on Morphology of Cellulose Acetate Films Prepared by Dry-Cast Process, Journal of Macromolecular Science, Part B, 51 (2012) 2266-2275.

[57] A. Phillips, M. Ulsh, J. Mackay, T. Harris, N. Shrivastava, A. Chatterjee, J. Porter, G. Bender, The Effect of Membrane Casting Irregularities on Initial Fuel Cell Performance, Fuel Cells, 20 (2020) 60-69.

[58] S. Chede, N.M. Anaya, V. Oyanedel-Craver, S. Gorgannejad, T.A.L. Harris, J. Al-Mallahi, M. Abu-Dalo, H.A. Qdais, I.C. Escobar, Desalination using low biofouling nanocomposite membranes: From batch-scale to continuous-scale membrane fabrication, Desalination, 451 (2019) 81-91.

[59] K.J. Ruschak, Limiting flow in a pre-metered coating device, Chemical Engineering Science, 31 (1976) 1057-1060.

[60] M. Kohlova, C.G. Amorim, A. da Nova Araújo, A. Santos-Silva, P. Solich, M.C.B. Montenegro, In vitro assessment of polyethylene glycol and polyvinylpyrrolidone as hydrophilic additives on bioseparation by polysulfone membranes, Journal of Materials Science, 55 (2020) 1292-1307.

[61] R. Dehghan, J. Barzin, Development of a polysulfone membrane with explicit characteristics for separation of low density lipoprotein from blood plasma, Polymer Testing, 85 (2020) 106438.

[62] J. Wang, Z. Zhang, J. Li, J. Zhu, X. Meng, X. Li, X. Wang, Effect of Peg on Polysulfone Support and Reverse Osmosis Membrane Property, in: IOP Conference Series: Materials Science and Engineering, IOP Publishing, 2020, pp. 012073.

[63] C.-y. Yang, G.-d. Zhu, Z. Yi, Y.-y. Qiu, L.-f. Liu, C.-j. Gao, Tailoring the pore size and permeability of isoporous membranes through blending with poly (ethylene glycol): Toward the balance of macro-and microphase separation, Journal of Membrane Science, 598 (2020) 117755.

[64] C.C. Pereira, J.F. Nascimento, W.M. Grava, C.P. Borges, Effect of different PVDF and additives on the properties of hollow fiber membranes contactors for CO2 separation, Journal of Applied Polymer Science, (2020) 49013.

[65] N.B. Darwish, A. Alkhudhiri, H. AlRomaih, A. Alalawi, M.C. Leaper, N. Hilal, Effect of lithium chloride additive on forward osmosis membranes performance, Journal of Water Process Engineering, 33 (2020) 101049.

[66] Z.M.H.M. Shafie, A.L. Ahmad, S.C. Low, S. Rode, B. Belaissaoui, Lithium chloride (LiCl)-modified polyethersulfone (PES) substrate surface pore architectures on thin poly (dimethylsiloxane)(PDMS) dense layer formation and the composite membrane's performance in gas separation, RSC Advances, 10 (2020) 9500-9511.

[67] I. Sadeghi, P. Kaner, A. Asatekin, Controlling and Expanding the Selectivity of Filtration Membranes, Chemistry of Materials, 30 (2018) 7328-7354.

[68] B.S. Lalia, V. Kochkodan, R. Hashaikeh, N. Hilal, A review on membrane fabrication: Structure, properties and performance relationship, Desalination, 326 (2013) 77-95.

[69] X. Tan, D. Rodrigue, A Review on Porous Polymeric Membrane Preparation. Part I: Production Techniques with Polysulfone and Poly (Vinylidene Fluoride), Polymers, 11 (2019) 1160.

[70] Z. Chen, M. Deng, Y. Chen, G. He, M. Wu, J. Wang, Preparation and performance of cellulose acetate/polyethyleneimine blend microfiltration membranes and their applications, Journal of membrane science, 235 (2004) 73-86.

[71] M. Sivakumar, D.R. Mohan, R. Rangarajan, Studies on cellulose acetate-polysulfone ultrafiltration membranes: II. Effect of additive concentration, Journal of Membrane Science, 268 (2006) 208-219.

[72] O. Kutowy, S. Sourirajan, Cellulose acetate ultrafiltration membranes, Journal of applied polymer science, 19 (1975) 1449-1460.

[73] R. Haddada, E. Ferjani, M.S. Roudesli, A. Deratani, Properties of cellulose acetate nanofiltration membranes. Application to brackish water desalination, Desalination, 167 (2004) 403-409.

[74] A.P. Duarte, M.T. Cidade, J.C. Bordado, Cellulose acetate reverse osmosis membranes: Optimization of the composition, Journal of Applied Polymer Science, 100 (2006) 4052-4058.

[75] A. Idris, L.K. Yet, The effect of different molecular weight PEG additives on cellulose acetate asymmetric dialysis membrane performance, Journal of Membrane Science, 280 (2006) 920-927.

[76] X. Wang, X. Ba, N. Cui, Z. Ma, L. Wang, Z. Wang, X. Gao, Preparation, characterisation, and desalination performance study of cellulose acetate membranes with MIL-53(Fe) additive, Journal of Membrane Science, 590 (2019) 117057.

[77] G. Arthanareeswaran, T.S. Devi, M. Raajenthiren, Effect of silica particles on cellulose acetate blend ultrafiltration membranes: Part I, Separation and Purification Technology, 64 (2008) 38-47.

[78] B. Van der Bruggen, Chemical modification of polyethersulfone nanofiltration membranes: a review, Journal of Applied Polymer Science, 114 (2009) 630-642.

[79] C. Zhao, J. Xue, F. Ran, S. Sun, Modification of polyethersulfone membranes – A review of methods, Progress in Materials Science, 58 (2013) 76-150.

[80] T.A. Otitoju, A.L. Ahmad, B.S. Ooi, Recent advances in hydrophilic modification and performance of polyethersulfone (PES) membrane via additive blending, RSC Advances, 8 (2018) 22710-22728.

[81] F. Liu, N.A. Hashim, Y. Liu, M.M. Abed, K. Li, Progress in the production and modification of PVDF membranes, Journal of membrane science, 375 (2011) 1-27.

[82] L. Eykens, K. De Sitter, C. Dotremont, L. Pinoy, B. Van der Bruggen, Membrane synthesis for membrane distillation: A review, Separation and Purification Technology, 182 (2017) 36-51.

[83] A. Alkhudhiri, N. Darwish, N. Hilal, Membrane distillation: A comprehensive review, Desalination, 287 (2012) 2-18.

[84] G.-d. Kang, Y.-m. Cao, Application and modification of poly (vinylidene fluoride)(PVDF) membranes–a review, Journal of Membrane Science, 463 (2014) 145-165.

[85] A. Colburn, R.J. Vogler, A. Patel, M. Bezold, J. Craven, C. Liu, D. Bhattacharyya, Composite Membranes Derived from Cellulose and Lignin Sulfonate for Selective Separations and Antifouling Aspects, Nanomaterials, 9 (2019) 867.

[86] F. Galiano, K. Briceño, T. Marino, A. Molino, K.V. Christensen, A. Figoli, Advances in biopolymer-based membrane preparation and applications, Journal of Membrane Science, 564 (2018) 562-586.

[87] S.S. Gaur, P. Dhar, A. Sonowal, A. Sharma, A. Kumar, V. Katiyar, Thermo-mechanically stable sustainable polymer based solid electrolyte membranes for direct methanol fuel cell applications, Journal of Membrane Science, 526 (2017) 348-354.

[88] M.I. Baig, E.N. Durmaz, J.D. Willott, W.M. de Vos, Sustainable membrane production through polyelectrolyte complexation induced aqueous phase separation, Advanced functional materials, 30 (2020) 1907344.

[89] P.S. Goh, T.W. Wong, J.W. Lim, A.F. Ismail, N. Hilal, Innovative and sustainable membrane technology for wastewater treatment and desalination application, in: Innovation Strategies in Environmental Science, Elsevier, 2020, pp. 291-319.

[90] Y. Zhu, C. Romain, C.K. Williams, Sustainable polymers from renewable resources, Nature, 540 (2016) 354-362.

[91] D.W. Lee, H. Lim, H.N. Chong, W.S. Shim, Advances in chitosan material and its hybrid derivatives: a review, The Open Biomaterials Journal, 1 (2009).

[92] T.D. Rathke, S.M. Hudson, Review of chitin and chitosan as fiber and film formers, Journal of Macromolecular Science, Part C: Polymer Reviews, 34 (1994) 375-437.

[93] C. King, J.L. Shamshina, G. Gurau, P. Berton, N.F.A.F. Khan, R.D. Rogers, A platform for more sustainable chitin films from an ionic liquid process, Green Chemistry, 19 (2017) 117-126.

[94] S.S. Silva, J.F. Mano, R.L. Reis, Ionic liquids in the processing and chemical modification of chitin and chitosan for biomedical applications, Green Chemistry, 19 (2017) 1208-1220.

[95] A.C. Galvis-Sánchez, A.M.M. Sousa, L. Hilliou, M.P. Gonçalves, H.K.S. Souza, Thermo-compression molding of chitosan with a deep eutectic mixture for biofilms development, Green Chemistry, 18 (2016) 1571-1580.

[96] A. Jafari Sanjari, M. Asghari, A Review on Chitosan Utilization in Membrane Synthesis, ChemBioEng Reviews, 3 (2016) 134-158.

[97] R. Lieder, M. Darai, G. Orlygsson, O.E. Sigurjonsson, Solution casting of chitosan membranes for in vitro evaluation of bioactivity, Biol Proced Online, 15 (2013) 11-11.

[98] B. Ma, X. Li, A. Qin, C. He, A comparative study on the chitosan membranes prepared from glycine hydrochloride and acetic acid, Carbohydrate Polymers, 91 (2013) 477-482.

[99] A. Ratcliffe, A. Baker, D. Smith, Successful management of 70% acetic acid ingestion on the intensive care unit: A case report, J Intensive Care Soc, 19 (2018) 56-60.

[100] L. Cui, S. Gao, X. Song, L. Huang, H. Dong, J. Liu, F. Chen, S. Yu, Preparation and characterization of chitosan membranes, RSC Advances, 8 (2018) 28433-28439.

[101] H.A. Le Phuong, N.A. Izzati Ayob, C.F. Blanford, N.F. Mohammad Rawi, G. Szekely, Nonwoven Membrane Supports from Renewable Resources: Bamboo Fiber Reinforced Poly(Lactic Acid) Composites, ACS Sustainable Chemistry & Engineering, 7 (2019) 11885-11893.

[102] I. Smallwood, Handbook of organic solvent properties, Butterworth-Heinemann, 2012.

[103] H.F. Smyth Jr, C.P. Carpenter, C.S. Weil, U.C. Pozzani, J.A. Striegel, J.S. Nycum, Range-finding toxicity data: List VII, American Industrial Hygiene Association Journal, 30 (1969) 470-476.

[104] R. Gold, J.T. Phillips, E. Havrdova, A. Bar-Or, L. Kappos, N. Kim, T. Thullen, P. Valencia, L. Oliva, M. Novas, J. Li, M.T. Sweetser, N. Kurukulasuriya, V. Viglietta, R.J. Fox, Delayed-Release Dimethyl Fumarate and Pregnancy: Preclinical Studies and

Pregnancy Outcomes from Clinical Trials and Postmarketing Experience, Neurology and Therapy, 4 (2015) 93-104.

[105] M. Razali, J.F. Kim, M. Attfield, P.M. Budd, E. Drioli, Y.M. Lee, G. Szekely, Sustainable wastewater treatment and recycling in membrane manufacturing, Green Chemistry, 17 (2015) 5196-5205.

[106] Y. Alqaheem, A. Alomair, A. Alhendi, S. Alkandari, N. Tanoli, N. Alnajdi, A. Quesada-Peréz, Preparation of polyetherimide membrane from non-toxic solvents for the separation of hydrogen from methane, Chemistry Central Journal, 12 (2018) 80.

[107] F. Liu, N.A. Hashim, Y. Liu, M.R.M. Abed, K. Li, Progress in the production and modification of PVDF membranes, J. Membr. Sci., 375 (2011) 1-27.

[108] J.-h. Wang, Y.-h. Zhang, Y.-y. Xu, B.-k. Zhu, H. Xu, Fabrication of hydrophilic and sponge-like PVDF/brush-like copolymer blend membranes using triethylphosphate as solvent, Chin. J. Polym. Sci., 32 (2014) 143-150.

[109] M.-m. Tao, F. Liu, B.-r. Ma, L.-x. Xue, Effect of solvent power on PVDF membrane polymorphism during phase inversion, Desalination, 316 (2013) 137-145.

[110] H. Karkhanechi, M. Vaselbehagh, S. Jeon, A.R. Shaikh, D.-m. Wang, H. Matsuyama, Preparation and characterization of polyvinylidenedifluoride-co-chlorotrifluoroethylene hollow fiber membranes with high alkaline resistance, Polymer, 145 (2018) 310-323.

[111] H.W. Paerl, D.R. Whitall, Anthropogenically-derived atmospheric nitrogen deposition, marine eutrophication and harmful algal bloom expansion: Is there a link?, Ambio, 28 (1999) 307-311.

[112] D.M. Anderson, P.M. Glibert, J.M. Burkholder, Harmful algal blooms and eutrophication: nutrient sources, composition, and consequences, Estuaries, 25 (2002) 704-726.

[113] J. Heisler, P.M. Glibert, J.M. Burkholder, D.M. Anderson, W. Cochlan, W.C. Dennison, Q. Dortch, C.J. Gobler, C.A. Heil, E. Humphries, Eutrophication and harmful algal blooms: a scientific consensus, Harmful algae, 8 (2008) 3-13.

[114] R. Ratti, Ionic Liquids: Synthesis and Applications in Catalysis, Advances in Chemistry, 2014 (2014) 16.

[115] R.D. Rogers, K.R. Seddon, Ionic Liquids--Solvents of the Future?, Science, 302 (2003) 792-793.

[116] J. Earle Martyn, R. Seddon Kenneth, Ionic liquids. Green solvents for the future, in: Pure Appl. Chem., 2000, pp. 1391.

[117] F. Heym, J. Haber, W. Korth, B.J.M. Etzold, A. Jess, Vapor Pressure of Water in Mixtures with Hydrophilic Ionic Liquids – A Contribution to the Design of Processes for Drying of Gases by Absorption in Ionic Liquids, Chemical Engineering & Technology, 33 (2010) 1625-1634.

[118] C. Dai, X. Sui, Z. Lei, Vapor pressure measurements and predictions for the binary systems containing ionic liquid [EMIM][BF4] and formic acid/acetic acid, J. Mol. Liq., 256 (2018) 471-479.

[119] D. Tomida, Y. Tani, K. Qiao, C. Yokoyama, Vapor pressure and liquid density of 1-butyl-3-methylimidazolium hexafluorophosphate and ammonia mixtures, High Temperatures--High Pressures, 47 (2018).

[120] I. Cichowska-Kopczynska, M. Joskowska, B. Debski, J. Luczak, R. Aranowski, Influence of Ionic Liquid Structure on Supported Ionic Liquid Membranes Effectiveness in Carbon Dioxide/Methane Separation, Journal of Chemistry, 2013 (2013) 10.

[121] D.Y. Xing, S.Y. Chan, T.-S. Chung, Molecular interactions between polybenzimidazole and [EMIM]OAc, and derived ultrafiltration membranes for protein separation, Green Chemistry, 14 (2012) 1405-1412.

[122] D.Y. Xing, W.Y. Dong, T.-S. Chung, Effects of Different Ionic Liquids as Green Solvents on the Formation and Ultrafiltration Performance of CA Hollow Fiber Membranes, Ind. Eng. Chem. Res., 55 (2016) 7505-7513.

[123] A. Colburn, N. Wanninayake, D.Y. Kim, D. Bhattacharyya, Cellulose-graphene quantum dot composite membranes using ionic liquid, Journal of Membrane Science, 556 (2018) 293-302.

[124] A. Romero, A. Santos, J. Tojo, A. Rodríguez, Toxicity and biodegradability of imidazolium ionic liquids, J. Hazard. Mater., 151 (2008) 268-273.

[125] K.M. Docherty, J.C.F. Kulpa, Toxicity and antimicrobial activity of imidazolium and pyridinium ionic liquids, Green Chemistry, 7 (2005) 185-189.

[126] T.P. Thuy Pham, C.-W. Cho, Y.-S. Yun, Environmental fate and toxicity of ionic liquids: A review, Water Res., 44 (2010) 352-372.

[127] S.P.M. Ventura, A.M.M. Gonçalves, T. Sintra, J.L. Pereira, F. Gonçalves, J.A.P. Coutinho, Designing ionic liquids: the chemical structure role in the toxicity, Ecotoxicology, 22 (2013) 1-12.

[128] N.T. Hassankiadeh, Z. Cui, J.H. Kim, D.W. Shin, S.Y. Lee, A. Sanguineti, V. Arcella, Y.M. Lee, E. Drioli, Microporous poly(vinylidene fluoride) hollow fiber membranes fabricated with PolarClean as water-soluble green diluent and additives, J. Membr. Sci., 479 (2015) 204-212.

[129] J.T. Jung, J.F. Kim, H.H. Wang, E. di Nicolo, E. Drioli, Y.M. Lee, Understanding the non-solvent induced phase separation (NIPS) effect during the fabrication of microporous PVDF membranes via thermally induced phase separation (TIPS), Journal of Membrane Science, 514 (2016) 250-263.

[130] T. Marino, E. Blasi, S. Tornaghi, E. Di Nicolò, A. Figoli, Polyethersulfone membranes prepared with Rhodiasolv®Polarclean as water soluble green solvent, Journal of Membrane Science, 549 (2018) 192-204.

[131] A. Randová, L. Bartovská, P. Morávek, P. Matějka, M. Novotná, S. Matějková, E. Drioli, A. Figoli, M. Lanč, K. Friess, A fundamental study of the physicochemical properties of Rhodiasolv®Polarclean: A promising alternative to common and hazardous solvents, Journal of Molecular Liquids, 224 (2016) 1163-1171.

[132] D.M. Alonso, S.G. Wettstein, J.A. Dumesic, Gamma-valerolactone, a sustainable platform molecule derived from lignocellulosic biomass, Green Chemistry, 15 (2013) 584-595.

[133] B. Girisuta, L.P.B.M. Janssen, H.J. Heeres, Kinetic Study on the Acid-Catalyzed Hydrolysis of Cellulose to Levulinic Acid, Industrial & Engineering Chemistry Research, 46 (2007) 1696-1708.

[134] B. Girisuta, L.P.B.M. Janssen, H.J. Heeres, A kinetic study on the decomposition of 5-hydroxymethylfurfural into levulinic acid, Green Chemistry, 8 (2006) 701-709.

[135] B. Girisuta, L.P.B.M. Janssen, H.J. Heeres, Green Chemicals: A Kinetic Study on the Conversion of Glucose to Levulinic Acid, Chemical Engineering Research and Design, 84 (2006) 339-349.

[136] M.A. Rasool, I.F.J. Vankelecom, Use of γ-valerolactone and glycerol derivatives as bio-based renewable solvents for membrane preparation, Green Chemistry, 21 (2019) 1054-1064.

[137] M.-L. Pellegrin, I. Mitra, K. Zhang, A. Menniti, K. Law, J. Wert, J. Lee, J. Aguinaldo, Membrane Processes, Water Environment Research, 80 (2008) 1113-1178.

[138] C.S.M. Pereira, V.M.T.M. Silva, A.E. Rodrigues, Ethyl lactate as a solvent: Properties, applications and production processes - a review, Green Chemistry, 13 (2011) 2658-2671.

[139] R.W. Baker, Membrane technology, Wiley Online Library, 2000.

[140] G. Wypych, Handbook of Solvents, Noyes Publications, 2001.

[141] C.M. Hansen, Hansen solubility parameters: a user's handbook, CRC press, 2002.

[142] H. Wan, N.J. Briot, A. Saad, L. Ormsbee, D. Bhattacharyya, Pore functionalized PVDF membranes with in-situ synthesized metal nanoparticles: Material characterization, and toxic organic degradation, Journal of Membrane Science, 530 (2017) 147-157.

[143] A. Behzad, K. Hooghan, C. Aubry, M. Khan, J. Croue, SEM-FIB Characterization of Reverse Osmosis Membrane Fouling, Microscopy and Microanalysis, 17 (2011) 1768-1769.

[144] Q.-Z. Zheng, P. Wang, Y.-N. Yang, D.-J. Cui, The relationship between porosity and kinetics parameter of membrane formation in PSF ultrafiltration membrane, Journal of Membrane Science, 286 (2006) 7-11.

[145] S.-i. Nakao, Determination of pore size and pore size distribution, Journal of Membrane Science, 96 (1994) 131-165.

[146] S. Kaur, Z. Ma, R. Gopal, G. Singh, S. Ramakrishna, T. Matsuura, Plasma-Induced Graft Copolymerization of Poly(methacrylic acid) on Electrospun Poly(vinylidene fluoride) Nanofiber Membrane, Langmuir, 23 (2007) 13085-13092.

[147] B. Chakrabarty, A.K. Ghoshal, M.K. Purkait, Effect of molecular weight of PEG on membrane morphology and transport properties, Journal of Membrane Science, 309 (2008) 209-221.

[148] P. Radovanovic, S.W. Thiel, S.-T. Hwang, Formation of asymmetric polysulfone membranes by immersion precipitation. Part I. Modelling mass transport during gelation, Journal of Membrane Science, 65 (1992) 213-229.

[149] P. Radovanovic, S.W. Thiel, S.-T. Hwang, Formation of asymmetric polysulfone membranes by immersion precipitation. Part II. The effects of casting solution and gelation bath compositions on membrane structure and skin formation, Journal of Membrane Science, 65 (1992) 231-246.

[150] A.W. Zularisam, A.F. Ismail, M.R. Salim, M. Sakinah, O. Hiroaki, Fabrication, fouling and foulant analyses of asymmetric polysulfone (PSF) ultrafiltration membrane fouled with natural organic matter (NOM) source waters, Journal of Membrane Science, 299 (2007) 97-113.

[151] H.K. Shon, S. Vigneswaran, I.S. Kim, J. Cho, H.H. Ngo, Fouling of ultrafiltration membrane by effluent organic matter: A detailed characterization using different organic fractions in wastewater, Journal of Membrane Science, 278 (2006) 232-238.

[152] S. Hernandez, C. Porter, X. Zhang, Y. Wei, D. Bhattacharyya, Layer-by-layer assembled membranes with immobilized porins, RSC Advances, 7 (2017) 56123-56136.

[153] T.J. Pillar-Little, N. Wanninayake, L. Nease, D.K. Heidary, E.C. Glazer, D.Y. Kim, Superior photodynamic effect of carbon quantum dots through both type I and type II pathways: Detailed comparison study of top-down-synthesized and bottom-up-synthesized carbon quantum dots, Carbon, 140 (2018) 616-623.

[154] P. Wagh, J. Spencer, B. Steele, I.C. Escobar, Membrane functionalization using bisamide-based organic frameworks for molecular weight cutoff reduction, Journal of Applied Polymer Science, 0 48327.

[155] R. Hausman, I.C. Escobar, A Fourier Transform Infrared Spectroscopic Based Biofilm Characterization Technique and Its Use to Show the Effect of Copper-Charged Polypropylene Feed Spacers in Biofouling Control, in: Modern Applications in Membrane Science and Technology, American Chemical Society, 2011, pp. 225-237.

[156] M. Flanagan, R. Hausman, B. Digman, I.C. Escobar, M. Coleman, T.-S. Chung, Surface Functionalization of Polybenzimidazole Membranes To Increase Hydrophilicity and Charge, in: Modern Applications in Membrane Science and Technology, American Chemical Society, 2011, pp. 303-321.

[157] R.W. Baker, Membrane Technology, in: Kirk-Othmer Encyclopedia of Chemical Technology, John Wiley & Sons, Inc., 2000.

[158] W. Ho, K. Sirkar, Membrane handbook, Springer Science & Business Media, 2012.

[159] D.R. Lloyd, S.S. Kim, K.E. Kinzer, Microporous membrane formation via thermally-induced phase separation. II. Liquid—liquid phase separation, Journal of Membrane Science, 64 (1991) 1-11.

[160] J.R. Werber, C.O. Osuji, M. Elimelech, Materials for next-generation desalination and water purification membranes, Nature Reviews Materials, 1 (2016) 16018.

[161] P.M. Roland Jacquot, Process for producing compounds comprising nitrile functions, in, Rhodia Operations Sas US, 2015.

[162] J.F. Kim, J.T. Jung, H.H. Wang, S.Y. Lee, T. Moore, A. Sanguineti, E. Drioli, Y.M. Lee, Microporous PVDF membranes via thermally induced phase separation (TIPS) and stretching methods, Journal of Membrane Science, 509 (2016) 94-104.

[163] J.Y. Kim, H.K. Lee, K.J. Baik, S.C. Kim, Liquid-liquid phase separation in polysulfone/solvent/water systems, Journal of Applied Polymer Science, 65 (1997) 2643-2653.

[164] A. Abdelrasoul, H. Doan, A. Lohi, C.-H. Cheng, Morphology Control of Polysulfone Membranes in Filtration Processes: a Critical Review, ChemBioEng Reviews, 2 (2015) 22-43.

[165] S.M. Mousavi, A. Zadhoush, Investigation of the relation between viscoelastic properties of polysulfone solutions, phase inversion process and membrane morphology: The effect of solvent power, Journal of Membrane Science, 532 (2017) 47-57.

[166] S.K. Yong, J.K. Hyo, Y.K. Un, Asymmetric membrane formation via immersion precipitation method. I. Kinetic effect, Journal of Membrane Science, 60 (1991) 219-232.

[167] B. Tansel, W.Y. Bao, I.N. Tansel, Characterization of fouling kinetics in ultrafiltration systems by resistances in series model, Desalination, 129 (2000) 7-14.

[168] C.M. Hansen, Hansen solubility parameters: a user's handbook, CRC press, 2007.

[169] K. Kamide, H. Iijima, S. Matsuda, Thermodynamics of Formation of Porous Polymeric Membrane by Phase Separation Method I. Nucleation and Growth of Nuclei, Polym J, 25 (1993) 1113-1131.

[170] A.F. Ismail, T. Matsuura, Membrane Technology for Water and Wastewater Treatment, Energy and Environment, CRC Press, 2016.

[171] Y. Liu, G.H. Koops, H. Strathmann, Characterization of morphology controlled polyethersulfone hollow fiber membranes by the addition of polyethylene glycol to the dope and bore liquid solution, Journal of Membrane Science, 223 (2003) 187-199.

[172] A. Iqbal, I. Ani, R. Rajput, Performance of microwave synthesized dual solvent dope solution and lithium bromide additives on poly(ethersulfone) membranes, Journal of Chemical Technology & Biotechnology, 87 (2012) 177-188.

[173] G. Delaplace, R. Guérin, J.C. Leuliet, Dimensional analysis for planetary mixer: Modified power and Reynolds numbers, AIChE Journal, 51 (2005) 3094-3100.

[174] G. Delaplace, R.K. Thakur, L. Bouvier, C. André, C. Torrez, Dimensional analysis for planetary mixer: Mixing time and Reynolds numbers, Chemical Engineering Science, 62 (2007) 1442-1447.

[175] D. Liu, Chen, L.C., Liu, T.J., Fan, T., Tsou, E.Y. and Tiu, C, An Effective Mixing for Lithium Ion Battery Slurries, Advances in Chemical Engineering and Science, 4 (2014) 515-528.

[176] S. Asapu, S. Pant, C.L. Gruden, I.C. Escobar, An investigation of low biofouling copper-charged membranes for desalination, Desalination, 338 (2014) 17-25.

[177] C.H. Durbin, R.; Escobar, I.C., An investigation of polymer dope and heating effects on hollow fiber membranes, Desalination and Water Treatment, (2013).

[178] M. Flanagan, Hausman, R., Digman B., I.C. Escobar, M.R. Coleman, and T-S Chung Surface Functionalization of Polybenzimidazole Membranes to Increase Hydrophilicity and Charge, American Chemical Society, Washington, DC, 2011.

[179] M.F. Flanagan, I.C. Escobar, Novel charged and hydrophilized polybenzimidazole (PBI) membranes for forward osmosis, Journal of Membrane Science, 434 (2013) 85-92.

[180] J. Albo, H. Hagiwara, H. Yanagishita, K. Ito, T. Tsuru, Structural Characterization of Thin-Film Polyamide Reverse Osmosis Membranes, Industrial & Engineering Chemistry Research, 53 (2014) 1442-1451.

[181] J. Albo, J. Wang, T. Tsuru, Gas transport properties of interfacially polymerized polyamide composite membranes under different pre-treatments and temperatures, Journal of Membrane Science, 449 (2014) 109-118.

[182] J. Albo, J. Wang, T. Tsuru, Application of interfacially polymerized polyamide composite membranes to isopropanol dehydration: Effect of membrane pre-treatment and temperature, Journal of Membrane Science, 453 (2014) 384-393.

[183] H. Strathmann, K. Kock, P. Amar, R.W. Baker, The formation mechanism of asymmetric membranes, Desalination, 16 (1975) 179-203.

[184] C.S. Tsay, A.J. McHugh, The combined effects of evaporation and quench steps on asymmetric membrane formation by phase inversion, Journal of Polymer Science Part B: Polymer Physics, 29 (1991) 1261-1270.

[185] D.B. Mosqueda-Jimenez, R.M. Narbaitz, T. Matsuura, G. Chowdhury, G. Pleizier, J.P. Santerre, Influence of processing conditions on the properties of ultrafiltration membranes, Journal of Membrane Science, 231 (2004) 209-224.

[186] D.B. Mosqueda-Jimenez, R.M. Narbaitz, T. Matsuura, Manufacturing conditions of surface-modified membranes: effects on ultrafiltration performance, Separation and Purification Technology, 37 (2004) 51-67.

[187] T. Nguyen, F. Roddick, L. Fan, Biofouling of Water Treatment Membranes: A Review of the Underlying Causes, Monitoring Techniques and Control Measures, Membranes, 2 (2012) 804.

[188] J. Marchese, M. Ponce, N.A. Ochoa, P. Prádanos, L. Palacio, A. Hernández, Fouling behaviour of polyethersulfone UF membranes made with different PVP, Journal of Membrane Science, 211 (2003) 1-11.

[189] S.T. Kelly, A.L. Zydney, Mechanisms for BSA fouling during microfiltration, Journal of Membrane Science, 107 (1995) 115-127.

[190] K.-J. Hwang, P.-Y. Sz, Membrane fouling mechanism and concentration effect in cross-flow microfiltration of BSA/dextran mixtures, Chemical Engineering Journal, 166 (2011) 669-677.

[191] M.D. Kennedy, H.K. Chun, V.A. Quintanilla Yangali, B.G.J. Heijman, J.C. Schippers, Natural organic matter (NOM) fouling of ultrafiltration membranes: fractionation of NOM in surface water and characterisation by LC-OCD, Desalination, 178 (2005) 73-83.

[192] W.W.Y. Lau, M.D. Guiver, T. Matsuura, Phase separation in polysulfone/solvent/water and polyethersulfone/solvent/water systems, Journal of Membrane Science, 59 (1991) 219-227.

[193] J. Wijmans, J. Kant, M. Mulder, C. Smolders, Phase separation phenomena in solutions of polysulfone in mixtures of a solvent and a nonsolvent: relationship with membrane formation, Polymer, 26 (1985) 1539-1545.

[194] R. Miao, L. Wang, M. Zhu, D. Deng, S.S. Li, J. Wang, T. Liu, Y. Lv, Effect of Hydration Forces on Protein Fouling of Ultrafiltration Membranes: The Role of Protein Charge, Hydrated Ion Species, and Membrane Hydrophilicity, Environ. Sci. Technol., 51 (2017) 167-174.

[195] S. Rajesh, K. Shobana, S. Anitharaj, D. Mohan, Preparation, Morphology, Performance, and Hydrophilicity Studies of Poly(amide-imide) Incorporated Cellulose Acetate Ultrafiltration Membranes, Ind. Eng. Chem. Res., 50 (2011) 5550-5564.

[196] J. Zhu, Q. Zhang, J. Zheng, S. Hou, S.B. Zhang, S. Li, Correlation of the polymer hydrophilicity and membrane fabrication process on the properties of asymmetric membranes in a vapor-induced phase-inversion process, J. Appl. Polym. Sci., 134 (2017).

[197] S. Kasemset, L. Wang, Z. He, D.J. Miller, A. Kirschner, B.D. Freeman, M.M. Sharma, Influence of polydopamine deposition conditions on hydraulic permeability, sieving coefficients, pore size and pore size distribution for a polysulfone ultrafiltration membrane, Journal of Membrane Science, 522 (2017) 100-115.

[198] P.S.T. Machado, A.C. Habert, C.P. Borges, Membrane formation mechanism based on precipitation kinetics and membrane morphology: flat and hollow fiber polysulfone membranes, Journal of Membrane Science, 155 (1999) 171-183.

[199] A. Alpatova, E.-S. Kim, X. Sun, G. Hwang, Y. Liu, M. Gamal El-Din, Fabrication of porous polymeric nanocomposite membranes with enhanced anti-fouling properties: Effect of casting composition, Journal of Membrane Science, 444 (2013) 449-460.

[200] P. Qin, X. Hong, M.N. Karim, T. Shintani, J. Li, C. Chen, Preparation of Poly(phthalazinone-ether-sulfone) Sponge-Like Ultrafiltration Membrane, Langmuir, 29 (2013) 4167-4175.

[201] J. Hwang, J. Choi, J.M. Kim, S.W. Kang, Water treatment by polysulfone membrane modified with tetrahydrofuran and water pressure, Macromolecular Research, 24 (2016) 1020-1023.

[202] F.W. Melpolder, C.E. Headington, Calculation of Relative Volatility from Boiling Points, Industrial & Engineering Chemistry, 39 (1947) 763-766.

[203] K. Nasirzadeh, R. Neueder, W. Kunz, Vapor Pressures of Propylene Carbonate and N,N-Dimethylacetamide, Journal of Chemical & Engineering Data, 50 (2005) 26-28.

[204] A.N.I.C.N.a.A. Scheme, Public report file STD/1544: Pentanoic acid, 5-(dimethylamino)-2-methyl-5-oxo-, methyl ester (Rhodiasolv PolarClean), in, 2015.

[205] Y. Wei, V. Chaudhary, Fast Quantitative Analysis of Stock Trading Points in Dual Period of DMAC, in: 2015 IEEE First International Conference on Big Data Computing Service and Applications, 2015, pp. 34-43.

[206] G. Jonsson, Methods for determining the selectivity of reverse osmosis membranes, Desalination, 24 (1977) 19-37.

[207] Z. Zhang, Q. An, T. Liu, Y. Zhou, J. Qian, C. Gao, Fabrication of polysulfone ultrafiltration membranes of a density gradient cross section with good anti-pressure stability and relatively high water flux, Desalination, 269 (2011) 239-248.

[208] B.K. Chaturvedi, A.K. Ghosh, V. Ramachandhran, M.K. Trivedi, M.S. Hanra, B.M. Misra, Preparation, characterization and performance of polyethersulfone ultrafiltration membranes, Desalination, 133 (2001) 31-40.

[209] C. Stropnik, V. Kaiser, V. Musil, M. Brumen, Wet-phase-separation membranes from the polysulfone/N,N-dimethylacetamide/water ternary system: The formation and elements of their structure and properties, Journal of Applied Polymer Science, 96 (2005) 1667-1674.

[210] G.S. Helm, J. Wei, N. Corner-Walker, Comparison of new polysulfone membrane GR70PE with other commercial membranes for concentration of proteins — long-term field test, Desalination, 191 (2006) 328-333.

[211] S.S. Madaeni, A. Rahimpour, Effect of type of solvent and non-solvents on morphology and performance of polysulfone and polyethersulfone ultrafiltration membranes for milk concentration, Polymers for Advanced Technologies, 16 (2005) 717-724.

[212] G. Arthanareeswaran, S. Velu, L. Muruganandam, Performance enhancement of polysulfone ultrafiltration membrane by blending with polyurethane hydrophilic polymer, in: Journal of Polymer Engineering, 2011, pp. 125.

[213] I.M. Wienk, R.M. Boom, M.A.M. Beerlage, A.M.W. Bulte, C.A. Smolders, H. Strathmann, Recent advances in the formation of phase inversion membranes made from amorphous or semi-crystalline polymers, Journal of Membrane Science, 113 (1996) 361-371.

[214] D. Antelmi, B. Cabane, M. Meireles, P. Aimar, Cake Collapse in Pressure Filtration, Langmuir, 17 (2001) 7137-7144.

[215] W. Zhang, J. Luo, L. Ding, M.Y. Jaffrin, A Review on Flux Decline Control Strategies in Pressure-Driven Membrane Processes, Industrial & Engineering Chemistry Research, 54 (2015) 2843-2861.

[216] K. Xiong, L. Hou, M. Wu, Y. Huo, W. Mo, Y. Yuan, S. Sun, W. Xu, E. Wang, From spin coating to doctor blading: A systematic study on the photovoltaic performance of an isoindigo-based polymer, Sol. Energy Mater. Sol. Cells, 132 (2015) 252-259.

[217] C. Sneha, G. Peter, E.I. C., H.T.A. L., Does casting method matter in filtration membranes? A comparison in performance between doctor blade and slot-die extruded polymeric membranes, J. Appl. Polym. Sci., 135 (2018) 45563.

[218] S.P. Deshmukh, K. Li, Effect of ethanol composition in water coagulation bath on morphology of PVDF hollow fibre membranes, J. Membr. Sci., 150 (1998) 75-85.

[219] S. Bonyadi, T.S. Chung, W.B. Krantz, Investigation of corrugation phenomenon in the inner contour of hollow fibers during the non-solvent induced phase-separation process, J. Membr. Sci., 299 (2007) 200-210.

[220] J. Eke, P. Wagh, I.C. Escobar, Ozonation, biofiltration and the role of membrane surface charge and hydrophobicity in removal and destruction of algal toxins at basic pH values, Sep. Purif. Technol., 194 (2018) 56-63.

[221] F. Liguori, C. Moreno-Marrodan, P. Barbaro, Environmentally Friendly Synthesis of γ-Valerolactone by Direct Catalytic Conversion of Renewable Sources, ACS Catalysis, 5 (2015) 1882-1894.

[222] I.T. Horváth, Introduction: Sustainable Chemistry, Chem. Rev., 118 (2018) 369-371.

[223] M. Poliakoff, J.M. Fitzpatrick, T.R. Farren, P.T. Anastas, Green Chemistry: Science and Politics of Change, Science, 297 (2002) 807-810.

[224] X. Dong, H.D. Shannon, C. Parker, S. De Jesus, I.C. Escobar, Comparison of two low-hazard organic solvents as individual and cosolvents for the fabrication of polysulfone membranes, AIChE Journal, 66 (2020) e16790.

[225] M. Taniguchi, S. Kimura, Estimation of transport parameters of RO membranes for seawater desalination, AIChE journal, 46 (2000) 1967-1973.

[226] A.M. Alklaibi, N. Lior, Membrane-distillation desalination: status and potential, Desalination, 171 (2005) 111-131.

[227] J.-W. Wang, L. Li, J.-Q. Gu, M.-Y. Yang, X. Xu, C.-S. Chen, H.-T. Wang, S. Agathopoulos, Highly stable hydrophobic SiNCO nanoparticle-modified silicon nitride membrane for zero-discharge water desalination, AIChE Journal, 63 (2017) 1272-1277.

[228] L. Li, C. Visvanathan, Membrane technology for surface water treatment: advancement from microfiltration to membrane bioreactor, Reviews in Environmental Science and Bio/Technology, 16 (2017) 737-760.

[229] T. Melin, B. Jefferson, D. Bixio, C. Thoeye, W. De Wilde, J. De Koning, J. Van der Graaf, T. Wintgens, Membrane bioreactor technology for wastewater treatment and reuse, Desalination, 187 (2006) 271-282.

[230] Y.-R. Chang, Y.-J. Lee, D.-J. Lee, Membrane fouling during water or wastewater treatments: Current research updated, Journal of the Taiwan Institute of Chemical Engineers, 94 (2019) 88-96.

[231] M.K. Mandal, M. Sharma, S. Pandey, K.K. Dubey, Membrane Technologies for the Treatment of Pharmaceutical Industry Wastewater, in: Water and Wastewater Treatment Technologies, Springer, 2019, pp. 103-116.

[232] G.R. Guillen, Y. Pan, M. Li, E.M. Hoek, Preparation and characterization of membranes formed by nonsolvent induced phase separation: a review, Industrial & Engineering Chemistry Research, 50 (2011) 3798-3817.

[233] A. Venault, Y. Chang, D.-M. Wang, D. Bouyer, A review on polymeric membranes and hydrogels prepared by vapor-induced phase separation process, Polymer Reviews, 53 (2013) 568-626.

[234] A. Saillenfait, F. Gallissot, G. Morel, Developmental toxicity of N-methyl-2-pyrrolidone in rats following inhalation exposure, Food and chemical toxicology, 41 (2003) 583-588.

[235] A. Saillenfait, F. Gallissot, I. Langonne, J. Sabate, Developmental toxicity of N-methyl-2-pyrrolidone administered orally to rats, Food and Chemical Toxicology, 40 (2002) 1705-1712.

[236] S.L. Baum, A.J. Suruda, Toxic hepatitis from dimethylacetamide, International journal of occupational and environmental health, 3 (1997) 1-4.

[237] K.-i. Tanaka, Toxicity of dimethylformamide (DMF) to the young female rat, Internationales Archiv für Arbeitsmedizin, 28 (1971) 95-105.

[238] T. Marino, F. Galiano, A. Molino, A. Figoli, New frontiers in sustainable membrane preparation: Cyrene™ as green bioderived solvent, Journal of Membrane Science, 580 (2019) 224-234.

[239] N. Evenepoel, S. Wen, M. Tilahun Tsehaye, B. Van der Bruggen, Potential of DMSO as greener solvent for PES ultra- and nanofiltration membrane preparation, Journal of Applied Polymer Science, 135 (2018) 46494.

[240] T. Marino, F. Galiano, S. Simone, A. Figoli, DMSO EVOL™ as novel non-toxic solvent for polyethersulfone membrane preparation, Environmental Science and Pollution Research, (2018).

[241] K.V. Peinemann, S.P. Nunes, Membranes for Water Treatment, Wiley, 2010.

[242] Microfiltration and Ultrafiltration: Principles and Applications, Taylor & Francis, 1996.

[243] C. Causserand, S. Rouaix, J.-P. Lafaille, P. Aimar, Ageing of polysulfone membranes in contact with bleach solution: Role of radical oxidation and of some dissolved metal ions, Chemical Engineering and Processing: Process Intensification, 47 (2008) 48-56.

[244] A.H. Landrock, Handbook of Plastic Foams: Types, Properties, Manufacture and Applications, Elsevier Science, 1995.

[245] X. Huang, B.T. McVerry, C. Marambio-Jones, M.C.Y. Wong, E.M.V. Hoek, R.B. Kaner, Novel chlorine resistant low-fouling ultrafiltration membrane based on a hydrophilic polyaniline derivative, Journal of Materials Chemistry A, 3 (2015) 8725-8733.

[246] R. Dach, J.J. Song, F. Roschangar, W. Samstag, C.H. Senanayake, The Eight Criteria Defining a Good Chemical Manufacturing Process, Organic Process Research & Development, 16 (2012) 1697-1706.

[247] S.M. Sen, D.M. Alonso, S.G. Wettstein, E.I. Gürbüz, C.A. Henao, J.A. Dumesic, C.T. Maravelias, A sulfuric acid management strategy for the production of liquid hydrocarbon fuels via catalytic conversion of biomass-derived levulinic acid, Energy & Environmental Science, 5 (2012) 9690-9697.

[248] N.C.f.B. Information, Methyl 5-(dimethylamino)-2-methyl-5-oxopentanoate, CID=58332853, in, PubChem Database.

[249] I.T. Horváth, H. Mehdi, V. Fábos, L. Boda, L.T. Mika, γ-Valerolactone—a sustainable liquid for energy and carbon-based chemicals, Green Chemistry, 10 (2008) 238-242.

[250] N.C.f.B. Information, Gamma-Valerolactone, CID=7921, in, PubChem Database.

[251] N.C.f.B. Information, N,N-Dimethylacetamide, CID=31374, in, PubChem Database.

[252] A.J. Reuvers, J.W.A. van den Berg, C.A. Smolders, Formation of membranes by means of immersion precipitation: Part I. A model to describe mass transfer during immersion precipitation, Journal of Membrane Science, 34 (1987) 45-65.

[253] S. Chede, P. Griffiths, I.C. Escobar, T.A.L. Harris, Does casting method matter in filtration membranes? A comparison in performance between doctor blade and slot-die extruded polymeric membranes, Journal of Applied Polymer Science, 135 (2018) 45563.

[254] P. Wagh, G. Parungao, R.E. Viola, I.C. Escobar, A new technique to fabricate high-performance biologically inspired membranes for water treatment, Separation and Purification Technology, 156 (2015) 754-765.

[255] C. Sprick, S. Chede, V. Oyanedel-Craver, I.C. Escobar, Bio-inspired immobilization of casein-coated silver nanoparticles on cellulose acetate membranes for biofouling control, Journal of Environmental Chemical Engineering, 6 (2018) 2480-2491.

[256] A. Rudin, H.L.W. Hoegy, H.K. Johnston, Estimation of viscosities of mixed polymer solutions, Journal of Applied Polymer Science, 16 (1972) 1281-1293.

[257] B.A. Miller-Chou, J.L. Koenig, A review of polymer dissolution, Progress in Polymer Science, 28 (2003) 1223-1270.

[258] M. Saxena, S. Sharma, A. Bhattacharya, Recycling of polysulfone: study properties of membranes, International Journal of Membrane Science and Technology, 2 (2015) 39-46.

[259] A. Mushtaq, H.B. Mukhtar, A.M. Shariff, Research Article FTIR Study of Enhanced Polymeric Blend Membrane with Amines, Research Journal of Applied Sciences, Engineering and Technology, 7 (2014) 1811-1820.

[260] S. Vico, B. Palys, C. Buess-Herman, Hydration of a polysulfone anion-exchange membrane studied by vibrational spectroscopy, Langmuir, 19 (2003) 3282-3287.

[261] Y. Wang, L. Liu, J. Xue, J. Hou, L. Ding, H. Wang, Enhanced water flux through graphitic carbon nitride nanosheets membrane by incorporating polyacrylic acid, AIChE Journal, 64 (2018) 2181-2188.

[262] C.A. Smolders, A.J. Reuvers, R.M. Boom, I.M. Wienk, Microstructures in phase-inversion membranes. Part 1. Formation of macrovoids, Journal of Membrane Science, 73 (1992) 259-275.

[263] C. Jao-Ming, W. Da-Ming, L. Fung-Ching, L. Juin-Yih, Formation and gas flux of asymmetric PMMA membranes, Journal of Membrane Science, 109 (1996) 93-107.

[264] Y. Termonia, Fundamentals of polymer coagulation, Journal of Polymer Science Part B: Polymer Physics, 33 (1995) 279-288.

[265] K. Kimmerle, H. Strathmann, Analysis of the structure-determining process of phase inversion membranes, Desalination, 79 (1990) 283-302.

[266] A. Idris, Z. Man, A.S. Maulud, M.S. Khan, Effects of Phase Separation Behavior on Morphology and Performance of Polycarbonate Membranes, Membranes, 7 (2017) 21.

[267] A. Idris, N. Mat Zain, M.Y. Noordin, Synthesis, characterization and performance of asymmetric polyethersulfone (PES) ultrafiltration membranes with polyethylene glycol of different molecular weights as additives, Desalination, 207 (2007) 324-339.

[268] H. Matsuyama, M. Teramoto, T. Uesaka, Membrane formation and structure development by dry-cast process, Journal of Membrane Science, 135 (1997) 271-288.

[269] X. Dong, T.J. Jeong, E. Kline, L. Banks, E. Grulke, T. Harris, I.C. Escobar, Eco-friendly solvents and their mixture for the fabrication of polysulfone ultrafiltration membranes: An investigation of doctor blade and slot die casting methods, Journal of Membrane Science, 614 (2020) 118510.

[270] M.H.D. Othman, M.R. Adam, M.A.B. Pauzan, S.K. Hubadillah, M.A. Rahman, J. Jaafar, Ultrafiltration Membrane for Water Treatment, in: Self-standing Substrates, Springer, 2020, pp. 119-145.

[271] W. Hirunpinyopas, P. Iamprasertkun, M.A. Bissett, R.A. Dryfe, Tunable charge/size selective ion sieving with ultrahigh water permeance through laminar graphene membranes, Carbon, 156 (2020) 119-129.

[272] P. Roccaro, R. Finocchiaro, J. Mamo, M.J. Farré, Monitoring NDMA precursors throughout membrane-based advanced wastewater treatment processes by organic matter fluorescence, Water Research, (2020) 115682.

[273] J. Sherwood, T.J. Farmer, J.H. Clark, Catalyst: Possible Consequences of the N-Methyl Pyrrolidone REACH Restriction, Chem, 4 (2018) 2010-2012.

[274] J. Coria, Policy Monitor—The Economics of Toxic Substance Control and the REACH Directive, Review of Environmental Economics and Policy, 12 (2018) 342-358.

[275] S. Dutta, K. Iris, D.C. Tsang, Z. Su, C. Hu, K.C. Wu, A.C. Yip, Y.S. Ok, C.S. Poon, Influence of green solvent on levulinic acid production from lignocellulosic paper waste, Bioresource Technology, 298 (2020) 122544.

[276] X. Tang, Y. Sun, X. Zeng, T. Lei, H. Li, L. Lin, γ-Valerolactone—an excellent solvent and a promising building block, in: Biomass, Biofuels, Biochemicals, Elsevier, 2020, pp. 199-226.

[277] A. Phillips, M. Ulsh, J. Mackay, T. Harris, N. Shrivastava, A. Chatterjee, J. Porter, G. Bender, The Effect of Membrane Casting Irregularities on Initial Fuel Cell Performance, Fuel Cells, n/a.

[278] H. Rezania, V. Vatanpour, A. Arabpour, A. Shockravi, M. Ehsani, Structural manipulation of PES constituents to prepare advanced alternative polymer for ultrafiltration membrane, Journal of Applied Polymer Science, 137 (2020) 48690.

[279] M.A. Frommer, D. Lancet, The mechanism of membrane formation: membrane structures and their relation to preparation conditions, in: Reverse Osmosis Membrane Research, Springer, 1972, pp. 85-110.

[280] K.B. Hatzell, X.C. Chen, C.L. Cobb, N.P. Dasgupta, M.B. Dixit, L.E. Marbella, M.T. McDowell, P.P. Mukherjee, A. Verma, V. Viswanathan, Challenges in lithium metal anodes for solid-state batteries, ACS Energy Letters, 5 (2020) 922-934.

[281] X. Dong, H.D. Shannon, C. Parker, S. De Jesus, I.C. Escobar, Comparison of two low‐hazard organic solvents as individual and cosolvents for the fabrication of polysulfone membranes, AIChE Journal, 66 (2020) e16790.

VITA

Xiaobo Dong

Education

Doctor of Philosophy, Chemical Engineering — August 2015-April 2020

University of Kentucky, Lexington, Kentucky, USA

Bachelor of Chemical Engineering and Technology — August 2008–June 2012

Ocean University of China, Qingdao, Shandong, China

Professional positions

Intern — June 2019-July 2019

Polymer Thin Film Processing Group, Georgia Institute of technology, Atlanta, Georgia, USA

Engineer — October 2014-June 2015

SOFCMAN Energy Technological Co., LTD., Ningbo, Zhejiang, China

Engineer — March 2013-October 2014

Institute of Industrial Technology, Chinese Academy of Sciences, Ningbo, Zhejiang, China

Awards

American Membrane Technology Association- Ian C. Watson fellowship — February 2019

Kentucky NSF EPSCoR Super Collider- Mark of Distinction poster award — April 2019

University of Kentucky CME Department- Outstanding Graduate Student Award — April 2019

American Filtration and Separation Society- Student poster competition honorable mention — April 2017

Kentucky NSF EPSCoR Super Collider- Mark of Distinction poster award — February 2017

North American Membrane Society Annual Conference- Elias Klein award — June 2016

Publications

X. Dong, T. Jeong, E. Kline, L. Banks, E. Grulke, T. Harris, I. C. Escobar. **Low-Hazard Solvents and their Mixture for the Fabrication of Polysulfone Ultrafiltration Membranes: An Investigation of Doctor Blade and Slot Die Casting Methods.** *Journal of Membrane Sciences*. (Accepted).

M. Wang, X. Dong, I. C. Escobar, Y. T. Cheng. **Lithium ion battery electrodes made using dimethyl sulfoxide (DMSO)- a green solvent.** *ACS Sustainable Chemistry and Engineering.* (Accepted)

X. Dong, H. Shannon, A. Amirsoleimani, G. Brion, I.C. Escobar. **Thiol-affinity immobilization of casein-coated silver nanoparticles on polymeric membranes for biofouling control.** *Polymers*. 2019, 11, 2057.

X. Dong, H. Shannon, C. Parker, S. De Jesus, I.C. Escobar. **Comparison of two low-hazard organic solvents as individual and co-solvents for the fabrication of polysulfone membranes.** *AIChE Journal*. 2020; 66: e16790.

X. Dong, H. Shannon, I.C. Escobar. **Investigation of PolarClean and gamma-valerolactone as solvents for polysulfone membrane fabrication.** ACS books: *Green Polymer Chemistry: New Products, Processes, and Applications*. Washington: ACS Publications, 2018. 385-403.

X. Dong, A. Al-Jumaily, I.C. Escobar. **Investigation of the use of a bio-derived solvent for the non-solvent-induced phase separation (NIPS) fabrication of polysulfone membranes.** *Membranes*. 2018, 8(2), 23.

Y. Lu, X. Dong, L. Wang, Y. Liu, C. Zhu, H. Xu. **Electrochemical oxidation of ammonium nitrite in absorption solution of flue gas.** *Journal of Electrochemistry*. 2014, 20(1): 1